A Thesis

entitled

A Real-Time Computational Decision Support System for Compounded Sterile Preparations using Image Processing and Artificial Neural Networks

by

Hem K. Regmi

Submitted to the Graduate Faculty as partial fulfillment of the requirements for the Master of Science Degree in Electrical Engineering

---

Dr. Vijay Devabhaktuni, Committee Chair

Dr. Jerry Nesamony, Committee Co-Chair

Dr. Devinder Kaur, Committee Member

Dr. Ezzatollah Salari, Committee Member

Dr. Amanda Bryant-Friedrich, Dean
College of Graduate Studies

The University of Toledo
August 2016

An Abstract of

A Real-Time Computational Decision Support System for Compounded Sterile Preparations
using Image Processing and Artificial Neural Networks

by

Hem K. Regmi

Submitted to the Graduate Faculty as partial fulfillment of the requirements for the Master of Science Degree in Electrical Engineering

The University of Toledo
August 2016

The purpose of this research is to design a computational decision support system (DSS) for compounded sterile preparations (CSP). Error-free compounding is dependent on the proper selection of components and adherence to procedure during compounding. A material selection system (MSS) based on a graphical user interface (GUI), coupled with a barcode scanner and back-end database, has been developed and tested for proper selection of items involving three different medication orders (MO). A video processing system (VPS) has been implemented in MATLAB that evaluates the live video feed from the compounding hood to monitor the compounding procedure when compounding the MO's. Surf detection is used to detect and locate compounding items placed in the hood. Various algorithms have been developed and tested to enhance the accuracy and robustness of the VPS. The Decision Support System (DSS) is further improved with integration of another digital camera to ensure that correct volume of medicine with appropriate syringe is performed during the whole compounding process. The template matching and SURF object detection application on the digital image of the syringe, along with minimum distance classifier and artificial neural networks (ANNs) on the previously collected data from several experimental observations, were explored in classification and volume measurement

of a syringe.

The MSS was tested for all items used in compounding the MO's and performed error-free. The VPS evolved to VPS.03 from VPS.01 and VPS.02. The greatest accuracy and ability for real-time realization were seen in VPS.03. All deliberate mistakes made when compounding the tested medication orders were captured by VPS.03. Leur-lock syringes of different sizes from 1 mL to 30 mL were tested, and an accuracy of 95+ % was obtained with very high precision.

The new computational decision support system facilitates error-free selection of components and is able to monitor and evaluate the compounding process and correct volume measurement in real time. The platform may be used in CSP compounding rooms to audit techniques and procedures as well as in training or educational settings.

To my parents, Krishna Prasad Regmi and Man Kumari Regmi, who are thousands of miles away from me.

Acknowledgments

First and foremost, I would to express my words of gratitude and appreciation for my advisor and thesis committee chairman Dr. Vijay Devabhaktuni and my co-advisor Dr. Jerry Nesamony for all of the guidence, support, advice, and motivation that he provided me over my entire graduate studies. I would also like to thank Dr. Devinder Kaur and Dr. Ezzatollah Salari for agreeing to serve as members of my thesis committee.

Secondly, I would like to thank The University of Toledo's Department of Electrical Engineering and Computer Science as well as the Dean's office for providing me with financial support in the forms of graduate assistantships and tuition waivers. I especially wish to extend gratitude towards Dr. Thomas Stuart, P.E. for enriching my graduate experience with teaching assistant opportunities. I also want to thank the student disability services department of university of Toledo, most notably Sandesh Modhe and Tony Howard, for providing me with part-time employment during the first fall and spring semesters of my graduate studies.

In addition, I want to thank my lab mate Colin Elkin and my research colleague Tashnim Jabir Shovan Chowdhury for assisting in the editing and proofreading of this thesis. My research group members of NE 2042 and NE 2033 are also greatly acknowledged. Most importantly, I would like to thank my family for continuous love, support, and motivation throughout my graduate studies.

Contents

List of Tables

List of Figures

List of Abbreviations

1-D	One-dimensional
2-D	Two-dimensional
ABS	Ampule Break Stage
ANN(s)	Artificial Neural Network(s)
APR	Automatic Prescription Reader
CA	California
CCL	Connected Component Labeling
CNS	Changing Needle Stage
CS	Cleaning Stage
CSP	Compounded Sterile Preparation
CSS	Computational Support System
DT	Detection Time
DSS	Decision Support System
EAN	European Article Number
GHz	Gigahertz
GUI	Graphical User Interface
HCL	Hydrogen Chloride
IAPP	Image Acquisition & Preprocessing
IIBS	Injecting into IV Bag Stage
IPA	Isopropyl Alcohol
IV	Intravenous
LAFW	Laminar Air Flow Hood
MATLAB	Matrix Laboratory
mg	milligram

ml ..... milliliter
MLP ..... Multilayer Perceptron
MO(s) ..... Medication Order(s)
MSE ..... Mean Square Error
MSS ..... Material Selection System

NCC ..... Normalized Correlation Coefficient

OCR ..... Optical Character Recognition
OR ..... Oregon
OSNS ..... Opening Syringe and Needle Stage

PC ..... Personal Computer
PCB ..... Printed Circuit Board

RAM ..... Random Access Memory
ROI ..... Region of Interest

SCS ..... Syringe Classification System
SCVMS ..... Syringe Classification and Volume Measurement System
SD ..... Standard Deviation
Sec ..... Seconds
SIFT ..... Scale Invariant Feature Transform
SSD ..... Sum of Squared Difference
SURF ..... Speeded Up Robust Features
SVM(s) ..... Support Vector Machine(s)
SVMS ..... Syringe Volume Measurement System

US ..... United States
USP ..... United States Pharmacopeia

VPS ..... Video Processing System

List of Symbols

η	NCC coefficient
ζ	SSD value
X	Features vector
$g(x)$	Decision boundary for classifier
w_i	Set of classes for classifier
$T(x)$	Transfer function
y_i	Network output of ANN for i^{th} data
x_i	Network input of ANN for i^{th} data
D_i	Targeted output of ANN for i^{th} data
$B_i(s)$	Bias(s) to ANN
$W_i(s)$	Weight(s) of branches of ANN
L	Barrel length
W	Barrel Width
PL	Plunger Length

Chapter 1

Introduction

Compounding is the process of making pharmaceutical preparations by a licensed pharmacist or a pharmacy technician according to the unique needs of an individual patient when commercially available drugs fail to meet the requirement or when a patient may specifically need those drugs. The pharmacists prepare compounded preparations based on a prescription provided by physicians for a specific patient. Compounding is categorized into compounded sterile preparations and compounded non-sterile preparations. Compounded sterile preparations are used or administered through a route that directly introduces the dosage form into the blood or systemic circulation, open wounds, surgical incisions, internal organs, eyes, nasal cavity, and lungs. Non-sterile preparations can be taken orally or used topically by applying to the skin or body orifices. Thus, compounded sterile preparations pose a greater risk to patient health and safety if prepared using incorrect ingredients, methods, and devices. The state boards of pharmacy regulate the practice of compounding. Introduction of technology during compounding process, such as compounding robots, makes the preparation efficient and error free but carries prohibitive costs related to procurement and production. The rationale for this work was to develop and evaluate a semi-automatic technical system that has a low cost to be integrated with existing compounding systems to augment and enhance the sterile compounding process.

1.1 Overview of Compounded Sterile Preparation

Frequently, errors that can cause patient death and serious adverse reactions are made when preparing CSP's using incorrect and defective materials [1] and when the person who is performing the compounding uses an incorrect method or procedure. Additionally, wrong decisions may be made in the stressful and often demanding environment of the clean room where CSP's are made due to personnel fatigue [2]. A wrong vial containing an injection that has a label similar to the required medication may be picked erroneously, causing eventual fatality. Even when the final CSP is released for patient administration after inspection and verification by the pharmacist, if an incorrect method was used when making the compounded injection, it can lead to deleterious effects and adversely affect patient health [3, 4].

Compounded sterile preparations made national news in the US following the tragic death of several patients spanning numerous states in 2012 [5]. Several reviews on the topic of safety of compounded sterile preparations, published prior to this tragedy and after, point to the prevalence of wide-ranging issues, including failure to meet specifications [2], contamination and/or sterility problems [6, 7], raw material purity issues [8], errors related to potency [9], content uniformity [10], and labeling [11]. A recent survey of practices related to CSP's in US hospitals show that integration, adoption, and updating of innovation and technology in this field are severely limited [12]. The current methods to evaluate, monitor, and correct these issues are based on direct personnel supervision and self-reporting. Thus, errors are identified after a minor or major event has occurred, followed by implementation of policies and procedures to limit, contain, and rectify the error. This approach, although helpful in verifying the cause of the problem and creating awareness of it among clinicians, is unable to prevent such events from occurring again. The introduction of checklists has been suggested to be useful in a variety of situations where

there is high probability of process-based errors [13, 14]. The earliest evidence for use of checklist-based decision support can be seen in aviation and other engineering fields. An intelligent decision support system based on integration of foundational knowledge, material properties, process selection, and equipment use for dosage form development has been proposed for use in the pharmaceutical industry during dosage form development [15]. Adoption of this type of strategy in the healthcare field has been slow but was initiated through use in nursing and in select areas of medicine and surgery [16, 17]. Numerous studies published in the recent past illustrate that the introduction of checklist-based systems in health-care and medicine has led to significant decreases in errors, substantial cost reduction, better patient outcomes, and thousands of lives saved [18-23].

1.2 Proposed Techniques for CSP

Until now, there has been no attempt to augment the existing compounded sterile preparations environment. Efforts to completely automate the preparation environment via robots are excessively and prohibitively expensive. In this study, an object and image tracking-based software system that can provide real-time support to identify and select materials, followed by monitoring, evaluation, and feedback during preparation of a compounded sterile preparation (CSP), was developed. A touch-free, gesture-controlled tool has been integrated into the system to enable hands-free navigation through the system, so as to simplify operating the system and minimize contamination risk from touch [24]. This system offers a cost-effective and user-friendly solution to problems encountered when preparing CSP's. A major innovation of this project is that it incorporates advances in digital and computational techniques in the CSP environment to reduce human error and ensure quality of the compounded preparation. Another important aspect of the project is the use of sensors such as bar-

Patient name:	**Room #:**
MRN #	
Promethazine HCL **(Strength 25 mg/ml)**	**12.5 mg**
Sodium chloride 0.9%	**50 ml**
DO NOT REFRIGERATE. **PROTECT FROM LIGHT.** **MONITOR VITAL SIGNS: BP, PULSE & RESPIRATIONS.** **IF GIVEN IV SPECIAL PRECAUTIONS NEED TO BE TAKEN.** **DO NOT ADMINISTER IN HAND OR WRIST.** **Q4HPRN** **Infuse over 15 minutes** **Qty: 1** **Prep Date:** **Time:** **Rx #:**	
Administration time:	**Time:** **Prepared by:** **Rx INIT:**
LABEL:	
Hospital Name **Address**	**Phone #**
Patient Name:	**Room #:**
MRN #	
PROMETHAZINE HCL **Sodium chloride 0.9%**	**12.5 MG** **50 ml**
DO NOT ADMINISTER IN HAND OR WRIST. **Q8HPRN** **Infuse over 15 minutes**	**DISP DATE:**
EXP. DATE and TIME:	**BY:**
BAR CODE	

Figure 1-1: Medication orders for Promethazine HCl infusion (MO-1).

code scanners and digital cameras to identify potential errors through object tracking, image tracking, and feedback mechanisms.

A computational support system (CSS) that helps to select proper materials before compounding and is capable of monitoring the procedure continuously and providing real time feedback to personnel preparing injections will help to address the problems related to CSP's. The system enables easy identification of material to be used when preparing an injection by coupling a standard bar-code scanner to an image database. After properly identifying, selecting, and verifying the items, the technician can then proceed to perform the compounding process. During this time, image analysis and

Patient name:	**Room #:**
MRN #	
LABETOLOL HCL **(Strength 100 mg/20 ml)**	**15 mg**
MONITOR VITAL SIGNS: BP, PULSE & RESPIRATIONS **Q12PRN** **INFUSE OVER 5 MINUTES** **Qty: 1** **Prep Date:** **Time:** **Rx #:**	
Administration time:	**Time:** **Prepared by:** **Rx INIT:**
Hospital Name **Address**	**Phone #**
Patient Name:	**Room #:**
MRN #	
LABETOLOL	**15 MG**
Q12HPRN **Infuse over 5 minutes**	**DISP DATE:**
EXP. DATE and TIME:	**BY:**
BAR CODE	

Figure 1-2: Medication orders for Labetalol HCl (MO-2).

real-time monitoring of the procedure are performed through a strategically placed digital camera. As key points are reached during the compounding process, the program will provide feedback to the personnel regarding the validity and propriety of the steps used during injection preparation.

The whole compounding process is generally characterized by various standard operation procedures. The procedures are formulated based on institutional policies of a particular hospital or compounding facility by taking into account the guidelines published in the United States Pharmacopeia General Chapter <797> [25], manufacturer's recommendations available through package inserts accompanying injections

that are used in compounding, and other guideline documents [26, 27]. Some generalizations can be made regarding the procedure to be used when preparing an injection, based on the nature of the compounded preparation being made. We have selected three commonly encountered CSP's, including one compound involving an injection available in an ampule referred to as medication order-1 (MO-1) (Fig. 1-1); a second preparation in which a certain volume of sterile liquid injection is withdrawn from a vial during the compounding process, called medication order-2 (MO-2) (Fig. 1-2); and a third type in which a sterile powder for injection is reconstituted, called medication order-3 (MO-3) (Fig. 1-3). All three CSP's have varying degrees of difficulty and complexity during compounding. The procedure used to prepare a particular CSP was developed from existing practices and guidelines and incorporated into the interactive decision support system (DSS), which is part of the CSS created, tested, and evaluated in this project. The procedure was further transformed into a sequence of steps comparable to a checklist-type visual aid that will help the technician to navigate through the compounding procedure effortlessly [28].

Patient name:	**Room #:**
MRN #	
PROTONIX	**40 mg**
SODIUM CHLORIDE 0.9%	**100 ml**
Q6PRN **INFUSE OVER 30 MINUTES** **Qty: 1** **Prep Date:** **Time:** **Rx #:**	
Administration time:	**Time:** **Prepared by:** **Rx INIT:**
Hospital Name **Address**	**Phone #**
Patient Name:	**Room #:**
MRN #	
PROTONIX **SODIUM CHLORIDE 0.9%**	**40 mg** **100 ml**
Q6HPRN **Infuse over 30 minutes**	**DISP DATE:**
EXP. DATE and TIME:	**BY:**
BAR CODE	

Figure 1-3: Medication orders for Protonix (MO-3).

1.3 Overview of Syringe Classification and Volume Measurement System

In hospitals and other institutional settings injections and in general the parenteral route of drug delivery is an important means of administering medication to patients. Recently there has been an increase in the number of medications that are prepackaged in syringes that are sealed with a syringe tip cap. In all these instances a liquid solution of the drug or diluent is taken in a syringe during compounding, while adding a diluent, when administering the medication to a patient, or and when

packaging injections or solutions after preparation. The accuracy of the volume of liquid present in the syringe can have a significant effect on the outcome or results related to the process in which the syringe is being used. For example, if a 500 mg dose is present in 5 ml solution, when the technician manually withdraws and visually checks the volume wrongly as 5 ml, although the actual volume drawn was 4.8 ml, the error associated with the dose will be 4%. Such inaccuracies in dose can impact the therapeutic effect related to a drug. The errors related to inaccurate volume do not occur deliberately rather it can happen by a genuine mistake made by the technician or pharmacist. The visual verification of the volume of liquid in a syringe is very subjective and can have errors due to differences between personnel such as the syringe holding technique, checking of syringe plunger position above or below the eye level, etc. Additionally numerous pharmaceutical products including pain medications, hormones, diluents, biotechnology-derived products, anticoagulants etc. are available in prepackaged syringes called as "prefilled syringes". The imprecision related to the fill volume in prefilled syringes can significantly alter the potency of the medication based on deviations from the label claim associated with the product. Automated compounding systems are still evolving and some examples include Diana Hazardous Drug Compounding System [34] and Cytocare [35], but these systems are prohibitively expensive. Currently there are no available systems that can automatize the volume measurement step during compounding or packaging of sterile preparations taken in a syringe. In the research reported in this thesis, a new semi-automatic system that can be integrated into existing technologies was developed and evaluated. The approach includes several features such as low cost, high accuracy, high efficiency, and robustness.

1.4 Proposed Techniques for SCVMS

The strategy used in this system was to automatize the volume reading process during compounding as well as during inspection stage by the pharmacist with the help of a digital camera using image processing and artificial neural networks in real-time. The system takes image frame from the digital camera which is integrated with MATLAB software program [36] and gives the type of syringe used and exact volume of medication present in the syringe. The digital camera serves as the source of information for processing. The detection of syringe tip cap using adaptive template matching [37] forms the basic foundation to extract features of syringe from the whole image. Adaptive template matching technique is widely utilized in object detection [38], image registration [39], object tracking [40] various types of machine vision, industrial, and surveillance applications [41]. Weighted threshold histogram equalization with improved switched median filtering technique [42] helps to remove the impulse noise in the image and preserves the edge information. A recursive segmentation approach that extends Otsu's method [43] extracts the brightest object from the darkest background at the final iteration [44]. The segmentation process converts the gray-scaled image into binary data and becomes suitable for further processing. The connected component labelling (CCL) [45] helps to separate the medication and/or plunger region of the syringe from the whole segmented binary image. Various popular algorithms for CCL were used, tested, and verified in real-time using various hardware interfaces [46]. The multi-class confidence level in conjunction with weighted minimum distance classifier [47] classified the six syringes used in the compounding process flawlessly. The feature vectors for all the syringes were widely spaced enhancing the efficiency and computation time related to the classifier [48]. The volume measurement in the system is accomplished by using artificial neural network (ANNs) for supervised learning environment [49]. The

Levenberg-Marquardt back propagation algorithm [50] trained the plunger length in pixels and corresponding volume to build a neural network model that was later utilized for volume calculation. The untrained neural network model of single input, 10 hidden neurons, and single output was developed using Neural Network Toolbox in the MATLAB [51]. The neural network was trained using previously established datasets obtained by conducting various experiments to record the plunger length of different syringes at different volumes under identical experimental environment. Training in machine learning using support vector machines (SVMs) [52] can perform better than ANNs due to its higher feature dimensions [53] in analysis. But SVMs are slow and very complex to implement and for single input-single output datasets with high linearity and that can be satisfactorily trained using ANNs.

The visual inspection techniques using several digital cameras, X-rays and various imaging devices were already implemented in pharmaceutical industry to inspect the defects, foreign material, cracks, missing or misapplied stoppers and seals, etc. [54]. Machines can provide visual inspection as effectively as human technicians with the advantage of high speed and throughput. However human inspection is taken as the standard for visual inspection according to USP <790> (1, 2) [55, 56]. The scope of automatic volume detection is not limited to health care industry but similar techniques are already being investigated in industrial sectors such as visual inspection for soft drink bottling plant [57], printed circuit boards (PCBs) [58], and remote visual inspections of aircraft surfaces [59].

The proposed approach demonstrates the use of the digital camera to classify and detect the volume of medicine inside Luer-lock syringes. Syringes normally used during compounding of sterile preparations ranges from 1 mL to 60 mL. The system reported in this manuscript, syringes of size from 1 mL to 30 mL were tested. The experiments were conducted for similar syringes at different times under identical experimental conditions to check the reproducibility of the system and accuracy in vol-

Table 1.1: Publications and contributions to thesis.

Type	Publication/Contribution
Journal Paper I	A new computational decision support system for material selection and real-time monitoring and evaluation of aseptic technique when compounding sterile preparations. (Journal of Pharmaceutical Innovations, Submitted, Under review)
Journal Paper II	A new Leur-lock syringe classification and volume measurement system using Image Processing and Artificial Neural Networks.(Under preparation)
Source Code	A re-usable MATLAB library containing the source code of the algorithm implementations

ume detection. The system was designed to make it realizable in real time to inspect and measure volume of compounding syringe while the technician is compounding the medication. It can also be utilized to obtain the volume and type information of finished products such as prefilled syringes or fill volume in syringes after compounding by pharmacists checking the volume after compounding was completed.

1.5 Publications and Contributions to Thesis

The major publications and contributions of this research are presented in Table 1.1.

1.6 Thesis Organization

This thesis unfolds as follows:

Chapter 2 provides a review of the literature that forms the foundation of this research. It covers a variety of theoretical backgrounds pertaining to prior established research methods in the areas of object detection and tracking, artificial neural network and training, various classifiers, and standard CSP's.

Chapter 3 describes the DSS for different CSP's which focuses on the proper selection of materials and video processing system.

Chapter 4 explains the addition of the new system to the DSS described in Chapter 3, which helps to measure the volume of medicine inside syringe precisely during compounding.

Chapter 5 draws conclusive remarks and discusses possible future directions in which this research could advance.

Finally, the thesis ends with three appendices, containing all of the C# and MATLAB source code required to simulate each proposed scheme. Appendix A holds the code for MSS developed in Microsoft Visual Studio using C# while Appendix B contains the code for the complete VPS developed in MATLAB for the methods as described in Chapter 3, and Appendix C includes the necessary MATLAB codes for SCVMS.

Chapter 2

Literature Acquisition and Analysis

This chapter gives the background of the methods and processes utilized in the entire research process, including already implemented techniques and methods. Included are CSP terminologies used, algorithms, and methods utilized to accomplish desired output in details.

2.1 Compounded Sterile Preparation Methods

There are numerous compounding sterile preparation methods available that can be utilized by a pharmacist to prepare drugs based on the necessity of patient and/or prescription of doctor. When a pharmacy technician receives prescription which are generally called a medication order (MO), he/she does necessary calculations and lists all the medicines and equipment required for this particular preparation. He/she places all the medicines and equipment in the Laminar Air Flow Hood (LAFH) and starts the compounding process, following one of the standard compounding procedure. Although there are numerous compounding processes that differ from one another, most of them could be addressed by following three standard compounding procedures.

2.1.1 Ampule Preparation

An ampule preparation is the one of most commonly utilized CSP. During compounding it involves following steps:

1. Perform calculations correctly and check calculations.

2. Collect all items correctly: ampule, IV bag, syringe, filter needle and regular needle.

3. Remain silent or engage in minimal conversation during compounding. If you have to talk direct the conversation away from the hood. Make sure that there are no erratic and rapid hand movements inside the IV hood. Place material appropriately in the hood. All items should be adequately spaced apart in the hood to prevent zones of turbulence. All aseptic manipulations must be done at least six inches within the hood.

4. Swab the ampule and IV bag using IPA prep pad.

5. Ensure that the entire injection liquid is in the body of the ampule. Tap lightly to allow injection present in the head (if any) to drain into the body of the ampule. Open ampule using proper technique. Place the left and right thumbs in line along the ampule; one thumb along the head and the other thumb along the body of the ampule. Snap the head of the ampule. Discard the head of the ampule in a sharps container.

6. Open the syringe and the filter needle using proper technique by peeling off the wrapper.

7. Insert the filter needle into the syringe using proper technique. Do not touch the syringe tip and needle hub. Use proper hand placements so as not to block first air.

8. Use proper technique to draw injection from the ampule into the syringe. Use a one-handed technique. Use proper hand placements so as not to block first air. Hold the ampule in one hand and manipulate the syringe using the other hand and draw a little more volume of injection than required.

9. Use proper technique to remove filter needle and discard the needle in a sharps container. Do not touch the syringe tip.

10. Open regular needle using proper technique by peeling off the wrapper.

11. Insert regular needle into the syringe using proper technique. Do not touch the syringe tip and needle hub. Use proper hand placements so as not to block first air.

12. Expel air bubbles (if any) present inside the syringe by gently tapping the syringe with knuckles.

13. Adjust the volume by slowly pushing the plunger to the desired position. Verify the volume of the liquid in the syringe by observing the plunger position at eye level.

14. Use proper technique to inject liquid into IV bag. Pierce the compounding port at a 90° angle. Introduce the liquid inside the syringe into the IV bag by pushing the plunger completely towards the tip of the syringe. Withdraw the syringe by pulling the needle out of the compounding port slowly. Dispose used syringe and needle assembly in the sharps container.

15. Inspect IV bag for any particulates or unusual discoloration or other visual signs of incompatibility. Place the label properly on the blank face/side of the IV bag.

16. Place a sterile seal around the compounding port covering the tip completely.

17. Place the IV bag, vial, and label in a bin for inspection.

2.1.2 Injection Vial Preparation

Procedure to take a certain volume of liquid from a vial and capping the syringe using a sterile syringe tip cap.

1. Perform calculations correctly and check calculations.

2. Collect all items correctly: Vial, syringe, regular needle, and sterile syringe tip cap.

3. Remain silent or minimal conversation during compounding. If you have to talk direct the conversation away from the hood. Make sure that there are no erratic and rapid hand movements inside the IV hood. Place material appropriately in the hood. All items should be adequately spaced apart in the hood to prevent zones of turbulence. All aseptic manipulations must be done at least six inches within the hood. All waste generated should be disposed adequately and in a timely manner.

4. Check the vial for particulates or any unusual discoloration. Open vial using proper technique. Flip off the plastic vial top. Do not touch the rubber stopper.

5. Swab the vial using IPA prep pad and place it back in the hood. Make sure that all waste generated is disposed off appropriately.

6. Open the syringe using proper technique by peeling off the wrapper. Open the needle using proper technique by peeling off the wrapper.

7. Insert needle into the syringe using proper technique. Do not touch the syringe tip and needle hub. Use proper hand placements so as not to block first air.

8. Use proper technique to draw the injection from the vial. Pull the plunger back to take in first air from the IV hood. Take air in the syringe equal to the

volume of liquid desired from the vial. Push the air inside the syringe slowly and intermittently while drawing the reconstituted injection from the vial. Ensure that a slightly more than desired liquid is pulled into the syringe. Pull out the syringe by slowly withdrawing the needle.

9. Expel air bubbles (if any) present inside the syringe by gently tapping the syringe with knuckles.

10. Adjust the volume by slowly pushing the plunger to the desired position. Verify the volume of the liquid in the syringe by observing the plunger position at eye level.

11. Remove the needle by unscrewing the needle in the anti-clockwise direction. Dispose the needle properly. Take care to not touch the syringe tip.

12. Peel off the packing of the sterile syringe tip cap. Do not take the syringe tip cap with hands from the packing. Insert the syringe cap by slowly screwing the syringe tip into the sterile syringe tip cap. Make sure that the syringe tip cap is securely attached to the syringe.

13. Place the label by flagging the label using a clear tape around the syringe. Place the syringe, vial, and label in a bin for inspection.

2.1.3 Powder Reconstitution Preparation

This is another important procedure in CSP which reconstitutes a powder medication in the vial. It involves following steps during compounding:

1. Perform calculations correctly and check calculations.

2. Collect all items correctly: vial, IV bag, syringe, and needle.

3. Remain silent or engage in minimal conversation during compounding. If you have to talk direct the conversation away from the hood. Make sure that there are no erratic and rapid hand movements inside the IV hood. Place material appropriately in the hood. All items should be adequately spaced apart in the hood to prevent zones of turbulence. All aseptic manipulations must be done at least six inches within the hood.

4. Open vial using proper technique. Flip off the plastic vial top. Do not touch the rubber stopper.

5. Swab the vial using IPA prep pad and place it back in the hood. Make sure that all waste generated is disposed off appropriately.

6. Swab IV bag using IPA prep pad and place it back in the hood.

7. Open the syringe using proper technique by peeling off the wrapper. Open the needle using proper technique by peeling off the wrapper.

8. Insert needle into the syringe using proper technique. Do not touch the syringe tip and needle hub. Use proper hand placements so as not to block first air.

9. Insert the needle into the compounding port of the IV bag by piercing the compounding port at a 90° angle. Use proper technique to draw diluent from IV bag. Withdraw the needle by slowly pulling out.

10. Use proper technique to add diluent to powder in the vial. Pierce the stopper at an angle of 45° after ensuring that the bevel is facing up. Push the needle down. Slowly push the plunger and let the diluent into the vial. Release the plunger to allow air from inside the vial to bubble into the syringe. The syringe may be left in vial after adding all the diluent in the syringe into the vial.

11. Swirl the vial to dissolve. Ensure that all the powder is completely dissolved. Check for any particulates or unusual discoloration or other visual signs of incompatibility.

12. Use proper technique to draw reconstituted injection from the vial. Push the air inside the syringe slowly and intermittently while drawing the reconstituted injection from the vial. Ensure that all the liquid is pulled into the syringe.

13. Use proper technique to inject reconstituted injection into IV bag. Pierce the compounding port at a 90° angle. Introduce the liquid inside the syringe into the IV bag by pushing the plunger completely toward the tip of the syringe.

14. Withdraw the syringe by pulling the needle out of the compounding port slowly. Dispose the used syringe and needle assembly in the sharps container.

15. Inspect the IV bag for any particulates or unusual discoloration or other visual signs of incompatibility. Place the label properly on the blank face/side of the IV bag.

16. Place a sterile seal around the compounding port covering the tip completely.

17. Place the IV bag, vial, and label in a bin for inspection.

2.2 Image Preprocessing and Segmentation

Digital image acquired from imaging device contains information as well as noise. Preprocessing on digital image helps to improve the quality of image and makes it ready for further processing. The image preprocessing involves various filters on the image which helps to enhance edge, suppress noise etc.

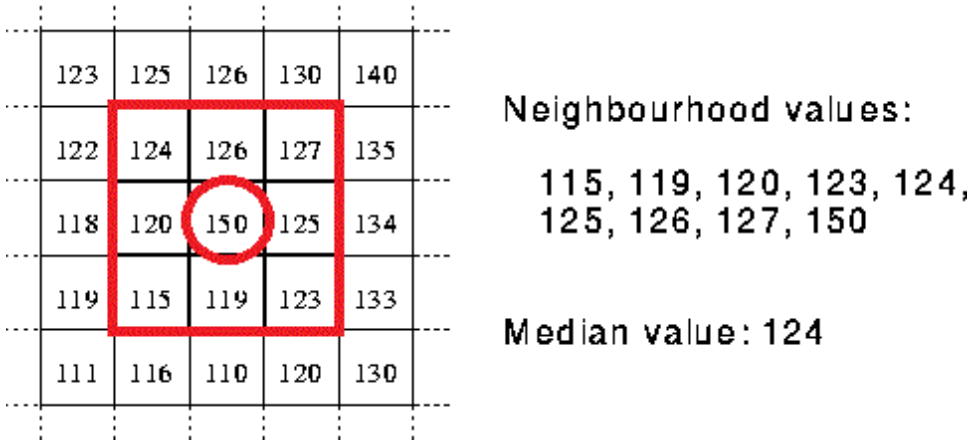

Figure 2-1: Example of Median Filter.

2.2.1 Image Enhancement

The main objective of image enhancement is to make it suitable for interpretation and analysis. The image enhancement techniques include spatial and frequency domain analysis. Mostly contrast enhancement using various transformation functions were utilized to enhance illumination of foreground object. Histogram equalization and histogram matching is also a widely used technique for image enhancement [42]. Median filtering and histogram equalization were used to enhance the image frame obtained from video. The 3×3 window mask of median filter as shown by red rectangle in Fig. 2-1. The median filter helps to remove salt and pepper noise in the image. The neighbors of intensity value 150 were considered in analysis. It has 3×3 mask window thus total 9 intensity values were first sorted in increasing order and median is picked. The median value replaces the previous intensity value denoted by red circle in Fig. 2-1. The process is repeated for all pixels in the image.

The histogram equalization [60] analyzes the intensity distribution of an image and tries to make the intensity distribution uniform. Histogram equalization assumes the total number of pixels in the image after transformation remains same and only the intensity distribution is made uniform. Let pixel x has value $0 < x < 1$, and

$y = f(x)$ maps the pixel value into the same range and we will have,

$$p(x) * dx = p(x) * dy \tag{2.1}$$

Thus, if $p(y) = 1$, then

$$dy = p(x) * dx \tag{2.2}$$

$$\frac{dy}{dx} = p(x) \tag{2.3}$$

For discrete level histogram equalization, the intensity value takes only one of the L discrete values for $0 \leq x < L$. The histogram equalization is first done for normalized function and later converted into the L intensity levels.

2.2.2 Image Thresholding and Analysis

The enhanced image becomes suitable to separate the background from the foreground object. There are several image thresholding techniques that are successfully implemented in different scenarios [61]. Image thresholding for this research is accomplished using Otsu's thresholding technique which is fast and accurate method [43], and this is based on discriminant analysis. Thresholding is obtained using partitioning of pixels of an image into two classes C_0 and C_1 (e.g. object and background) at certain gray level t. Thus, $C_0 = 0, 1, ..., t$ and $C_1 = t + 1, t + 2, ..., l - 1$. Let σ_W^2, σ_B^2, and σ_T^2 be the within class variance, between class variance, and the total variance respectively. Then an optimal threshold can be determined using a condition in which argument of minimum of η for all t belongs to G. where,

$$\eta = \frac{\sigma_B^2}{\sigma_T^2} \tag{2.4}$$

2.2.3 ROI Selection and Region Extraction

The thresholded image contains various regions as whole, among which a particular region will be utilized for further analysis. The ROI selection plays a very important role in image analysis, as it helps to narrow the subject of analysis and helps to avoid excessive computation time [62], which is highly necessary when a system has to be realized in real-time. The ROI selection is defined by the user and is easy when image acquisition system position is fixed and object position is also limited. In the system described in chapter 3, the selection of working zone and item placement zone is accomplished utilizing prior information of digital camera and LAFW compounding hood. After ROI selection, only required objects remain in the image and these objects have to be extracted for further analysis. The region extraction in the binary image is generally accomplished using connected component analysis [45, 63] which helps to obtain the geometrical information (size, location) of the different objects.

In the binary image, the single object gives the group of pixels which are neighbors to each other and are connected also. Thus a single object can be separated from entire image using connected component analysis. In connected component labeling the neighbor pixels with the same level of intensity are grouped together. In a binary image, all pixels with intensity value 1 that are neighbors of each other are said to be connected. The connectivity analysis can be done with 4 - connectivity and 8 - connectivity. The 8 - connectivity is utilized in the presented system to find the connected region. The connected component labelling operator scans the binary image by scanning a row until it finds the white pixel at point p (intensity at point p is 1) and checks for already scanned neighbor pixels. If all four neighbors have intensity 0, then assign a new label for p. Otherwise if only one neighbor has 1, then assign its label to p, but if more than one neighbors as 1, then assign one of the labels to p and make note of equivalences.

After completing the scanning process, equivalent labels are combined and assigned to a new label class. The label class contains the information about the number of connected pixels and their locations in the image, which is further processed to obtain the centroid and approximate area of the object.

2.3 Object Detection and Tracking

Object detection and tracking is the most utilized discipline in current automated systems. Object detection helps to identify the faults in the manufacturing plants, industrial finished goods, and mostly in video surveillance. Object detection is based on the shape, color, texture, and orientation, while motion tracking is based on the background subtraction methods and optical flow [64]. Detection of particular object in the whole image could be accomplished by the adaptive template matching and SURF object detection.

2.3.1 Template Matching

The template matching is one of the simplest and best techniques to detect an object in the scene image. For template matching we need one reference template image and another inspection image. Our main target is to inquire whether or not reference template is present in inspection image. The normalized cross correlation calculation (NCC) is done using the formula shown in Equation 2.5, and the correlation values are obtained in matrix form.

$$\eta = \frac{\sum_{i,j \in W} I_1(i,j) \times I_2(x+i, y+j)}{\sqrt{\sum_{i,j \in W} I_1^2(i,j) \times \sum_{i,j \in W} I_2^2(x+i, y+j)}} \tag{2.5}$$

where, η = Normalized correlation coefficient, $I_i(x, y)$ = Intensity value at position

(x,y), and ζ = SSD correlation value.

$$\zeta = \sum_{i,j \in W} I_1^2(i,j) - I_2^2(x+i, y+j) \tag{2.6}$$

Similarly, sum of squared difference (SSD) is another technique for correlation calculation, which is calculated using Equation 2.6. The correlation value at every point in the matrix is scanned and compared with some previously defined threshold. The threshold value is determined based on the experimental observations. For NCC, the perfect match of template to the inspection image gives the correlation value of +1 while the correlation value with negative of template will give -1. Thus, the NCC value lies in the range of [-1, +1]. For SSD, the correlation value is greater than zero and will have low value for perfect matching while remains high for less matched cases. Matching points are detected by comparing correlation value with some predefined threshold. Let the template image has a size of 3×3 and inspection image has a size of 100×100. Thus, when the correlation value is calculated on every pixel in inspection image by running template image over the inspection image. A matrix of correlation value will have size of 100×100, will have values in range between $[-1, +1]$ for NCC, and will have non-negative value for SSD.

2.3.2 SURF Detection

Speeded up robust features is the scale and rotation invariant local feature descriptor, which is robust yet faster than other methods [33]. In the SURF detection process, the SURF features of template and inspection image is calculated at first, and then the feature points of the template are compared with the feature points of the inspection image to find the best match points. The best match points collectively give the region of the inspection image where the region resembles the template image. SURF is faster than SIFT and other feature descriptor methods. SURF ap-

Figure 2-2: (a) Original with eye template in green rectangle and showing direction of scanning by blue arrows (b) Result image showing best match point by red asterisk, SSD matching, and NNC [65].

proximates the Laplacian of Gaussian with Box filter and has great advantage, since convolution with box filter can be easily calculated with integral images and that can be done in parallel with different scales. SURF relies on determinant of Hessian matrix for both scale and location while orientation is determined using sum of all wavelet responses within 60° as shown in Fig. 2-3.

The total window size near the interest points in the image is further divided into smaller sub regions. From there, wavelet components are calculated. Based on these components, the feature vector for smaller sub regions is given as

$$V = \{\sum x, \sum y, \sum dx, \sum dy\} \tag{2.7}$$

while other features have been developed based on the magnitude and sign of dx and dy to provide better accuracy with cost of computation. The wavelet response is not affected by illumination in the targeted image. SURF features also allow the

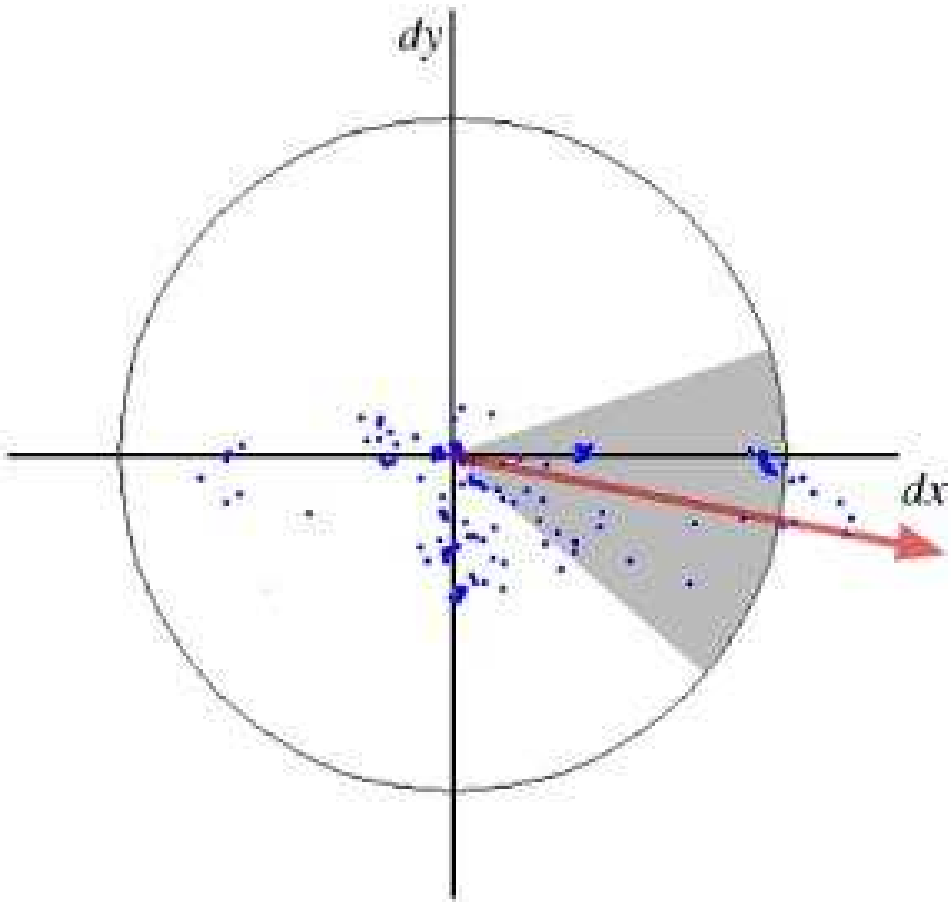

Figure 2-3: Wavelet in x and y direction in sub regions of image with in 60°. Where, dx is Haar wavelet component in horizontal direction and dy is Haar wavelet component in vertical direction degree [66].

detection of object in the cluttered scenario. SURF feature of specific object only matches with SURF features of the image where that object is located. Once the centroid of the detected object in clutter scene is obtained, it will be easy to calculate the difference with centroid in previous frame for that object. This technique helps to find if the specified object is moving or have changed its position.

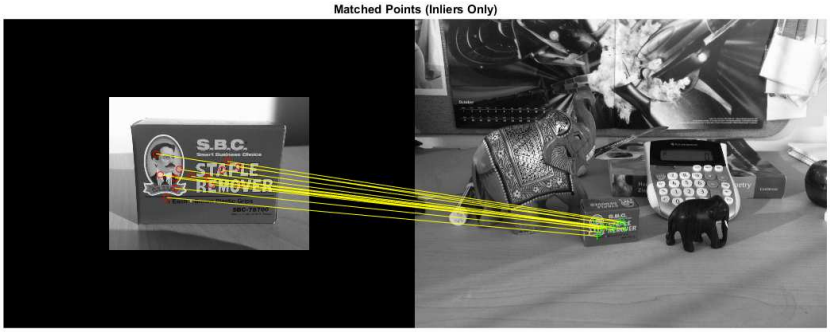

Figure 2-4: Example of SURF object detection in cluttered scene [67].

2.4 Minimum Distance Classifier

Minimum distance classifier using Euclidian distance measure is the simplest yet faster and accurate for simple data set with very little variations that other established classifiers and the fact is established in face recognition with eigenface which uses minimum distance classifier [68]. Classifier helps to classify a new sample into previously defined classes.

A pattern is the vector of measured features and our goal is to assign x into one of a set of classes $\{w_i\}$.

$$X = \begin{bmatrix} x_1 \\ x_2 \\ \vdots \\ x_n \end{bmatrix} \tag{2.8}$$

The decision boundary for x is given as,

$$g(x) = W^T X + W_0 \tag{2.9}$$

where,

$$W = M_1 - M_2 \tag{2.10}$$

$$W_0 = \{M_2^T M_2 - M_1^T M_1\}/2 \tag{2.11}$$

if $g(x) > 1$, assign x to class W_1. If $g(x) < 1$, assign x to class W_2. And if $g(x) = 0$, can be assigned to any class.

2.5 Artificial Neural Networks and Training

An artificial neural network is the information processing system which is inspired by the working principle of the biological nervous system. The neurons in neural networks are interconnected as in a biological system, and each synaptic connection has its own weights to process information. Neural networks help to solve the problems that do not fit with any algorithmic approach. It helps to derive very useful information from complicated and imprecise data [69].

Training in neural network can be done in supervised and unsupervised learning. The supervised learning requires the input pattern and output pattern for training, while unsupervised learning learns from mistakes that the network previously made and only have input patterns. The supervised learning is generally used for training data patterns that are complex to analyze and hardly fit in any mathematical functions. The supervised learning is controlled by calculating the mean square error (MSE) of the output, which gives how output produced by the neural network is deviated from its actual output for the same input. The complete datasets available for training are usually divided into learning data and validation data. The learning data is used for training while validation data, never used for training, is utilized define the criteria to stop the learning procedure. Usually training is stopped when learning and validation error are very close and less than maximum error is allowed. An artificial neural network consists of following elements:

In the Fig. 2-5, an example of an multi-layered perceptron (MLP) network with single input, single output, and three hidden neurons is shown, where x is input, D

is targeted output, H is hidden neuron, I is input neuron, O is output neuron, B_i is bias supplied to network, and W_i is weight of the network. Let $\{\gamma\}$ be the input to the hidden neurons. Then,

$$\gamma_1 = W_1 \times x + B_1 \tag{2.12}$$

$$\gamma_2 = W_2 \times x + B_2 \tag{2.13}$$

$$\gamma_3 = W_3 \times x + B_3 \tag{2.14}$$

Hidden layer neurons have sigmoid unipolar transfer function as given in Equation 2.15, while input and output neurons just copies the input to output.

$$T(x) = \frac{1}{1 + \exp(-x)} \tag{2.15}$$

if $Z_i = T(\gamma_i)$, then output y from network is given as,

$$y = B_4 + W_4 \times Z_1 + W_5 \times Z_2 + W_6 \times Z_3 \tag{2.16}$$

Output y is calculated for each input x available in dataset for training (sample dataset shown in Fig. 2-5), and mean square error (MSE) is calculated as,

$$MSE = \frac{\sum_{i=1}^{n} (y_i - D_i)^2}{n} \tag{2.17}$$

where n gives the total number of samples in dataset.

2.5.1 The Neuron

The neuron is the main element of neural network. It receives input from external world or from another neuron and sends output to the outer world or to another neuron for further processing. Inside the neuron there is an excitation function that

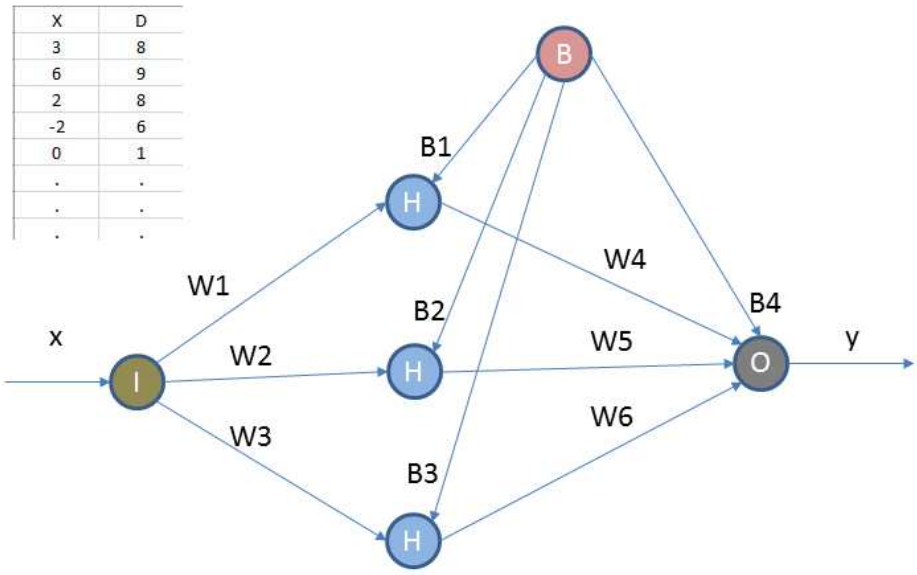

Figure 2-5: Example of Feed Forward MLP Neural Network.

might be linear, a threshold, and a sigmoid, which transforms input into output. Sigmoid transfer function is generally utilized in feed-forward MLP neural networks.

2.5.2 Input Layer

The input layer of neural network is the point in which the input data pattern is supplied. The input layer might contain more than one input neuron, and each input neuron should represent an independent feature that has significant effect in output produced. The input layer is connected to a hidden layer.

2.5.3 Output Layer

The output layer of neural network gives the output desired for which the network is trained. The number of output neurons might be different for different applications. The output is presented to outer world through output layer and it is connected to the hidden layer.

2.5.4 Hidden layer

The hidden layer does the main processing work and may have a large number of neurons based on the accuracy and computational efficiency desired. Neural networks may have more than one hidden layer to make the network more accurate and precise.

Chapter 3

Decision Support System for Material Selection and Real-Time Video Monitoring

This chapter provides the complete insight about the systems required for pharmaceutical compounding process for selected standard procedures. This includes how computational support could be provided to the existing CSP to reduce error, how to enhance working efficiency and how to promote a patient's health with low investment. It also debates the proposed system with previously existing semi-automatic and fully automated systems that are very costly and hardly integrate with the current existing CSP process. The key factors that introduce the error in compounded product like contamination, wrong selection of medication and medical equipment, and following the wrong procedure are addressed in the proposed system. The proposed system comprises a GUI that is integrated with a barcode reader that helps to select the correct medicines required for compounding and gives warnings and suggestions to the technician if wrong material has been selected. In the background process, it also has a video monitoring system that works in parallel with a GUI and invigilates the compounding methods followed by the pharmacy technician and gives

warnings, suggestions, and stops the program if a critical error is encountered.

The complete system was tested for different medication orders (MO-1, MO-2, and MO-3), which involves preparation of different medicines using three general CSP procedures. In material selection, error regarding wrong item selection, expired medicine, insufficient items, etc. were successfully tested while in compounding procedure monitoring errors like missing cleaning of items, selecting wrong needle, missing certain critical step, putting needle in wrong order, forget to put syringe tip cap after preparation, etc. were deliberately made during compounding and were successfully detected in real-time.

The remainder of this chapter is organized as follows. Section 3.1 explains about material selection system and its contribution in error reduction. Section 3.2 explains the video processing systems and its importance in CSP. Section 3.3 discusses the detailed methodologies involved in material selection and video processing systems. Section 3.4 presents the experimental results for both systems and explanation about it, and lastly, brief conclusions are drawn in Section 3.5.

3.1 Introduction to Material Selection System

Generally, when a pharmacy technician receives the medication orders they do all necessary calculations, collect materials required for that specific medicine, place all these items in hood, and then finally start compounding. Due to humanly nature; they generally pick up the wrong medicine that looks similar, forgot to check the expiry date even for correct medicine, and/or do not collect all items required before starting compounding that leads to preparation of contaminated wrong medication, which is very dangerous when administered to the patient and could lead to fatal disease. Thus, the material selection system ensures the proper selection of items from store room to the LAFW compounding hood. It does not allow the technician

to start compounding until the previous necessary steps were accurately followed. It also provides the gesture controlled GUI to prevent errors from contamination. The GUI system is integrated with camera-mouse [24] to enable such feature. The material selection system GUI communicates with the video monitoring system to provide the synchronization between two cross platform systems.

3.2 Introduction to Video Processing System

Another important aspect of error introduction in CSP is due to following the wrong procedure during compounding. The pharmacy technician performing compounding is generally in a hurry and also exhausted, sometime forgetting to clean the IV Bag, Vial, ampule etc. The technician may also forgot to use the filter needle (ampule preparation), which is very critical mistake since the ampule has to be broken before it is injected into the IV bag and if the technician forgets to use a filter needle, small glass particles also go directly into the IV bag. Thus, based on normal compounding guidelines as explained in Chapter 2, we have selected the 3 most commonly used CSPs for analysis and research. They have several steps during the whole compounding process, but only vital 5-6 steps for each CSP were considered in the video processing system (VPS). The final working video processing system was developed by combining various constraints and limiting certain parameters in video acquisition and item placement area in order to work in real-time. The working principle of VPS is based on the detection of items (medicine and medical equipments) inside the hood and sequential detection of steps during the compounding process by allowing hand movements near the item placement area.

3.3 Methods and Materials

All experiments and testing were done in a horizontal laminar airflow hood that is approved, tested, and routinely used to train PharmD students to compound CSPs in an instructional compounding laboratory. The semi-automatic system developed and tested contains two separate interfaces equipped with required hardware. The system can be further divided into the following two major subsystems.

3.3.1 Material Selection System

The MSS is a barcode scanner subsystem comprising of a barcode reader (*Magellan 1100i Barcode Scanner, Datalogic ADC Inc., Eugene, OR*) along with a Graphical User Interface (GUI) (developed on Microsoft Visual Studio 13 using C# language) designed specifically for selecting materials such as ampules, vials, IV bags, needles, syringes, alcohol swab pad, etc. that are used to prepare a particular type of CSP [29].

The flowchart of the MSS is shown in Fig. 3-1. The MSS helps to select only the desired material needed for performing the compounding. The first step during MSS usage is to perform all necessary calculations and select the appropriate items from those available, based on the CSP required, according to the medication order that is received from the physician. After this, the compounding procedure is selected (such as "*Protonix reconstitution*"). The next step is to assemble and choose the material available on the shelves for compounding. When the item (medication or medical equipment such as syringe, needle, etc.) is scanned using the barcode scanner, the barcode will be read and the MSS will check and verify that the item as the correct one (or not) based on the technician's earlier selection of the compounding procedure. When a wrong item is chosen by the technician, the system will provide a vocal feedback message to the technician. Additionally, it will not allow the com-

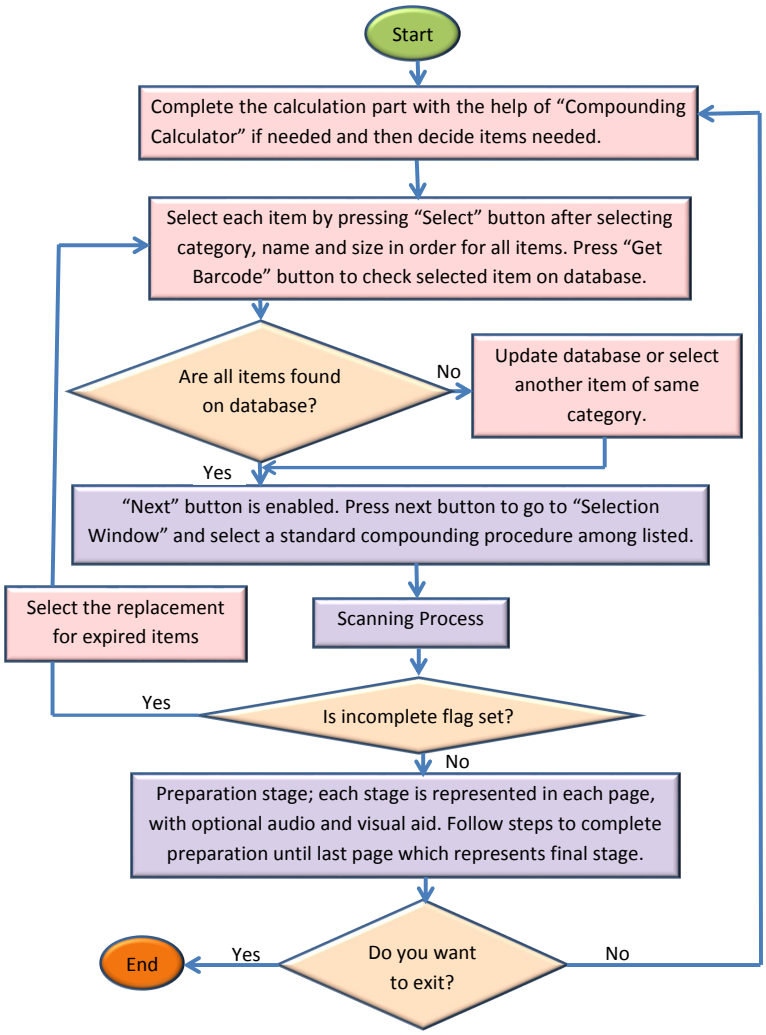

Figure 3-1: Flowchart of Material Selection System.

pounding process to proceed to the next step until the mistake is rectified. This is made possible by connecting the GUI with a backend database. The database stores information about the medication and medical equipment, including category, name, size, concentration, date of expiry, and the corresponding barcode. With the help of these fields, one can precisely select the correct medication and medical equipment through the GUI. Once all the correct items —including the correct medication, IV bag, and material such as needles, syringes, etc. —have been collected and staged in the Laminar Airflow Workbench (LAFW), the MSS proceeds to the next step in compounding. At this stage, the system also shows the actual procedure to be fol-

lowed in a sequential order from start to end, with appropriate audio and imagery related to a particular step on the GUI window so that the technician can see, hear, or read the compounding procedure. The technician has the ability to turn on the audio when the procedure text is displayed so as to enable the read-out-loud function when needed.

The MSS has the following seven elements as parts of the system.

3.3.1.1 Data Acquisition

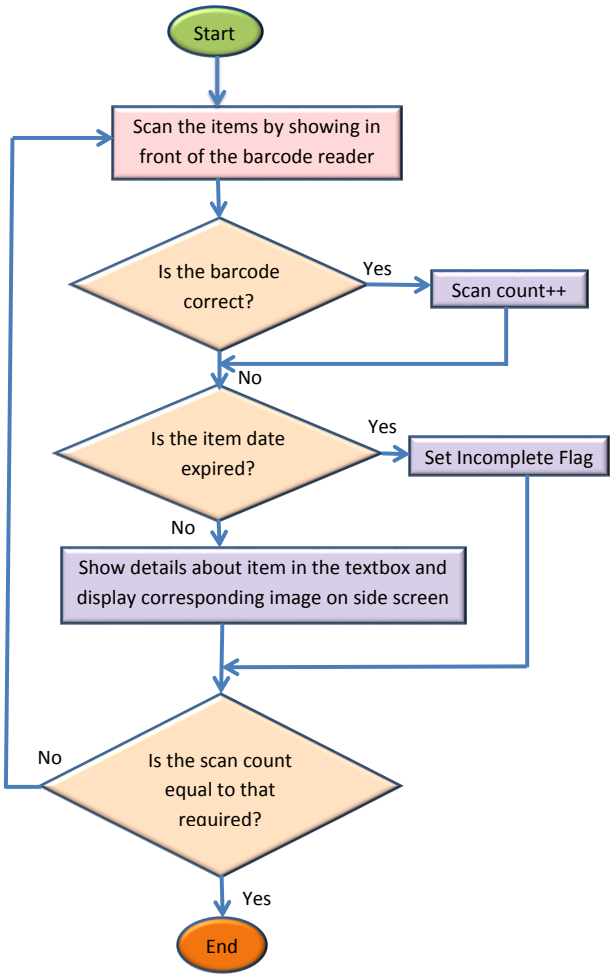

Figure 3-2: Flowchart of Barcode Scanning Process.

Data acquisition system for MSS is accomplished using a barcode reader. Bar-

codes have universally become a quick and easy method to identify different kinds of material in all walks of life. Due to the size, shape, and volume of medications and medical equipment, the healthcare field uses a very unique kind of barcode symbology. These barcode symbologies include linear 1D, stacked 1D, and 2D categories. The various types typically encountered are EAN-14, GS1-128 stacked, GS1-128 limited, GS1-128 truncated, GS1 data-bar, etc. The MSS employs a Magellan 1100i omni-directional presentation scanner manufactured by Datalogic S.p.A, Bologna, Italy. The scanner captures the image of the barcode using a high quality imaging sensor, decodes it using a barcode-decoding algorithm, and gives the barcode to a PC transmitted serially in a manner similar to that of a keyboard input. A flow chart of the barcode scanning process is shown in Fig. 3-2.

3.3.1.2 Compounding Calculator

The compounding calculator element was thought to be an essential part of this system since a large number of preventable medication errors from CSP's have been found to be due to a calculation-related or mathematical mistake [31, 32]. The starting window of the application has an embedded basic arithmetic calculator in which the technician can provide the dose required in milligrams (mg) and the concentration of medication in milligrams per milliliter (mg/ml). The volume of injection required to compound the CSP will be computed in milliliters. The calculation window is independent of the rest of the application program and uses a separate panel background color to denote a property.

3.3.1.3 Item Selector

The MSS has an item selector interface that contains category, name and size fields for quick and easy selection of material. A tree-based architecture was used in the database to store the properties of medications. This feature helps the interface

design to show only the names of the selected category and all the sizes of the selected name and category in a combo box. The user will first select a category such as vial, syringe, ampule, IV bag, etc. Subsequently, the combo box is updated and shows only those item(s) that match(es) the category previously selected in the category combo box. Then the user will select the next field which is the "name" in the name combo box. Following this, the size combo box is updated and displays available sizes that match with the previously selected category and name. At this stage the correct size can be selected. Thus the MSS leads and guides the technician to accurately and precisely select the desired medication and medical equipment.

3.3.1.4 Expiration Date-check

When a particular medication is selected the expiration date check automatically verifies the date of expiry. This is an important safety check point since medication past its expiration date may have its quality compromised and hence can adversely affect the health and safety of patients. If the selected item is expired then the technician will not be permitted to go beyond this point until that mistake is corrected. The expiration date-check compares the stored expiry date of a medication in the database with the date when the item is being selected for preparing a CSP and displays an appropriate recommendation.

3.3.1.5 Image Confirmation

When a particular item is selected, the image confirmation element in the MSS will display the corresponding image of that item on screen allowing the user to visually check and verify if correct item is being selected for use in the CSP. This feature is made possible in the interface by placing a link of the item image in the database so that the program will load an image based on the stored link when the item is selected.

3.3.1.6 Database Operation

The database used in this system is a local database connected to the MSS interface application using a connection string. The database has a table to store information about the medication, with columns that store information such as barcode data, category, name, image link, expiration date, and concentration in mg/ml. The table is organized in a manner such that columns contain discrete types of information while rows array the number of data stored in the database. There are basic buttons to add, edit and delete information from the database. New information will be automatically updated to every window when a change is presented.

3.3.1.7 Read-out-Loud and Visual-Aid

For a particular CSP preparation procedure, all critical and necessary steps are listed on various pages of a tab. Each page exhibits the steps in text format of sufficiently large and visible font size to be used after a previous step has been followed and concluded. These steps can also be read out loud with an optional speak button placed on each page. There is also a picture that displays each particular step on a side screen so that the technician can augment and crosscheck the activities being performed to the visual and audio.

3.3.2 Video Processing System

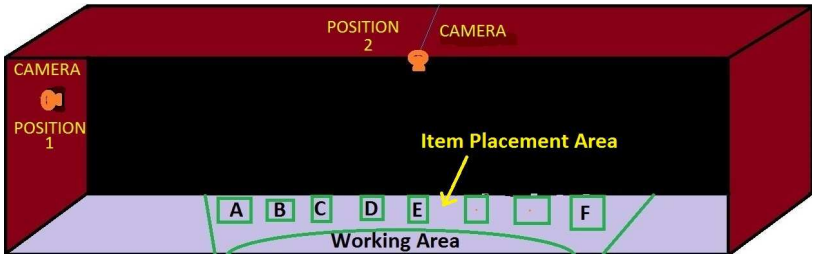

Figure 3-3: Schematic Diagram of Experimental Setup in LAFW.

Once the proper material has been selected using the MSS, the CSP compounding process can start. The primary objective of VPS is to analyze the technician's compounding procedure in real time to issue accurate and timely warnings when mistake(s) occur. The experimental and system setups (Fig. 3-3) that are needed to run the VPS in real time are enumerated below.

3.3.2.1 Video Acquisition and Preprocessing

Video acquisition for VPS is facilitated by the Image Processing and Computer Cision Toolbox in MATLAB. A digital camera (Webcam C615, Logitech, Newark, CA) is fixed to the LAFW at the proper orientation and connected to the computer interface. The real-time video feed is received in MATLAB program and the image frames are utilized for further processing.

Before applying any image and video processing algorithms, the image frame received from video is preprocessed, which includes the median filtering and histogram equalization as described in Section 2.3.1.

3.3.2.2 Weighted Frame Correlation Technique (VPS.01)

The camera position was fixed so that when compounding is performed, the images captured will have good spatial and temporal resolution. This arrangement helps to reduce the computational overhead to register the object position in new image frame. Video capturing generally occurs at 25 to 30 frames per second (fps), but in the VPS it was reduced to 10 fps by taking into consideration the fact that information will not change in the millisecond time range. The video has distinct sequential stages and is unique for each compounding procedure.

To compute the similarity of input video frames with previously defined stages, there are 25 images for each stage that are used as reference for correlation calculation. As we are considering 10 frames per second, the total window considers 2.5 seconds

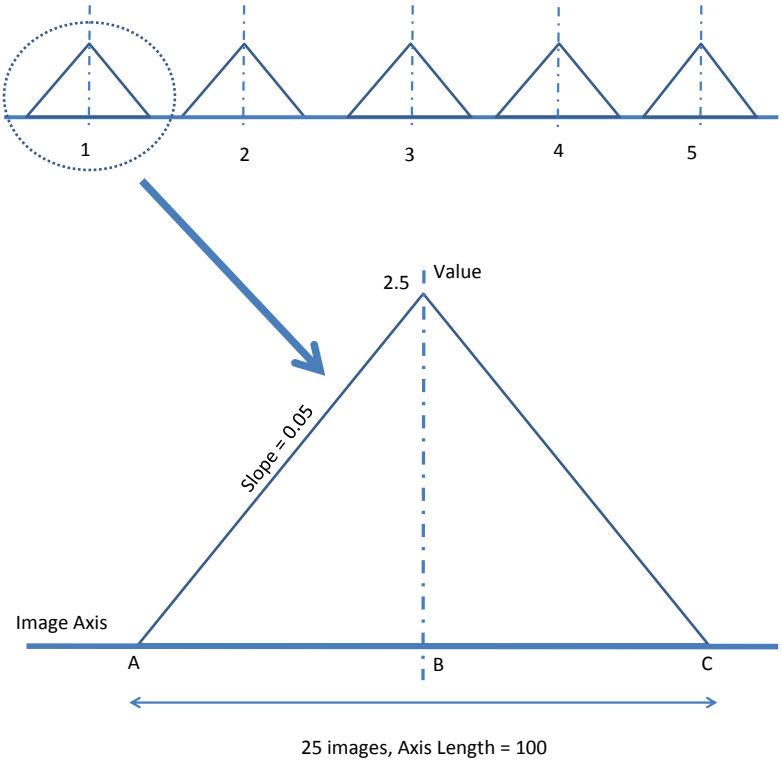

Figure 3-4: Window model for weighted frame correlation calculation (VPS.01).

of video for analysis as reference. The correlation values are filtered by the window, as shown in Fig. 3-4, and the cumulative similarity of the video frame to each stage is calculated. Whichever stage has the highest similarity value will be the most probable candidate for registration in the weighted frame correlation.

The flowchart of VPS.01 is shown in Fig. 3-5. The algorithm for weighted frame correlation decides which stage the current frame indicates based on similarity calculation and probability. Probability signifies the likeliness of occurrence of a particular stage based on the previous stage registered. For example, if stage 1 was registered previously, then it is highly probable that stage 2 will follow stage 1, so probability

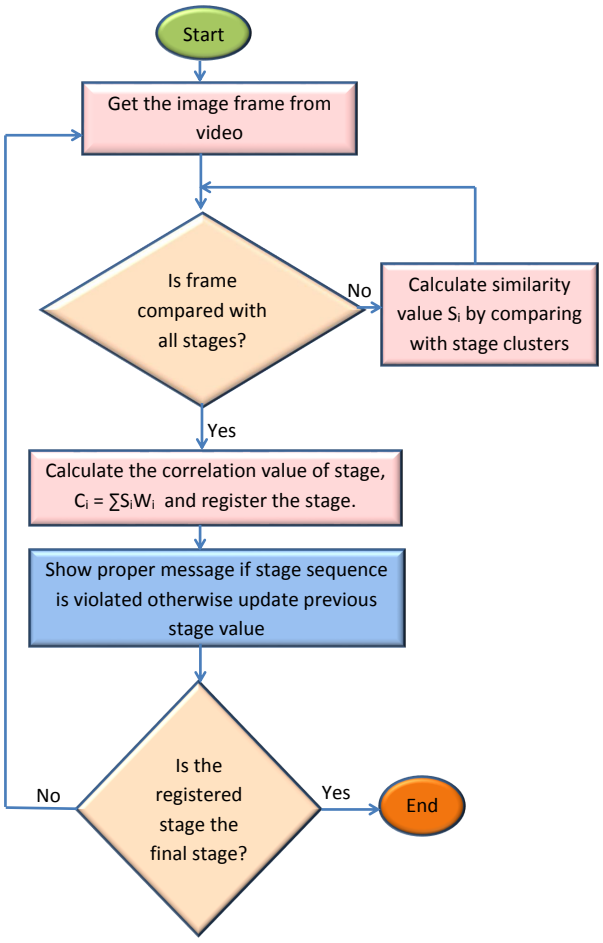

Figure 3-5: Flowchart of Weighted Frame Correlation Technique.

assignment for stage 2 at a time point immediately after stage 1 will be higher than for stages 3, 4, etc. Additionally, if a stage downstream has been registered at a particular time point, the probability of a stage upstream occurring at that same time point is zero. That is, if stage 3 was registered at a time point, it is not probable for events following stage 3 to be stage 2, 1, etc.

3.3.2.3 Component Detection Technique (VPS.02)

The approach discussed here is to detect various steps used during the compounding procedure in a sequential manner and analyze the steps to determine whether

steps are missed. The imaging region within the LAFW was confined to the field of view of the camera lens and had a finite boundary drawn along the region. The item placement areas were fixed within this region and referred to as the region-of-interest (ROI). This technique helps to reduce the search area for items placed within the area and enhances item recognition. To detect items such as an IV bag, ampule, vial, syringe, filter needle, regular needle, alcohol swab pad, etc., object detection using SURF (Speeded up Robust Features) was implemented [33]. SURF object detection helps to detect the template object in an image containing several objects. The detection scheme was implemented for each item that was going to be used during a compounding process. Thus, by applying object detection, we can obtain the position of each item and select the region of interest in the image frame based on the placement area of a particular item. The general flowchart of VPS.02 is shown in Fig. 3-6.

As an example, in the CSP preparation involving use of an injection ampule, the first activity is to clean the appropriate IV bag and ampule using an alcohol swab pad. First, the technician will pick the alcohol pad from the alcohol swab pad area and then clean each of these items. During video processing, the hand-movement near the ROI of alcohol pad is detected. When hand-movement in the alcohol swab pad area is detected along with movement in the IV bag region and ampule region, then it can be concluded that the compounding process is in the cleaning stage. Hence, if hand-movement is detected toward other items without having movement at the alcohol swab pad along with concurrent movement in the IV bag and ampule regions, then it can be inferred that the cleaning stage was omitted during the compounding process. This is a critical error during the preparation of a CSP. After cleaning the ampule and IV bag, the next step is to open the syringe and assemble the filter needle. To detect this stage, hand-movement in the syringe and filter needle ROIs were detected. The next step in the compounding process is the ampule breaking stage. Applying

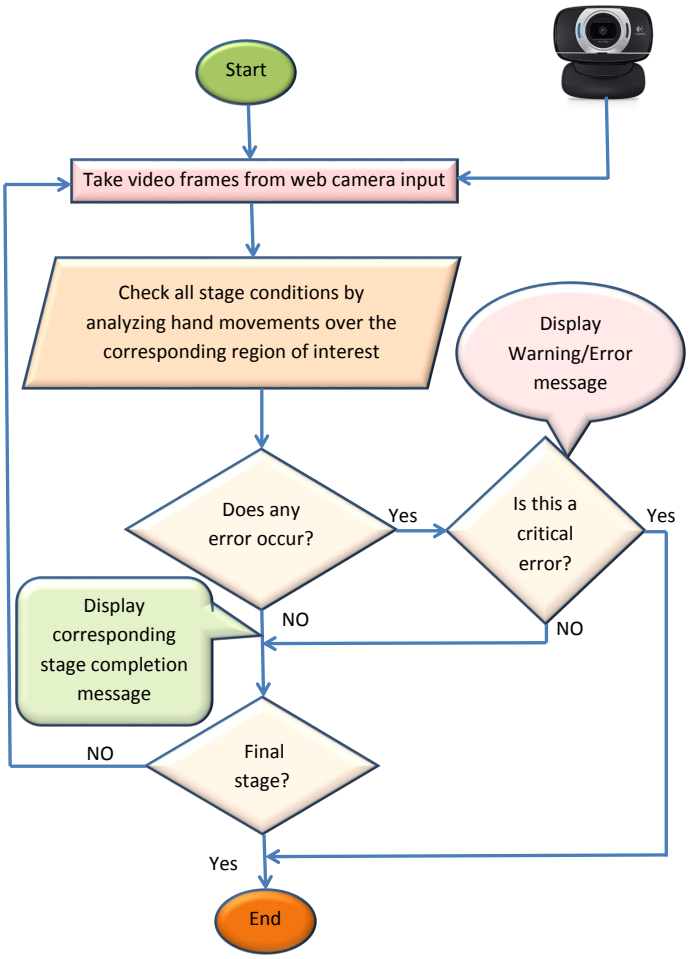

Figure 3-6: Flowchart of Component Detection Technique.

similar logic as described above during each stage, the progress of the compounding process was estimated during the entire compounding process.

3.3.2.4 Modified Component Detection Technique (VPS.03)

The principal time-consuming process in the component detection algorithm described above was the proper detection of each item inside the LAFW. The rest of the processing absolutely relies on the perfection of this detection. The items used during compounding are small and can be placed in any orientation in the LAFW. This warranted extracting and comparing features from several different samples of

a particular item, with the image frame captured as video via the digital web-cam for detection of that particular item. The size of the sample population determines the accuracy of detection and the processing time. This led to significant lag time in processing and updating the progress of the compounding procedure. Hence, the implementation and running of the component detection part of the system was not realized in real time. In the modified component detection technique, to reduce the processing time for item detection, the search zone for item detection was limited by creating marked rectangular areas inside the LAFW. Only one particular type of item can be placed in each rectangular area, as indicated by A-F shown in Fig. 3-3. This minor modification of limiting the random positioning of items substantially reduced the detection time, and the algorithm was realized in real time.

3.3.2.5 Robustness of VPS.03

The ability of the system to detect errors made during the compounding process was tested by deliberately making mistakes during the compounding process. Some common mistakes were recorded for the three standard compounding procedures used in this system. The mistakes that were made are skipping cleaning stage, not using filter needle, not using regular needle, not using medication, and not following the correct sequence of events in a particular procedure.

3.4 Experimental Results

The medication order for each CSP was processed in a manner identical to how it will be handled in the IV compounding room of an in-patient hospital pharmacy. One CSP was compounded at a time, and the procedure started with the material selection being tracked by the MSS, followed by the compounding process being monitored by the VPS. The entire compounding procedure was performed with the implementation

of various algorithms. The results from MSS were recorded by capturing screenshots of the computer GUI in the proper sequence. The VPS performed video processing by implementing various algorithms when the CSP(s) such as ampule preparation, powder for reconstitution, and liquid injection vial were made in the LAFW.

3.4.1 Material Selection System

A typical workflow during the material selection stage for preparing a CSP is shown in Fig. 3-7. The example shown in the Fig. 3-7 is the preparation of a labetolol injection. The items are selected first (Fig. 3-7(a)), followed by the relevant procedure, as shown in Fig. 3-7(b). Following this, the combo-box automatically enables selecting the first appropriate item that is needed to perform this compounding. In Fig. 3-7(a), the item "syringe" is displayed under the category, followed by the name "luer-lock with needle", and size/volume "3 ml" fields. In this manner, other items needed for compounding this CSP were selected including the syringe, sterile syringe tip cap, injection vial, and alcohol swab pad. After this, the items were gathered and scanned by clicking the "get barcode" button and bringing each item to the sensor of the barcode scanner (Fig. 3-7(c)). When each item is scanned, its image will be displayed as is shown in the case of the needle and the labetalol vial is shown in Fig. 3-7(d) and (e), respectively. Additionally, information coded in the barcode will be displayed in a box as well. Fig. 3-7(f) also shows an example of an error message that is displayed when an item was scanned that does not match the material previously selected for that particular CSP. The MSS window shown in Fig. 3-7(a) also shows the compounding calculator, which was used to calculate the volume of the injection that will provide the dose required for a patient, according to the medication order.

An example CSP in which this feature was used is the labetolol injection that was withdrawn into a 3 ml syringe and capped with sterile syringe tip cap. According

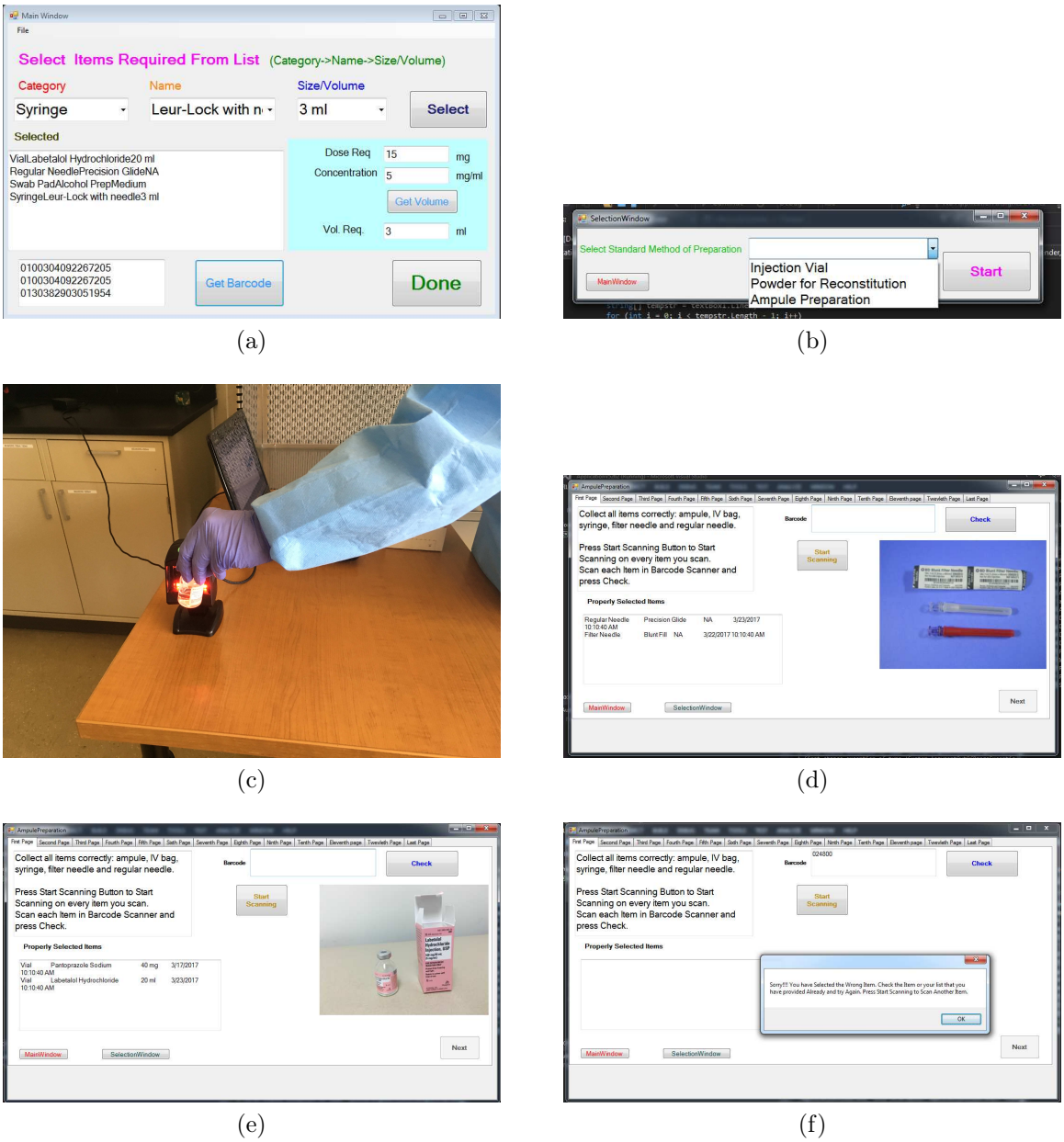

Figure 3-7: Output screenshots of MSS; (a) all selected items shown on screen with barcode, (b) Selection of standard compounding procedure, (c) item shown in front of barcode scanner, (d) showing scanned result for needle, (e) Showing scanned result for labetolol, and (f) Error message for wrong selection of item.

to the product label, the labetolol injection is available in a concentration of *100 mg/20 ml*, and the dose required in the medication order was 15 mg. The dose required was typed into the "dose required" box, and the concentration of the injection that was used in the compounding was provided in the "concentration" box (Fig. 3-7(a)). Following this, when the "get volume" button is clicked, the "volume req" window displays the volume of injection that is to be used in the CSP as 3 ml. This process will help to eliminate numerous errors that are typically observed in the CSP compounding setting, such as using wrong items for compounding, using the wrong procedure when preparing the CSP, and miscalculating the volume of injection needed to supply a dose in the CSP. The MSS functioned flawlessly during the compounding of all three CSP's prepared in this work.

3.4.2 Video Processing System

3.4.2.1 VPS.01

The Phenergan infusion CSP (MO-1) was selected to test the VPS.01 since it had the highest number of manipulations and steps involved during preparation. The camera fixed in position 1, as shown in Fig. 3-3, collected the video. The five major stages and the corresponding abbreviations used in Table 3.1 during Phenergan infusion preparation are: 1. cleaning stage (CS) –during this stage, the ampule and the compounding port in the 50 ml normal saline IV bag are cleaned; 2. opening syringe and needle stage (OSNS) –during this stage, the syringe and filter needle are taken out of the plastic wrapping material and the needle is attached to the syringe; 3. ampule break stage (ABS) –during this stage, the ampule is broken using proper technique; 4. changing needle stage (CNS) –during this stage, the filter needle is removed from the syringe that contains injection withdrawn from the ampule and a regular needle is attached to the syringe; and 5. injection into IV bag Stage (IIBS)

–this is the final stage of the CSP preparation when the injection in the syringe is slowly injected into the 50 ml NS IV bag through the compounding port. Image frames obtained from the video camera were fed into VPS, which calculated the correlation value of a current image frame when compared to each of the five stages described above using the filter window, as shown Fig 3-4. Results obtained from three trials are shown in Table 3.1. The correlation values obtained for each stage are similar within a particular test trial, but the value for a particular stage fluctuated among the three test trials. This led to improper and erroneous identification of the stage of infusion preparation. As an example, in test trial 1, the wrong stage was identified two times: once when the actual stage was ABS, it was wrongly identified as CNS, and the other mistake was when the IIBS stage was wrongly identified as CS. These two errors brought the accuracy of the VPS.01 down to 60 in test trial 1. The overall accuracy in the stage classification on all three trials was found to be 53.3 % $\pm$ 11.5 %, which is low and insufficient to make it applicable on a CSP decision support system.

The poor accuracy of VPS.01 was attributed to the camera position and the nature of the algorithm used to classify stages. Camera position 1 (Fig. 3-3) gave an angular side view of the compounding area and the items placed and used there. The algorithm used in VPS.01 uses the correlation between the whole image frame of a particular current image and reference images of each stage. During the compounding process, successive image frames had only small differences, leading to similar correlation values for each stage. This led to poor discretion between various compounding stages. Additional tests were performed after moving the camera to position 2 (Fig. 3-3), but only marginal improvement in accuracy was observed. It was during this stage that it was noted that the processing time using VPS.01 was high and did not allow for implementation of this method as a DSS in real time. However, the algorithm did yield promising results with slight modifications, but the results and decision regard-

Table 3.1: Correlation values of different stages and accuracy of VPS.01.

Trial	Observed Stage in Video	Stage Detected By System	Correlation Value	Accuracy (%)
	CS	CS	12.54	
	OSNS	OSNS	11.32	
1	ABS	CNS	10.54	60
	CNS	CNS	12.45	
	IIBS	CS	10.69	
	CS	CS	13.12	
	OSNS	ABS	11.25	
2	ABS	CNS	11.68	60
	CNS	CNS	12.65	
	IIBS	IIBS	12.47	
	CS	CS	13.55	
	OSNS	OSNS	12.35	
3	ABS	CNS	11.56	40
	CNS	ABS	10.98	
	IIBS	CS	11.67	

ing the compounding process were obtained after completion of the CSP preparation. Thus, it was concluded that VPS.01, with some more modifications, may be useful when evaluating the compounding skills and technique of technicians or students in a training or educational laboratory.

3.4.2.2 VPS.02

The low accuracy of VPS.01 led to the use of video acquisition orientation and the use of a component detection algorithm in compounding procedure monitoring. The camera position was fixed at position 2 in VPS.02. From the new camera position, better quality video and images were captured that enabled better differentiation between various items used in the CSP compounding process. In VPS.02, rather than analyzing the whole image, the algorithm focuses on detecting each component (item) used in compounding and detects compounding stages based on whether that particular component (item) is utilized by the technician. When the system starts, VPS.02

first detects all the items required to prepare the CSP placed inside the hood with multiple scanning until it detects all the components. During the scanning, the region property (area and centroids) of each detected item is obtained. After all components placed inside the hood are detected, appropriate messages and warnings, when applicable, were displayed based on items being utilized during the compounding stage.

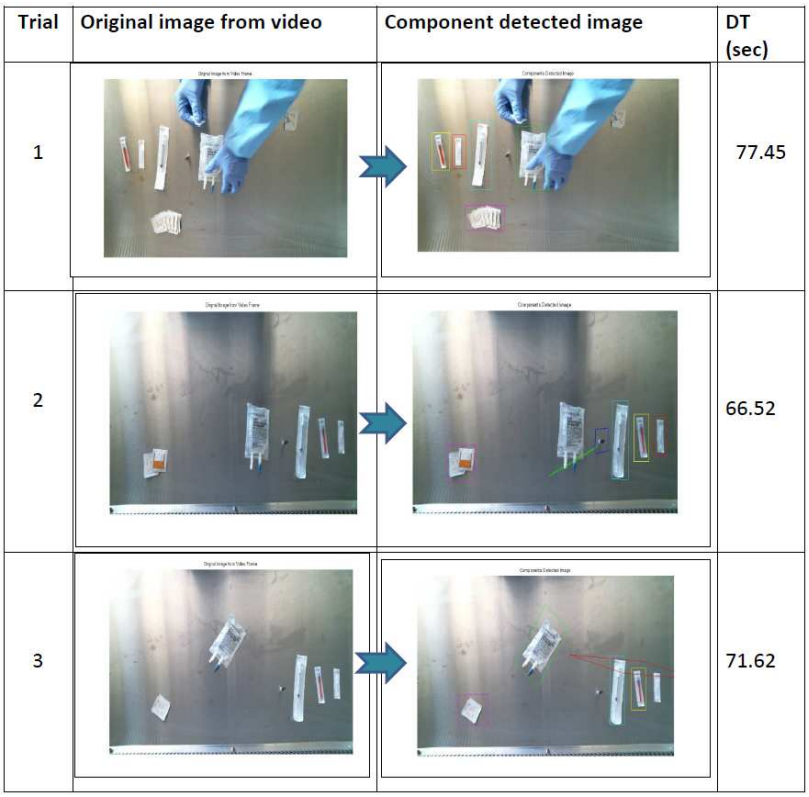

Figure 3-8: Component detection and detection time (DT) of VPS.02 (MO-1).

The component detection stage in VPS.02 was accomplished using the surf detection technique, as shown in Fig. 3-8. In this method, the items were placed randomly inside the LAFW in the item staging (placement) area that was in front of the working zone, as shown in Fig. 3-3. During trial 1 of ampule preparation, as in Table 3.2, all items except the ampule were detected. Detected items were indicated on the computer screen by rectangular boundaries of varied colors around the item. As shown in Fig. 3-8, yellow, red, cyan, green, purple, and blue were used to represent the filter needle, regular needle, syringe, IV bag, and ampule, respectively. During

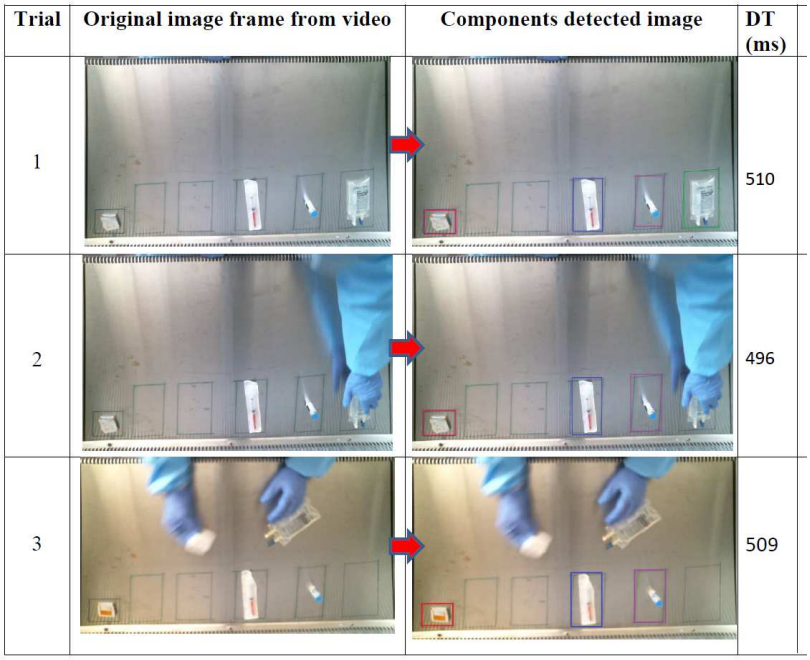

Figure 3-9: Component detection and detection time (DT) of VPS.03 (MO-3).

the three trials, trial 1 failed to detect the ampule (1 item), trial 2 failed to detect the IV bag (1 item), and trial 3 failed to detect the ampule and the regular needle (2 items) (Table 3.2). If we consider all three trials together, it may be concluded that all the items were successfully detected, but there was still the likelihood of at missing at least one item during a particular compounding process. All items placed inside the LAFW have to be detected by the VPS.02 to monitor and evaluate the compounding process and to function as a real-time decision support system. Since the objective of the research is to develop DSS in real time, detection time (DT) makes this algorithm not suitable to implement in VPS. The average detection time (DT) for a particular item during a single scanning in VPS.02 was found to be 71.9 $\pm$ 5.5 secs. It was also found that the VPS.02 required at least five scans to completely detect all items in the LAFW, contributing to a total DT of approximately 6 minutes during the detection stage of the process. We estimated that to implement VPS.02 in real time, the detection process should at least be completed within 5 secs from when VPS starts. This estimate was based on the observation that it generally took

Table 3.2: Components detection for 3 trials in VPS.02.

Trial	Items on image frame	Items detected by system	Number of items missed (Total items = 6)
1	Filter Needle, Regular Needle, Syringe, Ampule, IV Bag, Swab Pad	All items detected except Ampule	1
2	Filter Needle, Regular Needle, Syringe, Ampule, IV Bag, Swab Pad	All items detected except IV Bag	1
3	Filter Needle, Regular Needle, Syringe, Ampule, IV Bag, Swab Pad	All items detected except Regular Needle and Ampule	2

about 5 secs from the time the camera started to when the technician actually began preparing the CSP using the items placed in the LAFW. Thus, the delayed DT did not allow for using VPS.02 to provide real-time support during the compounding process. However, VPS.02 can still be used to analyze and evaluate a pre-recorded video of the compounding process. Based on the results obtained from VPS.02, the process and algorithm were modified to develop VPS.03.

3.4.2.3 VPS.03

An important change that was made in VPS.03 was that the item placing area in the LAFW was limited by drawing rectangular boxes using a green colored marker inside which a particular item had to be placed before the compounding started (Fig. 3-3, boxes labeled A to F). In this configuration, the items were placed in the assigned specific rectangular areas before the compounding process started. The rectangular areas now limited the position and orientation of items, as shown in Fig. 3-9. The pictures on the left side of the figure represent the items in the LAFW before

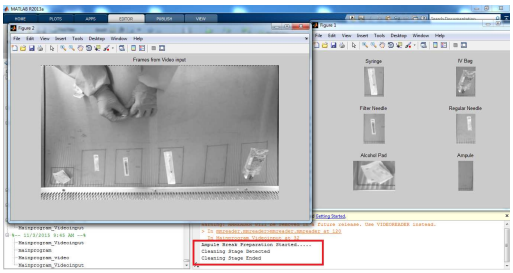

(a)

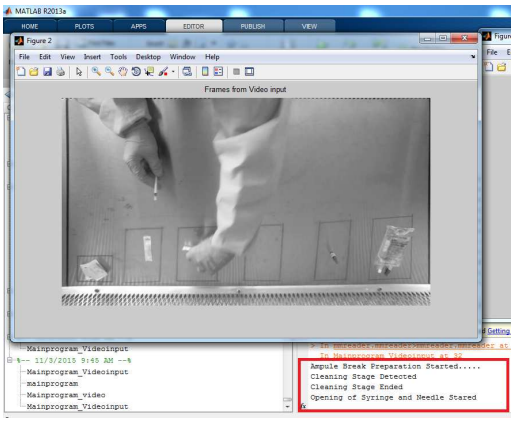

(b)

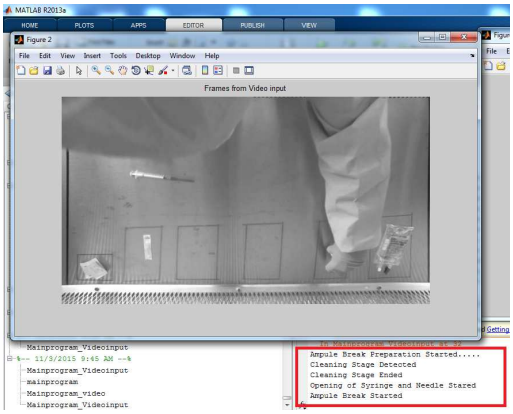

(c)

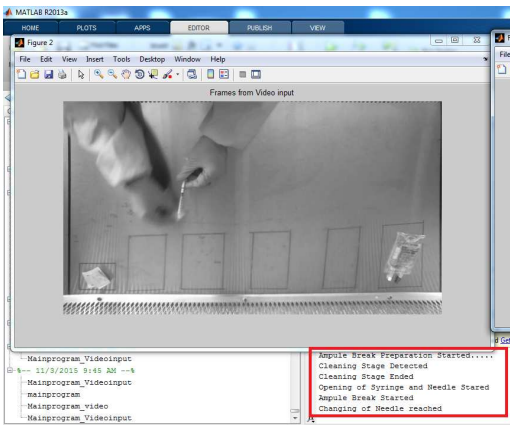

(d)

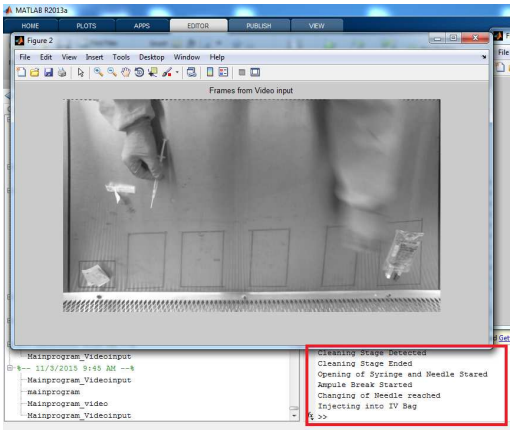

(e)

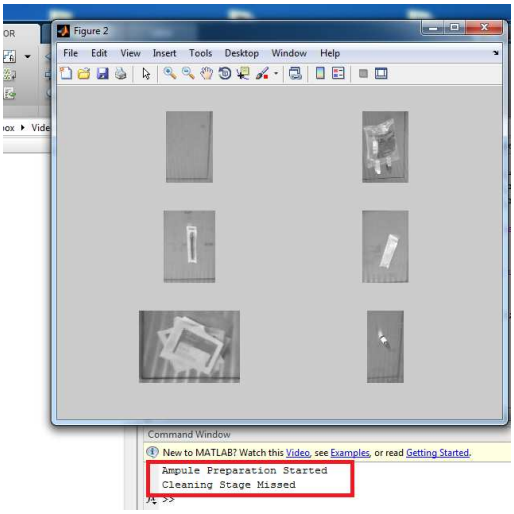

(f)

Figure 3-10: Output screenshots of VPS.03 of MO-1; (a) cleaning stage reached, (b) opening of syringe and needle stage, (c) breaking of ampule stage, (d) changing of needle stage, (e) injecting medicine into IV bag, and (f) cleaning stage missed (mistake).

Table 3.3: Summary of the results from VPS.03 for MO-1.

Compounding Process	Tests	Descriptions	Results
Ampule Preparation	Experiment I (Preparation of MO-1 without any mistakes)	Compounding was performed 3 times without making any mistakes from technician to evaluate accuracy of the system	All the stages for ampule preparation were detected without any error during all three trials
	Experiment II (Preparation of MO-1 with possible mistakes)	Compounding is performed under identical environment as in Experiment I. Mistakes are introduced deliberately during the compounding process. a. Missing Cleaning Stage b. Not using Filter Needle c. Not using Regular Needle d. Injecting into IV Bag without drawing medicine from ampule	All the errors introduced were detected and program gave warning message "Cleaning Stage Missed" for (a), "Medicine not used" and stopped program instantly for (d) while continued program till end for (b) and (c).

detection, while those on the right side show items after the detection was completed. When detection is completed, a colored rectangle will appear in the computer screen surrounding the object that was digitally detected. This process is identical to that described under VPS.02. Fig. 3-9 shows the detection of items needed for MO-3 placed inside the LAFW. During the three trials, perfect detection of all the items was observed (Fig. 3-9).

Additionally, the detection time for compounding MO-3 was reduced to 505 $\pm$ 7.8 ms, making VPS.03 realizable in real time. Additionally, the detection times for MO-1 were 516 $\pm$ 9.1 ms and for MO-2 were 491 $\pm$ 10.6 ms. Although the position and orientation of items placed inside the LAFW had to be specifically set

Table 3.4: Summary of the results from VPS.03 for MO-2.

Compounding Process	Tests	Descriptions	Results
Injection Vial	Experiment III (Preparation of MO-2 with no mistakes)	Compounding was performed 3 times without making any mistakes	All the important stages in injection vial were detected in every trials.
	Experiment IV (Preparation of MO-2 with possible mistakes)	Compounding was performed under similar environment as in Exp. III. Following mistakes were introduced: a. Cleaning stage Missed b. Syringe tip cap not used	During compounding process following messages were produced: a. "Cleaning stage missed" and program aborted instantly. b. "Syringe tip cap not used" and program aborted instantly.

in VPS.03, this arrangement made the program provide real-time support during the compounding process. During preliminary testing with the MO-1 preparation, VPS.03 demonstrated high accuracy, excellent robustness, and the ability to provide real-time decision support during the compounding process. Hence, VPS.03 was tested systematically by implementing it during the preparation of MO-1, MO-2, and MO-3. The CSP required according to each medication order was prepared three times, and the compounding process was monitored and evaluated in real time during the process.

Fig. 3-10 shows data from VPS.03 when MO-1 was prepared. Fig. 3-10(a) shows the detection of the cleaning stage, and the text highlighted with the red box within the screenshot indicates the prompt that the technician will be able to see, showing successful completion of the cleaning stage. Fig. 3-10(b) shows the

Table 3.5: Summary of the results from VPS.03 for MO-3.

Compounding Process	Tests	Descriptions	Results
Powdered Reconstitution	Experiment V (Preparation of MO-3 with no mistakes)	Compounding was performed 3 times without making any mistakes	All the important stages in powdered reconstitution were detected perfectly in every trials.
	Experiment VI (Preparation of MO-3 with cleaning mistakes)	Compounding was performed under similar environment but cleaning stage was deliberately missed	Program started normally and gave "Cleaning Stage Missed" message when technician went for syringe without using swab pad and program aborted instantly.

stage when the filter needle is attached to a 1 ml syringe, Fig. 3-10(c) shows the Phenergan ampule breaking, Fig. 3-10(d) shows filter needle being switched with regular needle, and Fig. 3-10(e) shows the completion of the compounding process when the injection in the syringe is introduced into the IV bag. At each stage, the text highlighted with a surrounding red box displays the message corresponding to the successful detection of a particular step during the compounding process. MO-1 was repeated three times, and Table 3.3 summarizes the key findings during each experiment. As can be seen from the table, Experiment I, which was a preparation of MO-1 (without any mistakes), was accurately detected, monitored, and evaluated in real time throughout various stages of compounding.

Fig. 3-11(a) displays the screenshot data during the first step of MO-2 compound-

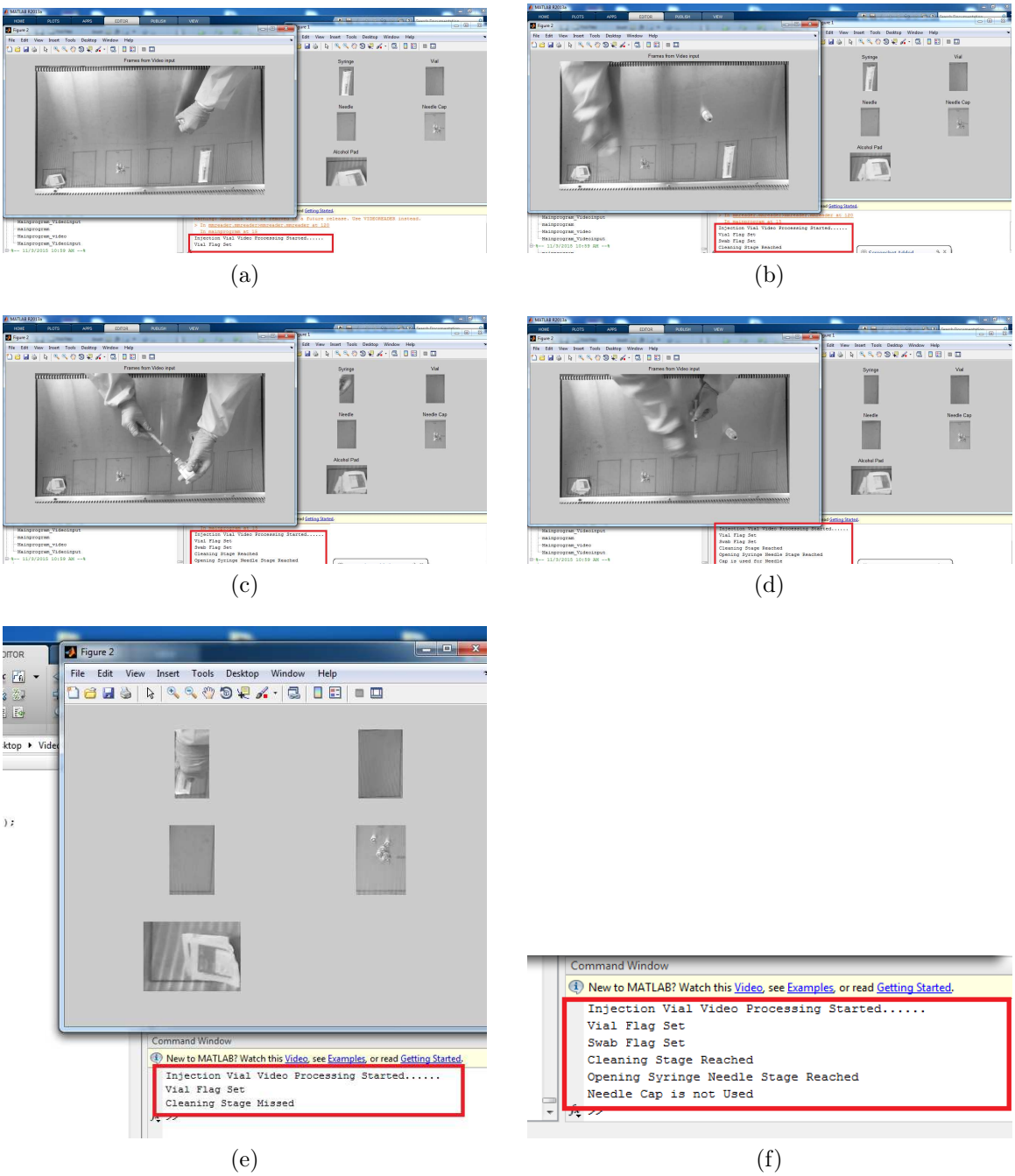

Figure 3-11: Output screenshots of VPS.03 of MO-2; (a) Picking up vial for cleaning, (b) Cleaning stage reached, (c) opening syringe and needle to get medicine from vial, (d) syringe tip cap used at the end of procedure, (e) cleaning stage missed (Mistake - 1), and (f) message box enlarged, syringe tip cap is not used at the end (Mistake - 2)).

ing. In this picture, the labetolol vial is picked up for cleaning followed by completion of the task, as is shown in Fig. 3-11(b). In Fig. 3-11(c), the 3 ml syringe and 11/2 inch 18 G needle assembly are used to draw the required volume of injection from the vial. This is followed by the final step wherein the needle was removed and a sterile luer-lock syringe tip cap was attached to the syringe, as shown in Fig. 3-11(d). The summary of observations made during MO-2 compounding is shown in Table 3.4 in the row titled "Experiment III".

Fig. 3-12(a) shows the IPA swab pad being picked to clean the IV bag when the compounding of MO-3 started. Subsequently, in Fig. 3-12(b), the cleaning stage was detected. After this step, the needle was assembled onto the 10 ml syringe detected in Fig. 3-12(c), and the syringe-needle assembly was detected being used to draw the proper volume of liquid from the 100 ml normal saline IV bag in Fig. 3-12(d). The liquid in the syringe was used to reconstitute protonix powder in the vial shown in Fig. 3-12(e), and the concluding step in this process occurred when the reconstituted (dissolved) protonix was injected into the IV bag in Fig. 3-12(f). The key findings during the compounding of MO-3 are shown in Table 3.5 along the row "Experiment V". VPS.03 functioned flawlessly when MO-3 was compounded.

3.4.2.4 Robustness of VPS.03

VPS.03 was able to perform flawlessly and provide real-time monitoring of the compounding process. Its ability to warn the technician when a mistake/error was made during compounding was tested by deliberately making some common compounding mistakes when each CSP was compounded. Several errors were made when MO-1 was compounded, and in Fig. 3-10(f), the screenshot data shows when the cleaning stage was missed during CSP preparation. The dialog box in the middle of the screenshot image displays all the items that were detected at that particular time. The 50 ml normal saline bag, the filter needle, the regular needle, IPA swab pad, and

Figure 3-12: Output screenshots of VPS.03 of MO-3; (a) alcohol swab pad used for cleaning IV bag, (b) vial picked for cleaning (Cleaning Stage), (c) opening syringe and needle to get liquid from IV bag, (d) picking IV bag to get liquid, (e) picking up powder vial to inject liquid inside, and (f) mixed solution finally injected back into IV bag.

the promethazine HCl ampule are visible in the picture. However, the technician picked up the 1 ml syringe (missing in the picture) first without cleaning the ampule and the compounding port in the IV bag. This led to the algorithm to detect that the cleaning step was missed and the warning message "cleaning stage missed" was shown as in the text highlighted with a red box in the picture. This mistake was made during three trials when the CSP was compounded, and each time the mistake was made, VPS.03 detected the mistake and warned the technician with the message "cleaning stage missed". Other mistakes that were made when the Phenergan infusion was being compounded are the filter needle not being used, filter needle not being switched to a regular needle when the injection in the syringe was injected into the 50 ml NS IV bag, and the drug ampule itself being missed during CSP preparation. A filter needle has to be used when liquid injections are withdrawn from a glass ampule into a syringe. This precautionary measure will prevent any small pieces of glass that may dislodge and fall into the liquid inside the ampule while it is opened. If a filter needle is not used, then small glass pieces can be taken inside the syringe along with the injection liquid and eventually reach the patients body when the injection is administered. After withdrawing the injection from an ampule into a syringe using a filter needle, the filter needle has to be removed and a regular needle attached to the syringe before injecting the liquid inside the syringe into the IV bag. This switching will prevent any glass pieces or other debris that may be filtered by the filter needle when the injection is withdrawn into the syringe from being injected into the IV bag. All the errors were detected as the mistakes were committed during the compounding stage.

This information is summarized in Table 3.3 in the row titled "Experiment II". Similar mistakes were made intentionally, such as missing the cleaning stage and not using the luer-lock syringe tip cap when MO-2 was compounded. Fig. 3-11(e) shows the screenshot image of data from when the cleaning stage was missed during

MO-2 compounding. During compounding of any CSP, after the items required for a particular CSP are placed in the IV hood, the compounding port of the IV bag, vial top, and ampule as applicable are cleaned using an IPA swab pad. This step is necessary to prevent any dust or other contaminant from entering the final compounded CSP. At all times, when the cleaning stage was missed, VPS.03 detected the error and displayed the warning message as shown in Fig. 3-11(e). MO-2 was for a labetolol injection, which in this case was to be administered as an IV push injection typically administered to a patient through a cannula inserted in a patient. When this injection is compounded in the IV room of an in-patient hospital pharmacy, the required volume of the injection is withdrawn into an appropriate syringe, the regular needle is removed, and the syringe closed by using a luer-lock syringe tip cap before dispensing. The syringe tip cap prevents any spillage from the syringe and inhibits contamination. When the luer-lock syringe tip cap was intentionally missed during MO-2 compounding, VPS.03 detected this error and displayed the error message, as shown in Fig. 3-11(f). Similarly, one mistake was made during the compounding of MO-3. The summary of observations of mistakes made during the compounding of MO-2 is given in Table 3.4 in the row titled "Experiment IV", and that made during the compounding of MO-3 is given in the Table 3.5 in the row titled "Experiment VI". As was observed during robustness testing of VPS.03, all the errors were detected in real time, and relevant warning messages were displayed when a particular error was detected.

3.5 Conclusion

A computational decision support system for use during preparation of compounded sterile preparations comprising of two main components, including material selection system (MSS) and video processor system (VPS), was successfully developed

and tested. The MSS consisted of a barcode reader and GUI. The MSS enabled proper identification and selection of items and components required to compound a particular CSP. The seven unique elements constituting the MSS, such as compounding calculator, item selector, expiration date-check, image confirmation, database operation, read-out loud and visual-aid, and barcode reader, were optimized during the development stages and functioned without any errors during implementation and testing. The algorithms related to the MSS were modified and rearranged as needed to produce the final version. Three different versions of the VPS, named VPS.01, VPS.02, and VPS.03, were developed sequentially to accommodate shortcomings of a previous version. VPS.01, using the weighted frame correlation technique, could not be implemented in real time due to certain deficiencies such as detection errors and unsuitable detection times. VPS.02 used the component detection technique but suffered delays in detection due to the lag time associated with video capture and the SURF detection technique. The final optimized VPS.03 utilized a modified algorithm and technique of that used in VPS.02 and successfully detected, monitored, and evaluated the compounding of three CSPs in real-time. VPS.03 also detected various compounding errors that were deliberately made during the CSP compounding stages. A system similar to that presented in this work is not currently available in training, educational, or practice settings. Additional systematic and elaborate experimentation with VPS.03 will allow use of this computational decision support system in the CSP preparation environment.

Chapter 4

Leur-lock Syringe Classification and Volume Measurement System

Decision support system for compounded sterile preparation is explained detailed in Chapter 3. In Chapter 3, the research is focused basically on two stages; the first is to make sure that all the medicines and medical equipment's which are brought to LAFW compounding after necessary calculations are correct (explained by MSS), and the second makes sure that the pharmacy technician compounding the medicine follows the correct procedure (explained by VPS). However, the VPS do not check for the volume of medicine drawn into the syringe and/or injected from the syringe. Along with correct item selection and compounding procedure, volume of medicine inside syringe after final preparation or volume of medicine before injecting into the IV bag is also a crucial factor in CSP. Thus, this research will now focuses on how to give feedback about the correctness of medicine inside syringe during compounding.

The proposed system integrates the extra web camera along with the web camera for VPS at suitable location, which classifies and gives the volume measured to the technician by implementing image processing algorithms. Generally, the syringe utilized in compounding ranges from 1 ml to 50 ml; hence, it is necessary to first classify which syringe is used during compounding, which affects the correctness of volume

drawn and/or injected during compounding. Thus, the system proposed first classifies the syringe used and measures the precise volume (more than 95 % accuracy) of medicine inside syringe.

The remainder of this chapter is organized as follows. Section 4.1 gives the idea about syringe classification system and how it is necessary to provide robustness to the system. Section 4.2 discusses how result obtained from Section 4.1 are utilized to measure the volume of medicine inside the syringe using ANN(s). Section 4.3 provides an overview of how the research was conducted, materials utilized for research, and methods implemented for classification and measurement systems. Section 4.4 explains the results of the research presenting a brief introduction about the result, and lastly, conclusions are drawn in Section 4.5.

4.1 Syringe Classification System

As explained in Chapter 3, CSP involves various compounding procedures and requires different medical equipment like syringe, needle, swab pad, etc. Among the listed syringes, they generally comes with different sizes for different preparations. The size of the syringe is selected based on the medication order so that we have a possible available resolution during compounding. For instance, the syringe utilized in MO-1 is 1 ml syringe, since the volume that has to be measured is less than 1 ml (1 ml denotes the maximum capacity of the syringe). However, 3 ml syringe is utilized in MO-2 because volume needs to be measured is greater than 1 ml. Thus, selection of syringe is based on the volume of medicine that has to be drawn by syringe obtained after necessary calculations. If 2.5 ml volume of medication needs to be drawn, the 3 ml syringe is used rather than 5 ml syringe to have best resolution.

Syringes generally utilized in CSPs are 1 ml, 3 ml, 5 ml, 10 ml, 20 ml, 30 ml and more. Thus in order to measure the volume inside syringe precisely it is necessary to

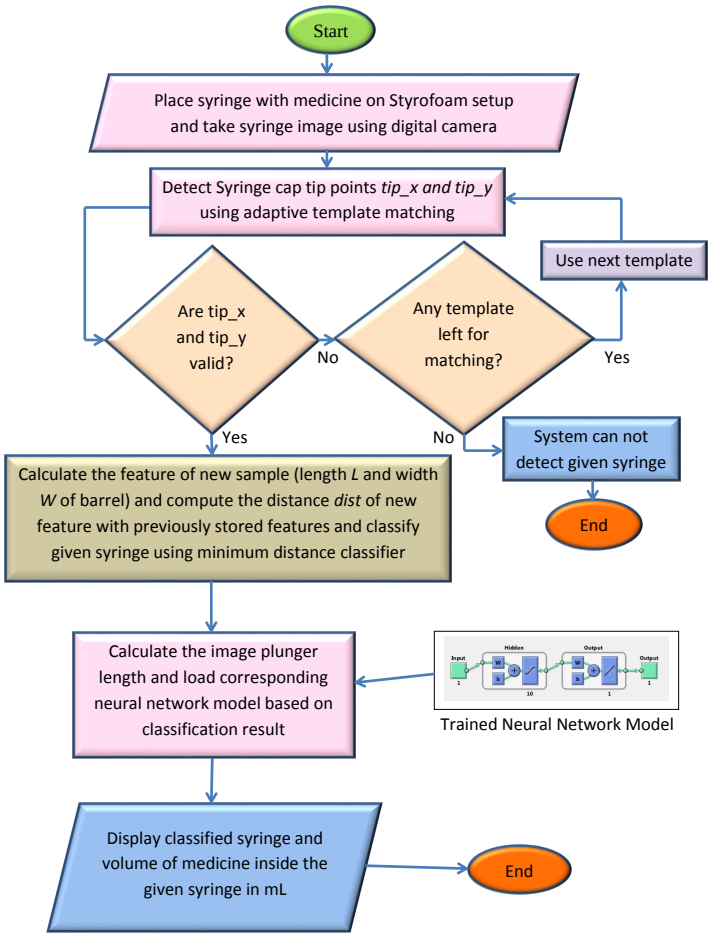

Figure 4-1: Flowchart of the complete system (SCVMS).

have information about the maximum capacity of syringe. The syringe classification system proposed here considers 6 leur-lock syringes 1 ml, 3 ml, 5 ml, 10 ml, 20 ml, and 30 ml and by using image analysis and minimum distance classifier it becomes able to differentiate among them. The classification was obtained flawlessly, which crucial for volume measurement because volume measurement systems starts with the assumption that classification result is 100 % accurate.

4.2 Syringe Volume Measurement System

Volume measurement system (VMS) occurs after the syringe classification and heavily relies on the decision base during the classification stage. Volume measurement utilizes the length between syringe tip cap and black rubber region obtained after application of different image processing algorithms. The VMS gives the volume inside syringe irrespective of any color and system was tested for various colors with different syringes. The trained neural network model helps in perfect input-output mapping. Although experimental observations show the linear relationship, accuracy is increased with trained model.

4.3 Methods and Materials

Syringe classification and volume detection are achieved using image analysis followed by a trained artificial neural network. The system includes two separate stages; classification stage and measurement stage. The measurement stage is loaded based on the result of classification stage. The system is capable of separating and calculating volumes for leur-lock syringe ranging from 1 mL to 30 mL. The complete flow chart of working of the system is given in Fig. 4-1. The experimental setup is shown in Fig. 4-2(a) which includes the styrofoam that provides the area to keep syringe during classification. Use of styrofoam with a desired depression on it helps to hold syringe firmly and believed to yield more accurate and precise results.

4.3.1 Image Acquisition and Preprocessing

The complete system works in real-time. Logitech webcam C615 digital camera is interfaced with control computer. A MATLAB program calls a special routine to start the digital camera which is fixed at a height of the surface of the styrofoam base

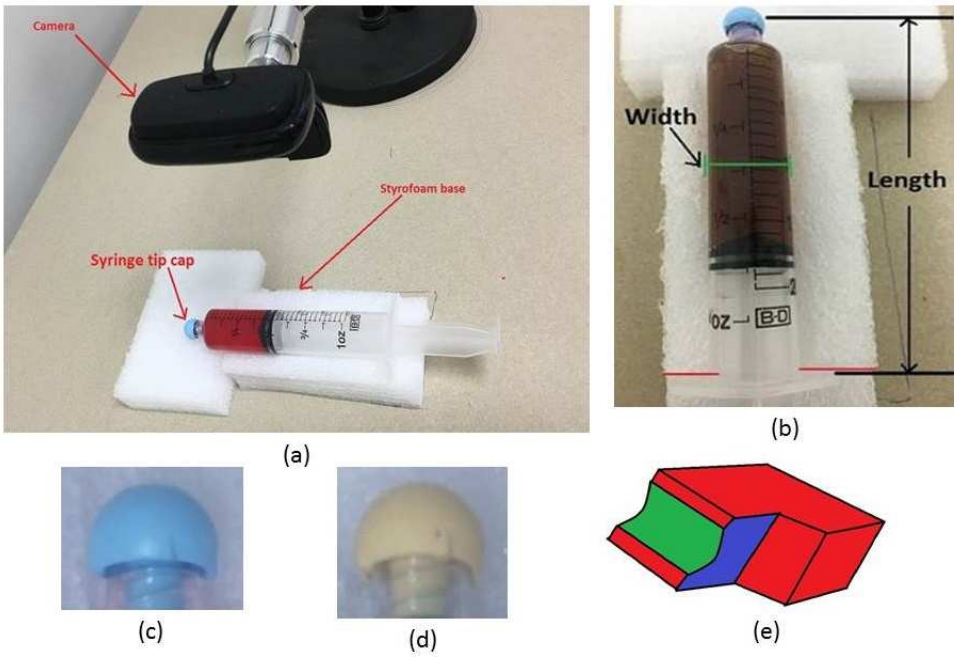

Figure 4-2: Components of SCVMS; (a) experimental setup of the complete system, (b) plan view of syringe on styrofoam base showing barrel length and width, (c) faint blue template of syringe tip cap, (d) yellow template of syringe tip cap, and (e) layout of Styrofoam lower region

where a syringe is placed as shown in Fig. 4-2(a). Real-time video input obtained from digital camera is supplied to the MATLAB program, which extracts the image from video. The image obtained is then enhanced using histogram equalization and median filtering to balance intensity and remove noise, respectively. A histogram equalization of image with 64 different levels is employed to get an image with intensity uniform distribution. The median filtering with window of size 3×3 is applied to remove small dots present in the syringe and background. The median filtering and contrast improvement makes the image appropriate for segmentation.

4.3.2 Neural Network Toolbox

Similar to the biological neurons network, an artificial neural network could recognize the pattern, find the best solutions, and classify from the data. The neural network training of the Neural Network Toolbox in MATLAB is utilized for the proposed

system to train the input data in supervised learning using the Lavenberg-Marquardt algorithm. It has MATLAB commands as well as a GUI application where the neural network structure could be created (input neurons, output neurons, hidden neurons). For training of the neural network it has function *train()*, which takes a dataset and untrained neural network structure and trains the neural netowrk for given learning, validation, and test error and finally gives the trained neural network. The trained neural network could be saved so that it does not have to go again for the training process.

4.3.3 Syringe Classification System

The syringe tip cap in the image is detected using the template matching. Various templates images of syringe tip cap are already stored on the database. Fig. 4-2(c) and 4-2(d) shows the template for faint blue and yellow colored templates of the syringe tip cap. the template matching technique determines the perfect match of a given template image to the scene image based on correlation calculation as given in Equation 2.5 . Different templates of syringe tip cap with various colors and orientations are stored in the database. Templates have size of 150×200, and the scene image has size of 1080×1920. When the MATLAB program is fed with an image frame obtained from the digital camera, it loads the different templates of syringe tip cap of yellow and blue color. At a single time, one template is run over the scene image of the syringe to find the best match. It calculates the correlation of the template image to the scene image or syringe image and forms a two dimensional matrix of correlation values. In the matrix of correlation values, whichever index of the matrix has the maximum correlation value, the point corresponding to that pixel is said to be best match point for the given template image. If the point is not detected in the first run with one colored syringe tip cap, then the other colored template is loaded and again run over the target image to find the best match point.

The detection of best match point is decided by applying the experimental setup data. The best match point is validated according to the experimental setup because it also imposes limits on the region of interest for detection of the syringe tip cap. In the proposed experimental setup, the height of detected points should be between 150 and 700. These points are measured based on the experimental observations. Thus, if the detected point does not lie within this criteria and then the other templates with different orientations are loaded and the whole process is run again until it gives the valid detected point, which could lead to increased computational time of system. Then, the detected syringe tip cap point is further utilized for classification and barrel length calculation. The lower end of barrel is locked in the styrofoam as shown in Fig. 4-2(b). This point is always fixed in the image since the web camera is also fixed.

4.3.3.1 Data Generation and Modelling

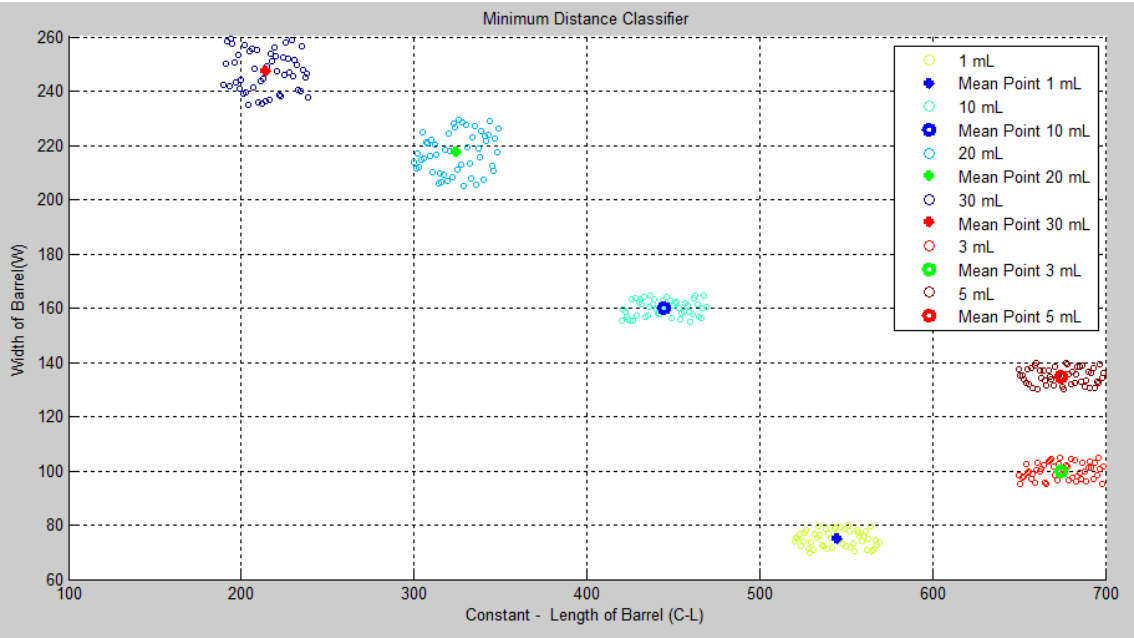

Figure 4-3: Experimental data and mean points plot of Minimum Distance Classifier.

Barrel length, the distance between lower end point of barrel and syringe tip cap point, is calculated. As given in Fig. 4-2(b), the distance between the blue colored

syringe tip cap and lower end point of barrel as indicated by red horizontal lines gives the barrel length while barrel width as indicated by green horizontal line is measured using the width of syringe. Fig. 4-2(e) shows the layout of the lower end of the styrofoam base where green colored surface indicates the depression introduced on the styrofoam upper part so that it could hold the syringe without any movement. The edge of the blue colored surface and green colored surface help to lock the syringe when lower end of barrel is placed on the given setup. Now the enhanced syringe image is subjected to into the segmentation for calculation of barrel width which is accomplished by measuring the width of the segmented and analyzed syringe image. After segmentation, the image is subjected to connected component analysis and this process yields the largest region as the plunger region along with medicine for colored medicine and/or the plunger region only for colorless medicine. The width of the largest connected region gives the barrel width. The Leur-lock syringe has a plunger usually made of black latex-free rubber, and syringe tip caps are made of usually red, yellow, and faint blue colors. During the experiments and data collection, two syringe tip caps (yellow and blue), plunger (black rubber), and medications with different colors (yellow, red, blue, colorless water) are used.

4.3.3.2 Classifier Implementation

Barrel length (L) is strong feature for syringe classification, as it can easily separate 30 mL, 20 mL, 10 mL, 1 mL syringes without any difficulties while 5 mL and 3 mL showed the same range of barrel length. Thus, barrel width (W) is also considered to make classification robust and efficient as shown in Fig. 4-3. Mean feature vector for each syringe is computed from 50 previously recorded data vectors as shown in Fig. 4-3. In the Fig. 4-3, the cluster of data points for six different syringes were shown with corresponding mean point as described in the legends of the figure. The distance between the mean points signifies the system effectiveness, and as shown in the figure

there is sufficient distance between clusters, which convinces the highest accuracy. Thus, when a new sample is received from video camera, it has been enhanced and filtered in IAPP stage (Section 4.3.1), and L and W are calculated and distance *dist* is calculated using Equation 4.1. Let new sample $S = \{L, W\}$ and the mean of six syringes be M_i, where $i = 1$ to 6. Then,

$$dist = |S - M_i| \tag{4.1}$$

The *dist* vector contains the distance of the new sample as the mean of six syringes considered in classification. The minimum value in *dist* vector is determined, and a new sample is classified as that type of syringe. Thus, feature vector with two features is believed to be able to classify the new sample into the six mentioned syringes.

4.3.4 Syringe Volume Measurement System

Measuring the volume of medicine inside a syringe is the second step of the complete system. After successful classification of the syringe to its corresponding category, the information about the type of syringe used in the given compounding process is obtained.

4.3.4.1 Plunger Length Calculation

Volume of medicine measured inside syringe basically relies on the plunger length (PL) calculation as described in Fig. 4-4. Plunger length is the length between the centroid of syringe tip cap and the lower region centroid of the rubber plunger as shown in Fig. 4-4(e). In Fig. 4-4(e) a green dot denotes the syringe tip cap centroid, while the red dot gives the centroid of the plunger rubber region. The city-block distance, which is the vertical distance between two points, is calculated by taking difference of y-coordinate of the two centroids. The digital camera and

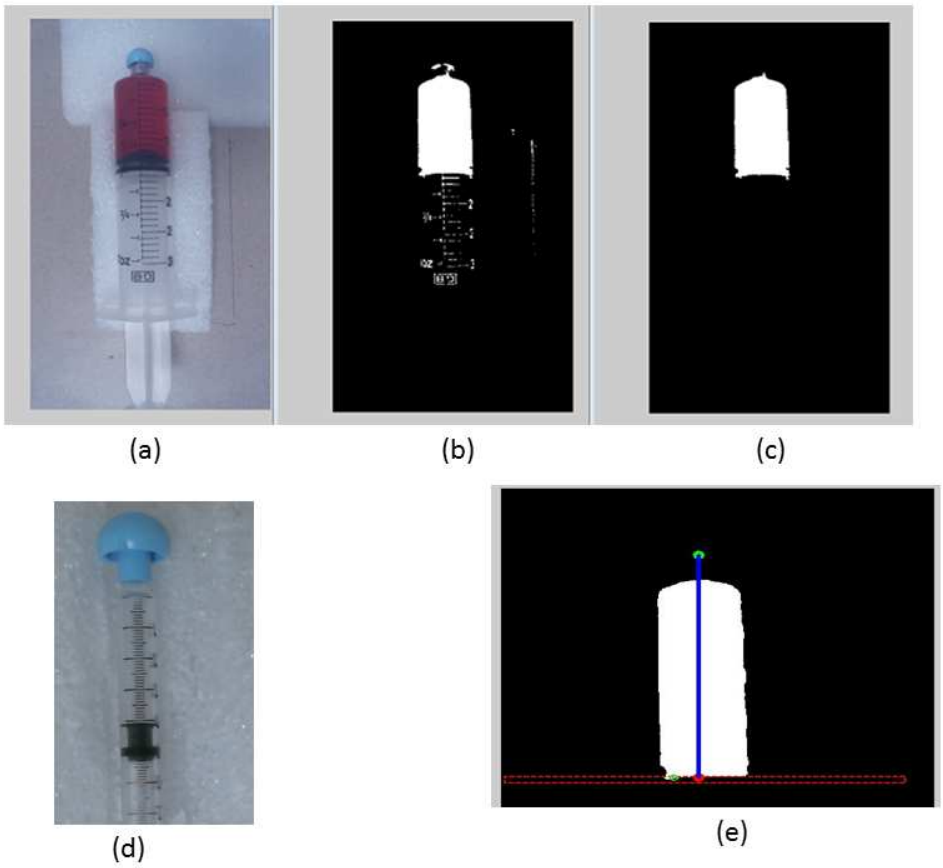

Figure 4-4: Screenshots output of (a) original image of syringe from video with colored medicine for 30 mL, (b) binary output image, (c) largest connected region of given binary image, (d) original image of syringe with colorless medicine for 1 mL, and (e) plunger length calculation process.

styrofoam setup are fixed at certain positions so that the syringe with medication is placed as shown in Fig. 4-2(a), that keeps the syringe tip cap always at the top portion of image and plunger rubber (Fig. 4-2(b)) at the bottom. The syringe tip cap is detected and its centroid calculated with same method described in the Syringe Classification section. In order to compute the centroid of lower region of rubber plunger, the grayscale image of the syringe is subjected to segmentation after IAPP process with the sufficiently large threshold value so that it can clearly separate the background image and foreground object. The main aim of segmentation to preserve the black rubber plunger region thus threshold value is set to keep only regions with very low intensity, although perfect segmentation is not necessary. Experimental

studies have shown that after segmentation process, the largest connected region in the binary image for every type of syringes is the rubber plunger region without colored medicine, as shown in Fig. 4-4(d) and/or rubber plunger along with medicine region for colored medicine inside syringe as shown in Fig. 4-4(a). After segmentation, the binary image is obtained as shown in Fig. 4-4(b) and then the 8-connected analysis is applied in the binary image, and the largest region is extracted and separated from the original binary image as shown in Fig. 4-4(c). Thus, the obtained plunger region is first eroded and then dilated to remove noise on the edges of the obtained region. Since the plunger region in the extracted image is at the bottom side of the image according to the experimental setup. The lowest 200 pixels of the plunger region are considered, and the centroid is calculated as shown in Fig. 4-4(e), the red dotted rectangular window shows the region containing lowest 200 pixels and green dot shows the calculated centroid. This technique helps to obtain an accurate and precise value of reference point for the rubber plunger region in each experiment and minimizes the dependency of the calculated centroid to the thresholding technique. In order to make the plunger length more consistent during each experiment, only vertical distance is considered, which means the x-coordinate difference is neglected, which helps to minimize the error due to thresholding. Thus, the difference of y-coordinate between centroid of syringe tip cap and centroid of plunger region gives the plunger length.

4.3.4.2 Data Generation and Training

For training, the volume of medicine inside the syringe is manually changed for different volumes and is fed into the MATLAB program for PL calculation. The program calculates the plunger length with the above described procedure in Section 4.3.4.1. Thus, obtained PL and corresponding observed volume makes the data-pair. Frome there, these data-pairs are stored in Microsoft Excel spread sheet as shown

in Fig. 4-6(a) and 4-6(b) to create the database. The same procedure is repeated for all six syringes, and database is developed for each of six syringes. The database contains 500 data-pairs for each syringe; thus, in total there will be six different data files. Databases thus developed are utilized to train an artificial neural network (ANNs) having 10 hidden neurons, a single input, and a single output. From the database, plunger length is used as an input and observed volume is used as a target for training. After training, there will be 6 different trained neural network models representing each syringe that takes plunger length as input and gives volume of medicine inside syringe as output.

4.3.4.3 Volume measurement using Trained model

When syringe classification gives the result in the string form as described in section 4.3.3, the text is compared with a previously stored array of text, given as follows:

$$Array = \{'One','Three','Five','Ten','Twenty','Thirty'\} \tag{4.2}$$

The resultant string matches with one of these six strings in the array and calls the corresponding trained neural network model that passes the plunger length PL to the model and gives volume of medicine inside the syringe as an output. For example, let syringe classification result produces the string "One" then, when the program compares this string with array of strings, it matches with the first string in the array and calls the neural network model for a 1 mL syringe, which is already trained and stored in the database. The neural network model takes plunger length PL as an input and gives the corresponding volume of medicine as the output.

4.4 Experimental Results

The syringes used in the experiments are the similar type of syringes used during the compounding process. During labetalol preparation, a leur-lock syringe of 3 mL capacity is used while during protonix preparation a syringe of 1 mL is utilized. In this experiment, all the types of syringes that are common in pharmaceutical compounding are used. The experimental setup could be imitated easily and with low cost in any pharmaceutical laboratory. The whole system was developed in MATLAB R2013a, which utilizes the neural network training and image processing toolboxes. By single acquisition of image frame from video, the system becomes capable of promptly classifying the type of syringe utilized and volume of medication inside it. The system also has the capability to classify and measure a syringe with any color of medicine inside it.

4.4.1 Syringe Classification System

Classification of the syringe is achieved without any error, which is indeed needed since the entire volume measurement system depends on proper classification of syringe. The classification result obtained decides which trained neural network model to load in order to map the plunger length calculated in the previous stages into the volume of medicine inside the particular syringe. The barrel length and barrel width were computed and utilized for classification and gave very promising results. Fig. 4-3 clearly indicates that based on the barrel length (major feature) and barrel width (minor feature), six syringes utilized during compounding process could be easily classified, and a small circle of different colors shows the plot of 50 different samples collected to compute the mean feature vector for each syringe. Length described in Fig. 4-3 is the length between two centroid points for plunger region and cap region in the image, which has unit of pixels. The constant C used in Fig. 4-3 has value

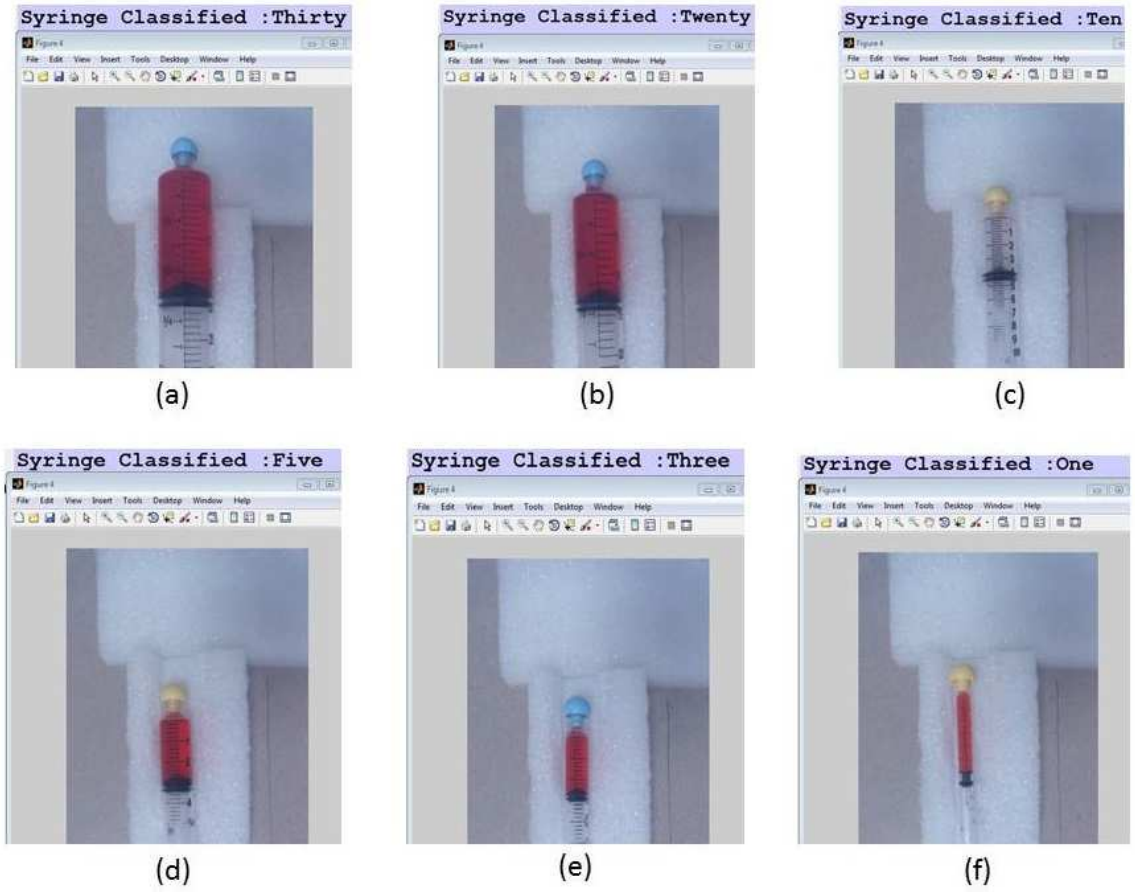

Figure 4-5: Output screenshots of SCS for (a) 30 mL, (b) 20 mL, (c) 10 mL, (d) 5 mL, (e) 3 mL, and (f) 1 mL.

of 1400 and its value only depends on position of camera and position of styrofoam base. Since both parameters are fixed in the experiment, C is considered to be a constant. The output obtained from this classification section is the string (name of syringe) indicating one of six syringes utilized in the compounding process. The efficiency of the system to classify the syringe was tested and found to be flawless during 50 trials for each syringe. During these trials, the position of rubber on the plunger was changed from lower range to higher range of the corresponding syringe so that the performance of the system can be measured for the entire range. For 30 ml, classification was tested with plunger rubber from 29 ml to 1 ml. A similar arrangement was developed for 20 ml, 10 ml, 5 ml, 3 ml, and 1 ml with plunger rub-

ber at different positions based on its maximum capacity. The snapshots of different plunger positions used for different syringes during classification are shown in Fig. 4-5. Fig. 4-5 shows the classification output string and the original image for a 30 ml syringe at 18 ml, 20 ml syringe at 13 ml, 10 ml syringe at 4 ml, 5 ml syringe at 3 ml, 3 ml syringe at 1.3 ml, and 1 ml syringe at 0.6 ml.

4.4.2 Syringe Volume Measurement

For the volume measurement, a dataset were collected as described in the methodology section. The portion of dataset for 5 ml and 10 ml is shown in Fig. 4-6(a) and Fig. 4-6(b). The dataset contains the plunger length on the left side and corresponding volume on the right side, as indicated by column A and column B respectively. In a 5 ml syringe, the syringe has scale resolution of 0.2 ml which indicates the minimum amount of volume that can be accurately measured using this syringe. In 5 ml syringe, there are small black lines between 3 ml and 4 ml indicating 3.2 ml, 3.4 ml, 3.6 ml, and 3.8 ml as shown in Fig. 4-6(c). the dataset for 5 ml was collected by changing the plunger position at every possible scale on the syringe from 0.2 ml to 5 ml. Experiments were conducted more with the same plunger position increase the sample size of dataset. Similar procedures were followed to collect datasets for other syringes too. The total number of samples in each dataset for given syringe was 500.

Since the SCS result was required for volume measurement and should be flawless, volume measurement performance was studied together with SCS, considering that SCS has 100 % accuracy and was illustrated in the Section 4.4.1. The experiment was conducted for all syringes at different volumes (plunger position), and volume obtained from the system was measured along with the time required for computation. For the single syringe, the complete system was tested with ample combinations of syringe tip caps and medications inside the syringe. Performances of different syringes were analyzed separately to find the accuracy, precision, and best working range for

each syringe.

4.4.2.1 Nerual Network Training

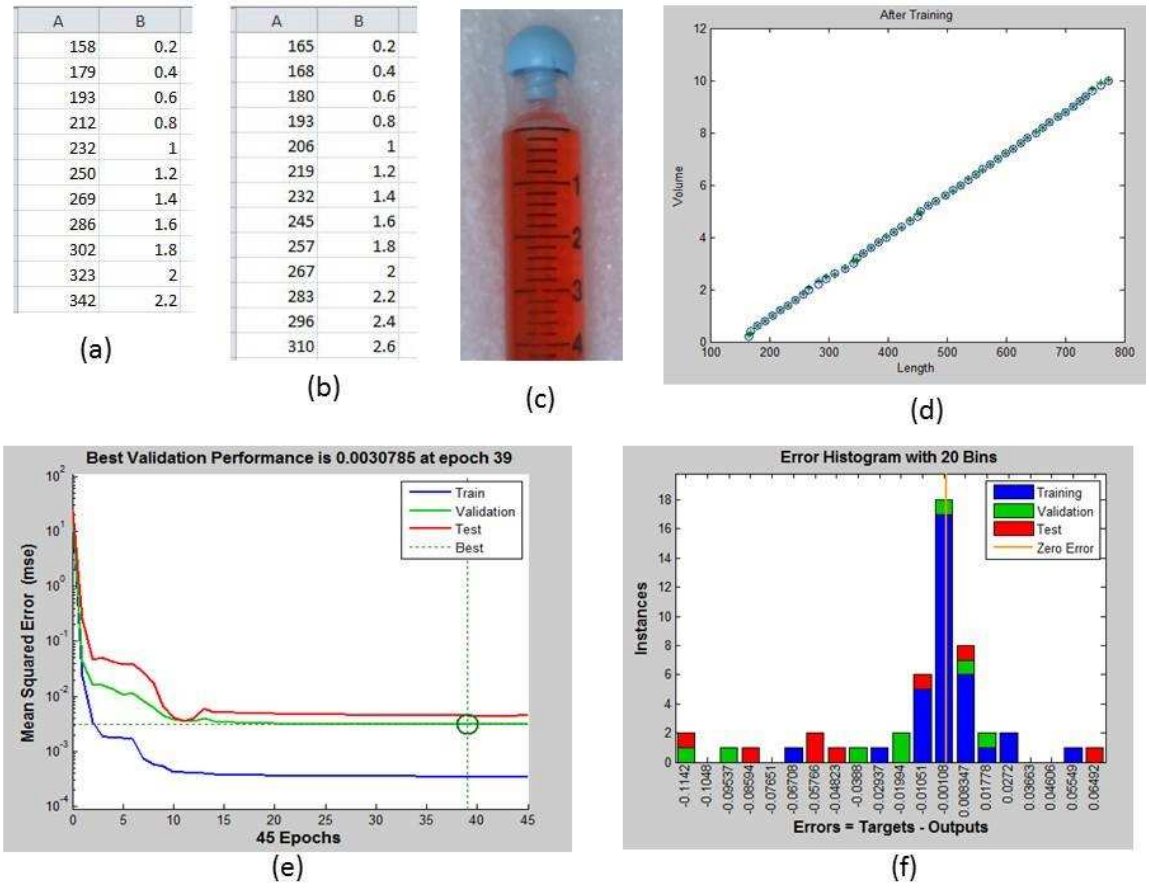

Figure 4-6: Output screenshots of SCVMS; (a) dataset for 5 mL, (b) dataset for 10 mL, (c) zoomed image of 5 mL, (d) input and output plot for 10 mL after training, (e) training, validation, test error plotted against mean square error (MSE) for 10 mL, and (f) error histogram diagram for 10 mL training.

The artificial neural network model was created in MATLAB using Neural Network Toolbox, which contains a single input, 10 hidden neurons, and a single output, and was trained with corresponding datasets for every syringe, and finally the trained model was saved to utilize in the volume measurement system. Figs. 4-6(d), 4-6(e), and 4-6(f) show the neural network training of 10 ml syringe, and Fig. 4-6(d) indicates the original data (blue circles) and output from network (green asterisk). The

network was trained using the Levenberg-Marquardt backpropagation method and performance was measured in mean squared error (MSE), as shown in Fig. 4-6(e), which shows the best error of approx. 0.003 for 45 epochs and also clarifies that MSE was large at the beginning, while it was decreasing after a few epochs, and finally constant, indicating the completion of training. Fig. 4-6(f) shows the error histogram, which indicates that for most instances of training, testing, and validation error are minimum and have value of 1e-3, signifying the completion of training. This histogram signifies that positive and negative errors are finally converging towards zero. As shown in the Fig. 4-6(e) the training error is generally low, but the training process is controlled by validation error, and finally, the trained model is tested using test error. Thus, validation and test error are always greater than training error, even for a trained model.

4.4.2.2 30 mL

For a 30 mL syringe, the neural network model was trained by the previously collected data. To test the accuracy and precision of the system for a 30 mL syringe, trials were performed using different volumes of medicine inside the syringe for four aforementioned colored medicines and two types of caps. Table 4.1 shows the performance of the 30 mL syringe at 5 mL, 15 mL, 20 mL, 25 mL, and 30 mL volume positions of medicine for 3 trials with yellow colored medicine with yellow and faint blue colored syringe tip caps. The table shows accuracy of 97 - 99 % for volume range of 15 - 30 mL, and thus gives the best working range, although it can be used with mediocre efficiency of 90 % and above from 5 mL. Standard deviation for best working range is found to be 0.003 - 0.0349, which efficiently describes the precision of system. This syringe has a resolution of 1 mL; thus, it can only be utilized to measure volume of difference of 1 mL visually, but with the proposed system it can precisely detect the correct volume with resolution of less than 1 mL, as illustrated

by Fig. 4-7(a). In this figure, it is hard to determine the exact volume by visual appearance of plunger position, since there is no scale available between 15 mL and 16 mL, but system gave the volume measure as 15.24 mL, which is more accurate. Similar results were obtained when other colors of medicines were used.

Table 4.1: Observed volume, computation time and accuracy for 30 mL syringe with yellow colored medicine.

Syringe Tip Cap Color	Actual Volume (ml)	Detected Volume (ml)	Detection Time (sec)	Mean ± SD	Accuracy (%)
Blue	5.0	5.3418	7.4689	5.3187 ± 0.0200	93.62
		5.3065	7.5848		
		5.3079	7.4982		
	15.0	15.4268	7.362	15.4125 ± 0.0236	97.25
		15.4254	7.3354		
		15.3853	7.3467		
	20.0	19.9458	7.4724	19.9420 ± 0.0270	99.71
		19.9669	7.4817		
		19.9133	7.4541		
	25.0	24.9481	7.3549	24.9499 ± 0.00168	99.79
		24.951	7.4219		
		24.9505	7.3674		
	30.0	30.0299	7.4582	30.0271 ± 0.0024	99.90
		30.0257	7.4806		
		30.0257	7.4731		
Yellow	5.0	5.3562	5.6312	5.3484 ± 0.0275	90.03
		5.3712	5.6762		
		5.3179	5.6816		
	15.0	15.2695	5.5527	15.3023 ± 0.0284	97.98
		15.3184	5.5211		
		15.3189	5.5512		
	20.0	19.9620	5.6320	19.9418 ± 0.0349	99.70
		19.9620	5.6373		
		19.9015	5.6976		
	25.0	24.8936	5.5793	24.8931 ± 0.0005	99.57
		24.8933	5.5518		
		24.8925	5.5580		
	30.0	29.9949	5.6234	29.9952 ± 0.0003	99.98
		29.9950	5.636		
		29.9956	5.7721		

4.4.2.3 20 mL

The neural network model for a 20 mL syringe was trained with previously collected data, and thus the obtained trained model is used to test the system performance for the 20 mL syringe. Table 4.2 shows the results obtained during trials for

the 20 mL syringe with red colored medicine along with both tip caps. It also has resolution of 1 mL and thus has a reading scale from 1 mL to 20 mL. Trials were performed for 1 mL, 5 mL, 10 mL, 15 mL, and 20 mL. Accuracy is very low (less than 75 %) for 1 mL volume measurement while it was measured 96.5 - 99+ % for 5 mL - 20 mL range; thus, 5 mL - 20 mL is the best working range for 20 mL syringe. Standard deviation for the best working range is found to be 0.008 - 0.0057, which explains the precision of the system. The output of the complete system for 20 mL when used to measure 5 mL volume is shown in Fig. 4-7(b). It shows the classified syringe output, volume measured, and computational time required for this particular setup in red, green, and blue rectangular windows respectively. The given syringe was tested with all medicines aforementioned inside it and found similar accuracy and precision.

Table 4.2: Observed volume, computation time, and accuracy for a 20 mL syringe with red colored medicine.

Syringe Tip Cap Color	Actual Volume (ml)	Detected Volume (ml)	Detection Time (sec)	Mean ± SD	Accuracy (%)
Blue	1.0	0.79245	7.3815	0.7591 ± 0.0592	75.91
		0.7942	7.3619		
		50.69075	7.3482		
	5.0	5.1762	7.3206	5.175 ± 0.0022	96.50
		5.1763	7.3191		
		5.1724	7.3958		
	10.0	10.0304	7.3306	10.0292 ± 0.0017	99.70
		10.0299	7.3697		
		10.0272	7.3403		
	15.0	14.4481	7.3311	14.4475 ± 0.0008	96.31
		14.4478	7.3296		
		14.4466	7.3554		
	20.0	19.6253	7.8535	19.6252 ± 0.0008	98.12
		19.6244	7.6066		
		19.6260	7.6212		
Yellow	1.0	0.69617	5.5965	0.6910 ± 0.0053	69.10
		0.69132	5.5478		
		0.68533	5.6518		
	5.0	5.1644	5.5303	5.1629 ± 0.0023	96.74
		5.1641	5.5351		
		5.1603	5.5443		
	10.0	9.95898	5.4774	9.9584 ± 0.0008	99.58
		9.9586	5.5399		
		9.9576	5.5541		
	15.0	14.4526	5.5078	14.4559 ± 0.0057	96.37
		14.4526	5.4474		
		14.4624	5.5711		
	20.0	19.6275	5.8215	19.6243 ± 0.0028	98.12
		19.6224	5.8093		
		19.6230	5.8065		

4.4.2.4 10 mL

The trained model was built using previously collected data for a 10 mL syringe and used to test system performance for a 10 mL syringe. The syringe has resolution of 0.2 mL, and trials were performed for 1.0 mL, 3.0 mL, 5.0 mL, 7.0 mL, and 9.0 mL for red colored medicine with both syringe tip caps, as shown in Table 4.3. From 3.0 mL - 9.0 mL, accuracy was observed to be consistent and found to be from 97 - 99 %; thus, the best working range for a 10 mL syringe is from 3 - 9 mL, although it also

gives good performance below 3 mL. For best working range standard deviation of 0.0017 - 0.0205 were observed, which describes the precision of the system. Below 1 mL, accuracy was low and the system was inconsistent. The output of the complete system for the 10 mL when used to measure 7 mL volume is shown in Fig. 4-7(c). It shows the classified syringe output, volume measured, and computational time required for this particular setup in red, green, and blue rectangular windows, respectively. Trials were performed for other colored medicines too and found similar results on accuracy and precision.

Table 4.3: Observed volume, computation time, and accuracy for 10 mL syringe with red colored medicine.

Syringe Tip Cap Color	Actual Volume (ml)	Detected Volume (ml)	Detection Time (sec)	Mean ± SD	Accuracy (%)
Blue	1.0	0.99478	7.4828	0.9902 ± 0.0592	99.02
		0.98495	7.5208		
		0.99095	7.9006		
	3.0	2.9608	7.5178	2.96 ± 0.0017	98.66
		2.958	7.5647		
		2.9612	7.6656		
	5.0	4.9548	7.6990	4.9311 ± 0.0205	98.62
		4.9187	7.6696		
		4.9198	7.7008		
	7.0	6.9310	7.7449	6.9309 ± 0.0004	99.01
		6.9305	7.7054		
		6.9313	7.7083		
	9.0	8.9791	7.3654	8.9792 ± 0.0002	99.76
		8.9794	7.5265		
		8.9790	7.3247		
Yellow	1.0	1.0522	6.5983	1.0484 ± 0.0033	95.16
		1.047	5.7334		
		1.046	5.6968		
	3.0	3.0943	5.6405	3.0908 ± 0.0034	96.97
		3.0876	5.6361		
		3.0904	5.9507		
	5.0	5.0086	5.7396	5.0052 ± 0.0078	99.89
		5.0107	5.7583		
		4.9963	5.7499		
	7.0	6.9592	5.6114	6.9701 ± 0.0121	99.57
		6.9763	5.5938		
		6.9779	5.5824		
	9.0	9.0567	5.3859	9.0625 ± 0.0094	99.30
		9.0574	5.5616		
		9.0733	5.5958		

4.4.2.5 5 mL

The trained model was used for testing 5 mL syringe by conducting trials for different volume positions of the syringe. Trials were performed at 1 mL, 2 mL, 3 mL, 4 mL, and 5 mL for colorless liquid (water) for both syringe tip caps, and observed data were collected as shown in Table 4.4. The 5 mL syringe has resolution of 0.2 mL, and results show that it has the best accuracy from 1.0 mL to 5.0 mL as 97 - 99 %, with standard deviation between 0.0002 - 0.0154 for best working range, thus illustrating how precise the system is. The accuracy degrades while going below 1 mL, so the best working range for 5 mL is found to be 1 mL to 5 mL. The output of the complete system for 5 mL when used to measure 1 mL volume is shown in Fig. 4-7(d). It shows the classified syringe output, volume measured, and computational time required for this particular setup in red, green and blue rectangular windows, respectively. Similar trials were also performed with other colored medicines inside the syringe and found accuracy and precision range within the same range.

Table 4.4: Observed volume, computation time, and accuracy for a 5 mL syringe with colorless (water) colored medicine.

Syringe Tip Cap Color	Actual Volume (ml)	Detected Volume (ml)	Detection Time (sec)	Mean ± SD	Accuracy (%)
Blue	1.0	0.96869	7.5453	0.9690 ± 0.0004	96.90
		0.96896	7.5378		
		0.96942	7.5476		
	2.0	2.0809	7.4915	2.0828 ± 0.0041	95.86
		2.0799	7.5207		
		2.0875	7.5747		
	3.0	2.9372	7.6427	2.9364 ± 0.0009	97.88
		2.9364	7.5619		
		2.9355	7.5365		
	4.0	3.9848	7.4891	3.9902 ± 0.0099	99.75
		3.9842	7.5646		
		4.0017	7.5337		
	5.0	4.9208	7.5161	4.92 ± 0.0007	98.40
		4.9196	7.5392		
		4.9196	7.5670		
Yellow	1.0	1.000	5.5497	0.9999 ± 0.0002	99.99
		0.9997	5.5721		
		1.0001	5.6118		
	2.0	2.0963	5.5457	2.0965 ± 0.0002	95.17
		2.0967	5.5563		
		2.0966	5.5432		
	3.0	2.9929	5.6084	2.9922 ± 0.0008	99.74
		2.9913	5.5610		
		2.9923	5.5614		
	4.0	3.9854	5.5933	3.9943 ± 0.0154	99.85
		3.9853	5.5916		
		4.0121	5.6044		
	5.0	4.9615	5.5322	4.9736 ± 0.0207	99.47
		4.9618	5.5839		
		4.9975	5.6097		

4.4.2.6 3 mL

A 3 mL syringe has the capacity to measure from 0.1 mL to 3.0 mL and has resolution of 0.1 mL. The trained model built from the previously collected data for 3 mL was used for testing of the system's ability and performance for a 3 mL syringe. Trials were performed for black colored liquid inside syringe at volumes of 0.5 mL, 1.0 mL, 1.8 mL, 2.5 mL, and 3.0 mL with both colored syringe tip caps. From 1.0 to 3.0 mL, the accuracy was observed to be between 97 - 99+ % as shown in Table

4.5 with standard deviation between 0.0001 - 0.0016, which gives the precision for 3 mL syringe. For 0.5 mL, accuracy was observed to be around 90 %; thus, it could still be used to measure volume of medicine from 0.5 mL - 3.0 mL with moderate accuracy. The output of the complete system for 3 mL when used to measure 3 mL volume is shown in Fig. 4-7(e). It shows the classified syringe output, volume measured and computational time required for this particular setup in red, green, and blue rectangular windows, respectively. Similar trials were performed with different colored medicines and results were found to be within the range of the given accuracy and precision.

Table 4.5: Observed volume, computation time, and accuracy for a 3 mL syringe with black colored medicine.

Syringe Tip Cap Color	Actual Volume (ml)	Detected Volume (ml)	Detection Time (sec)	Mean ± SD	Accuracy (%)
Blue	0.5	0.56861	7.3334	0.5683 ± 0.0003	86.34
		0.56808	7.4034		
		0.56808	7.5414		
	1.0	0.99975	7.5840	0.9972 ± 0.0047	99.72
		0.99174	7.3611		
		1.0001	7.8425		
	1.8	1.8108	7.4355	1.8107 ± 0.0001	99.40
		1.8106	7.6764		
		1.8106	7.6308		
	2.5	2.4379	7.4703	2.4380 ± 0.0002	97.52
		2.4382	7.3327		
		2.4379	7.3037		
	3.0	3.0155	7.5622	3.0172 ± 0.0026	99.42
		3.0159	7.3405		
		3.0202	7.4514		
Yellow	0.5	0.53957	5.5282	0.5364 ± 0.0052	92.72
		0.53924	5.5524		
		0.53046	5.8166		
	1.0	0.96968	5.4774	0.9699 ± 0.0003	96.99
		0.96985	5.5568		
		0.97024	5.5524		
	1.8	1.7939	5.6081	1.7929 ± 0.0016	99.60
		1.7910	5.6012		
		1.7938	5.6015		
	2.5	2.4285	5.4699	2.4293 ± 0.0012	97.47
		2.4286	5.5284		
		2.4307	5.5650		
	3.0	3.0238	5.5351	3.0246 ± 0.0007	99.18
		3.025	5.5626		
		3.025	5.5614		

4.4.2.7 1 mL

A 1 mL syringe has the capacity to measure from 0.01 mL to 1 mL thus it has resolution of 0.01 mL. However, the trained model for 1 mL syringe was tested after 0.05 mL because the plunger is indistinguishable from the syringe tip cap below 0.05 mL; thus, the system has limitation for detection below 0.05 mL. The built trained model was tested for different trials at different volume positions. Trials were performed for 0.05 mL, 0.25 mL, 0.5 mL, 0.75 mL, and 1.0 mL for red colored medicine

with both syringe tip caps. Observed volumes with average accuracy and precision were given in Table 4.6. Results show that the best working range was found to be 0.25 to 1.0 mL with accuracy of 96 - 99 % and standard deviation from 0.0001 - 0.0106. From 0.05 to 0.25 mL, accuracy was found to be between 85% - 95 %, still giving mediocre accuracy range for volume measurement. The output of the complete system for 1 mL when used to measure 0.31 mL volume is shown in Fig. 4-7(f). It shows the classification result and volume measured with red and green rectangular windows, respectively. Similar trials were conducted for other colored medicines, and results were observed and was similar to the results of red colored medicine.

Table 4.6: Observed volume, computation time, and accuracy for a 1 mL syringe with red colored medicine.

Syringe Tip Cap Color	Actual Volume (ml)	Detected Volume (ml)	Detection Time (sec)	Mean ± SD	Accuracy (%)
Blue	0.05	0.049172	7.3727	0.0477 ± 0.0012	95.40
		0.047029	7.3726		
		0.047045	7.3596		
	0.25	0.24142	7.3930	0.2417 ± 0.0003	96.68
		0.24194	7.4112		
		0.24184	7.3493		
	0.5	0.50972	7.3747	0.5097 ± 0.00001	98.06
		0.50968	7.3351		
		0.50967	7.3318		
	0.75	0.72895	7.3771	0.7288 ± 0.0001	97.17
		0.72878	7.3526		
		0.72879	7.4583		
	1.00	0.98828	7.3248	0.9894 ± 0.0016	98.94
		0.98867	7.5294		
		0.99118	7.4016		
Yellow	0.05	0.046449	5.5382	0.0453 ± 0.0019	90.60
		0.046344	5.5694		
		0.043050	5.5918		
	0.25	0.23957	5.6234	0.2397 ± 0.0001	95.88
		0.23986	5.5145		
		0.23969	5.5497		
	0.5	0.5181	5.5226	0.5190 ± 0.0008	96.2
		0.51945	5.5440		
		0.51944	5.7292		
	0.75	0.72532	5.5359	0.7258 ± 0.0009	96.77
		0.72527	5.6733		
		0.72692	5.7401		
	1.00	0.99058	5.5530	0.9892 ± 0.00106	98.92
		0.99904	5.7488		
		0.97802	5.6491		

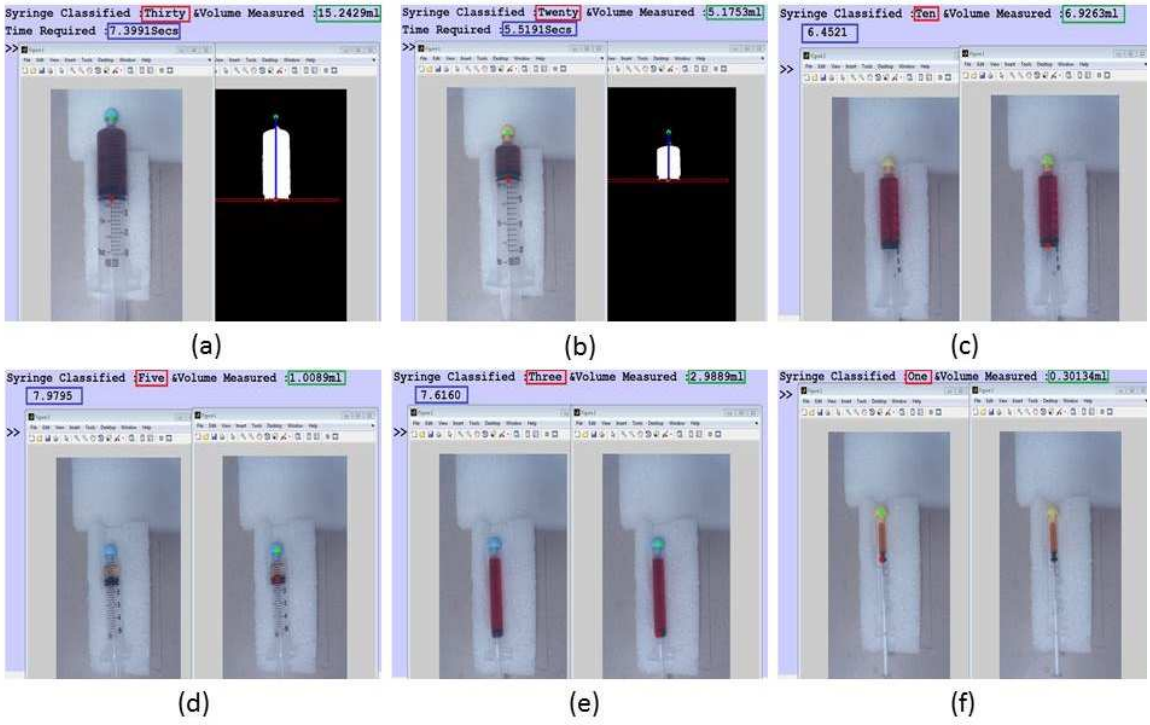

Figure 4-7: Screenshot of complete system output showing syringe type, volume measured, and computational time for (a) 30 mL, (b) 20 mL, (c) 10 mL, (d) 5 mL, (e) 3 mL, and (f) 1 mL.

4.4.2.8 Volume Measurement using Linear Model

This is vivid in the dataset that every syringe has an almost linear input-output relation with a little exception from only a few data points. Thus, alongside with training, the system was also tested with linear model, and results were observed. The linear model was built using only three points from the dataset; initial point (x_0, y_0), mid-point (x_m,y_m) and final point (x_f,y_f). For example, in the 5 ml syringe, plunger length and volume pair (158, 0.2) at 0.2 ml is initial point, pair (377, 2.6) at 2.6 ml is middle pint, and pair (596, 5.0) at 5 ml is the final point. Let x denote the plunger length obtained from analysis and y be the volume of medicine calculated as:

$$y = \frac{(y_m - y_0)}{(x_m - x_0)} \times (x - x_0) + y_0, \qquad x \leq x_m \tag{4.3}$$

$$y = \frac{(y_f - y_m)}{(x_f - x_m)} \times (x - x_m) + y_m, \qquad x > x_m \tag{4.4}$$

This method was tested for all the combinations as described for neural network training (data not shown). The output volume and accuracy are comparable to that obtained from trained neural network model. The average computation time using linear model is 7.1251 $\pm$ 0.0243 secs, for the blue colored syringe tip cap and 5.3120 $\pm$ 0.0531 secs, for the yellow colored syringe tip cap. Thus, on average, using the linear model will make the system 350 ms faster than trained network. Thus, from experimental observations there is a slight decrease in accuracy in exchange for computational efficiency. Rather, the efficiency was high at the extreme points for the linear model than that of the neural network model. (158, 0.2), (377, 2.6), and (596, 5.0) represent the initial, middle, and final data points for the 5 mL syringe. The recorded efficiency around these points is even better than with the trained neural network model, but for the volume scales in between these points, accuracy was better with the trained network. This is because of limited data point consideration in analysis for the linear model, while the neural network model considers every data points and trains the network so that it will have minimal possible error for working range.

4.4.2.9 Accuracy and Precision

The summary of performance of the complete system for the complete system is shown in Table 4.7. The table gives the range of accuracy for different syringes with different colors of medicines inside it and equipped with different syringe caps. The accuracy presented in the table is for the best working range of corresponding syringes. For the 30 mL syringe, the overall accuracy is reported from 96.37 % - 99.89 % shown by block letters in the 30 mL column and the worst precision is measured in standard deviation to be 0.0356. Similarly, for the 20 mL syringe, the overall accuracy

was reported from 96.31 % - 99.85 % as shown in the column of 20 mL of the table. The worst precision for 20 mL was recorded to be 0.0158. For 10 mL of syringe, overall accuracy ranges from 96.59 % to 99.89 %, and worst precision is 0.0205, as shown in 10 mL column. For a 5 mL syringe, overall accuracy ranges from 95.82 % to 99.91 %, and worst precision is 0.0162 as shown in the column for 5 mL. For the 3 mL syringe, the overall accuracy ranges from 96.72 % to 99.95 %, and the worst precision observed was 0.0057, as shown in the 3 mL column of the table. Finally, for 1 mL, the overall accuracy ranges from 96.14 % to 99.35 %, and worst precision was found to be 0.0110, as shown in the column 1 mL of the table.

Table 4.7: Summary of working accuracy of used syringes for different medicines and syringe tip caps for their best working range.

Color		Volume Measurement Accuracy (%)					
Tip	Medicine	30 mL	20 mL	10 mL	5 mL	3 mL	1 mL
Blue	Red	96.75 - 99.82	**96.31** - 99.70	96.97 - **99.89**	96.34 - 99.87	96.92 - 99.70	96.53 - 98.95
	Yellow	97.15 - **99.89**	96.52 - 99.57	97.08 - 99.75	96.17 - 99.54	97.18 - 99.52	96.68 - 98.87
	Black	96.45 - 99.62	96.72 - 99.38	97.16 - 99.82	96.37 - 99.81	96.93 - 99.65	96.25 - **99.35**
	Water	97.05 - 99.15	97.35 - 99.72	**96.59** - 99.73	**95.82** - **99.91**	97.21 - 99.72	96.75 - 98.96
Yellow	Red	96.54 - 99.24	97.18 - 99.76	97.02 - 99.81	95.92 - 99.33	97.14 - 99.87	**96.14** - 99.12
	Yellow	97.31 - 99.17	97.29 - **99.85**	97.15 - 99.34	96.50 - 99.84	**96.72** - **99.95**	96.22 - 98.95
	Black	96.68 - 99.45	96.67 - 99.52	96.86 - 99.84	96.19 - 99.77	97.26 - 99.78	96.52 - 98.83
	Water	**96.37** - 99.48	97.24 - 99.51	97.01 - 99.51	96.14 - 99.83	96.81 - 99.69	96.42 - 99.13

4.4.3 Computation Time

The computation time includes the time required for whole process, which also includes the classification, volume measurement, and display of images. The compu-

tation time for the core process will be slightly less than previously recorded and will also depend on processor and system RAM. All the experiments were conducted in MATLAB R2013a, which was installed in a computer with Windows 7 64-bit operating system with Intel Xeon W3550 @ 3.07 GHz processor and 12 GB of RAM. During classification of syringe, an adaptive template matching technique was applied, and the computation time for adaptive template matching depends on the template size and target image size. Yellow and faint blue colored syringe tip cap templates have size of almost the same; thus, this factor does not contributed much in computation time difference for yellow and blue colored syringe tip caps. It is because of the algorithms, which requires to check for both syringe tip caps, and the process is followed sequentially. For example, if there is yellow colored syringe tip cap then it doesn't have to go to check for blue syringe tip cap, but if there is blue tip cap then it has to go to check for yellow also. Thus, there is computation time difference between yellow and blue colored syringe tip caps with a difference of around 2 seconds. This time lagging could be reduced by applying parallel processing in the algorithm for adaptive template matching rather than a sequential approach. The total computation time includes image acquisition time, image pre-processing time, barrel length and plunger length calculation time, etc. along with adaptive template matching time. Therefore, the total computation time is recorded a little higher than for adaptive template matching. The total computation time was recorded for every trial performed for each syringe. For example, computation time for a 5 mL syringe can be observed in Table 4.4 with a table column named detection time (DT). The mean and standard deviation of these data were calculated, average detection time for the blue colored syringe tip cap was found to be 7.5446 ± 0.0371 secs, and average detection time for the yellow colored syringe tip cap was found to be 5.6055 ± 0.0830 secs. The above results show that the complete system is very computationally efficient and can be realized in real-time.

4.5 Reproducibility and Reliability of the Complete System

To study the reproducibility, the experiments for syringe classification and syringe volume measurements were conducted at different time schedules and with different personnel (including pharmacy technicians and non-technical persons). The results obtained were not different from previously recorded. The results obtained for Tables 4.1 and 4.2 were conducted by a PharmD student at different instances while results obtained for Tables 4.3 - 4.6 were conducted by a non-technical personnel under the same experimental environments. Thus, it can be concluded that the system is reproducible. The reliability could also be viewed from the precision of the results obtained. As seen in Table 4.1 - 4.6, the precision is high for the same volume of medicine in three different trials, which concludes that the system is highly reliable.

4.6 Conclusion

The SCVMS was successfully developed and tested using a digital imaging device and MATLAB. The classifications of syringes were obtained flawlessly for all six syringes with provided red, black, yellow, and colorless liquids inside the syringe. Both blue and yellow colored syringe tip caps were utilized in training as well as in testing.

A volume measurement system after SCS was also developed, trained, and tested successfully. The average accuracy of 95 % - 99+ % was obtained in each experimentation with high precision indicating system's perfect reproducibility and reliability with low computation time for the complete process.

Chapter 5

Conclusive Remarks

The ultimate goal of the research is to find out a way to minimize the general human errors in CSPs with the aid of technology. The proper selection of medicine and medical equipment along with a suitable procedure for given medication order is guaranteed in Chapter 3, while the proper volume of medicine along with proper syringe selection was ensured in Chapter 4. Thus, Chapter 3 and Chapter 4 together serve as the complete computational system for CSP.

The possible factors of human errors were analyzed and addressed in Chapter 3 by dividing the complete compounding task into two major problem statements. The first was performing necessary calculation according to a medication order, collecting all the required items from the store room, and bring them to the hood. With the help of barcode scanner integrated with a windows application developed in the Microsoft Visual Studio the technician is guided to select only necessary items inside the hood. Secondly, after keeping all the correct items inside the hood, the technician doing CSP should follow the standard procedure and should not miss certain steps like cleaning of all items, changing the needle in ampule preparation, putting the syringe tip cap in injection vial, etc. During the compounding process, the web camera was placed at the top of the compounding hood and backend MATLAB program provides the necessary feedback during compounding and ascertains that the technician is

following the right procedure.

Volume measurement of medicine using syringe is involved in almost every CSP. Thus, the volume of medicine inside the syringe after final preparation and/or injecting into IV bag is also a very critical error. A separate web camera is integrated in to the system as described in Chapter 3 for volume measurement. A second digital camera is dedicated for syringe classification and volume measurement and is thus tuned accordingly. Classification was done using a minimum distance classifier and obtained with 100 % accuracy while volume measurement gives an accuracy of 95% - 99+ % with high precision. The accuracy obtained is in the satisfactory range for the volume accuracy margin.

CSP is an important aspect of healthcare. Even small achievement obtained to reduce errors in CSP makes a difference between life and death of a patient. Thus, the proposed low cost computational decision support system serves as the medium to reduce errors when compounding with the currently existing manual CSP.

5.1 Future Work

The computational support system for CSPs is a less covered topic so far, although there are few high cost automatic robots already implemented for the whole compounding process. There is currently no support system that is low cost and can integrate with current existing compounding methods. Thus, most of the aspects of CSPs are untouched so far and give a new potential direction for new researchers.

5.1.1 Inclusion of More CSP's

The proposed system only considers the three most utilized compounding methods (Ampule, Injection, and Powder), but the whole CSP is not limited to only three methods. The proposed DSS facilitates the addition of more compounding methods

so that the complete system could have all the compounding methods followed during the preparation. Although addition of more methods will increase the computational overhead, it will also increase the robustness of the system.

5.1.2 Automatic Prescription Reader (APR)

The whole compounding process is based on the information provided on the prescription. When a compounding technician receives the prescription, he/she has to do some calculations to get the volume of medicine required. The necessary items are collected from the store room based on the nature of the preparation. There is enough room for a technician to make mistakes during calculation and misreading the prescription, which was not sufficiently addressed in the proposed system. The automatic prescription reader could be added to the current system, which will read the prescription applying optical character recognition (OCR) to the image obtained from a digital camera. Although the computational burden for MSS will be increased, the possibility of error during calculation and prescription reading will be ruled out.

5.1.3 Body Movement Tracking

The use of Microsoft Kinect sensor to estimate whole body movements could be another potential direction for this research. The current proposed system utilizes the combination of hand movements around the location of the object (item), and the accuracy of system highly depends on the utilization of the items placed in the LAFH compounding hood. Thus, only 5-6 important stages on each compounding procedure were considered in VPS. Tracking both hands of the technician may give the advantage of detecting more stages than detected by the current system and helps to increase the accuracy and precision of the VPS.

References

[1] Compounding P. Safe practices for parenteral nutrition. 2004.

[2] Morris AM, Schneider PJ, Pedersen CA, Mirtallo JM. National survey of quality assurance activities for pharmacy-compounded sterile preparations. AMERICAN JOURNAL OF HEALTH SYSTEM PHARMACY. 2003;60(24):2567-76.

[3] Trissel LA, Gentempo JA, Saenz LM, Woodard MY, Angeles CH. Effect of two work practice changes on the microbial contamination rates of pharmacy-compounded sterile preparations. American journal of health-system pharmacy. 2007;64(8):837-41.

[4] Goldberg RA, Flynn HW, Isom RF, Miller D, Gonzalez S. An outbreak of streptococcus endophthalmitis after intravitreal injection of bevacizumab. American journal of ophthalmology. 2012 Feb 29;153(2):204-8.

[5] Control CfD, Prevention. Multistate outbreak of fungal infection associated with injection of methylprednisolone acetate solution from a single compounding pharmacy-United States, 2012.

[6] Control CfD, Prevention. Pseudomonas bloodstream infections associated with a heparin/saline flush–Missouri, New York, Texas, and Michigan, 2004-2005. MMWR Morbidity and mortality weekly report. 2005;54(11):269.

[7] Health UDo, Services H, Food, Administration D. FDA Alerts Health Care Professionals of Infection Risk from Repackaged Avastin Intravitreal Injections. Washington, DC: Food and Drug Administration. 2011.

[8] Chollet JL, Jozwiakowski MJ. Quality investigation of hydroxyprogesterone caproate active pharmaceutical ingredient and injection. Drug development and industrial pharmacy. 2012;38(5):540-9.

[9] Control CfD, Prevention. Deaths from intravenous colchicine resulting from a compounding pharmacy error–Oregon and Washington, 2007. MMWR Morbidity and mortality weekly report. 2007;56(40):1050.

[10] Gudeman J, Jozwiakowski M, Chollet J, Randell M. Potential risks of pharmacy compounding. Drugs in R & d. 2013;13(1):1-8.

[11] Staes C, Jacobs J, Mayer J, Allen J. Description of outbreaks of healthcare associated infections related to compounding pharmacies, 2000-2012. American journal of health-system pharmacy: AJHP: official journal of the American Society of Health-System Pharmacists. 2013;70(15).

[12] Pedersen CA, Schneider PJ, Scheckelhoff DJ. ASHP national survey of pharmacy practice in hospital settings: dispensing and administration-2011. American Journal of Health-System Pharmacy. 2012;69(9):768.

[13] Augusto JC. Temporal reasoning for decision support in medicine. Artificial intelligence in medicine. 2005;33(1):1-24.

[14] Pronovost P, Needham D, Berenholtz S, Sinopoli D, Chu H, Cosgrove S et al. An intervention to decrease catheter-related bloodstream infections in the ICU. New England Journal of Medicine. 2006;355(26):2725-32.

[15] Zhao C, Jain A, Hailemariam L, Suresh P, Akkisetty P, Joglekar G et al. Toward intelligent decision support for pharmaceutical product development. Journal of Pharmaceutical Innovation. 2006;1(1):23-35.

[16] Stevens JD, Bader MK, Luna MA, Johnson LM. Cultivating Quality: Implementing Standardized Reporting and Safety Checklists. AJN The American Journal of Nursing. 2011;111(5):48-53.

[17] Sent D, Van der Gaag LC. Automated test selection in decision-support systems: a case study in oncology. Studies in health technology and informatics. 2006;124:491.

[18] Gwozdz R, Grass F. Contamination by human fingers: The Midas touch. Journal of radioanalytical and nuclear chemistry. 2004;259(1):173-6.

[19] Kundrapu S, Sunkesula V, Jury LA, Sitzlar BM, Donskey CJ. Daily disinfection of high-touch surfaces in isolation rooms to reduce contamination of healthcare workers' hands. Infection Control. 2012;33(10):1039-42.

[20] Haynes AB, Weiser TG, Berry WR, Lipsitz SR, Breizat A-HS, Dellinger EP et al. A surgical safety checklist to reduce morbidity and mortality in a global population. New England Journal of Medicine. 2009;360(5):491-9.

[21] Leape L, Berwick D, Clancy C, Conway J, Gluck P, Guest J et al. Transforming healthcare: a safety imperative. Quality and Safety in Health Care. 2009;18(6):424-8.

[22] Shojania KG, Duncan BW, McDonald KM, Wachter RM, Markowitz AJ. Making health care safer: a critical analysis of patient safety practices. Agency for Healthcare Research and Quality Rockville, MD; 2001.

[23] Berenholtz SM, Pronovost PJ, Lipsett PA, Hobson D, Earsing K, Farley JE et al. Eliminating catheter-related bloodstream infections in the intensive care unit*. Critical care medicine. 2004;32(10):2014-20.

[24] Betke M, Gips J, Fleming P. The camera mouse: visual tracking of body features to provide computer access for people with severe disabilities. Neural Systems and Rehabilitation Engineering, IEEE Transactions on. 2002;10(1):1-10.

[25] Pharmacopoeia US. USP General Chapter<797>. Pharmaceutical Compounding-Sterile Preparations. 2004.

[26] Rinehart JR, Chan D, Cunningham M, Geller RE, Grandfield G, Heckman S et al. ASHP guidelines on outsourcing sterile compounding services. American journal of health-system pharmacy: AJHP: official journal of the American Society of Health-System Pharmacists. 2010;67(9):757-65.

[27] KIENLE PC, MCELHINEY LF, OSTEEN RB, TROELL E, MASSOOMI F, SHEEHY K, CASSANO AT, BING CD, BUCHANAN C, FORREY RA, KASTANGO ES. ASHP guidelines on compounding sterile preparations. American journal of health-system pharmacy. 2014;71(2):145-66.

[28] Gawande A, Lloyd JB. The checklist manifesto: How to get things right. Metropolitan Books New York; 2010.

[29] Brown E. Windows Forms Programming with C#. Manning Publications Co.; 2002.

[30] Sekar A, Bialas AR, de Rivera H, Davis A, Hammond TR, Kamitaki N et al. Schizophrenia risk from complex variation of complement component 4. Nature. 2016;advance online publication. doi:10.1038/nature16549 http://www.nature.com/nature/journal/vaop/ncurrent/abs/nature16549.html - supplementary-information.

[31] Hicks RW, Becker SC. An Overview of Intravenous-related Medication Administration Errors as Reported to MEDMARX®., a National Medication Error-reporting Program. Journal of Infusion Nursing. 2006;29(1):20-7.

[32] Cowley E, Williams R, Cousins D. Medication errors in children: a descriptive summary of medication error reports submitted to the United States Pharmacopeia. Current Therapeutic Research. 2001;62(9):627-40.

[33] Bay H, Ess A, Tuytelaars T, Van Gool L. Speeded-up robust features (SURF). Computer vision and image understanding. 2008;110(3):346-59.

[34] Diana Hazardous Drug Compounding System | ICU Medical [Internet]. Icumed.com. 2016 [cited 19 May 2016]. Available from: http://www.icumed.com/products/oncology/pharmacy-compounding-automation/diana.aspx

[35] CytoCare - Automatic Compounding of Cytotoxic Drugs | Products | TOSHO [Internet]. Tosho.cc. 2016 [cited 19 May 2016]. Available from: http://www.tosho.cc/en/products/cytocare.html

[36] Acquire Images from Webcams - MATLAB & Simulink [Internet]. Mathworks.com. 2016 [cited 19 May 2016]. Available from: http://www.mathworks.com/help/supportpkg/usbwebcams/ug/acquire-images-from-webcams.html

[37] Mohr D, Zachmann G. Fast adaptive silhouette area based template matching. IfI Technical Report Series, 2010. URL http://www. in. tu-clausthal. de/forschung/technical-reports;.

[38] Banharnsakun A, Tanathong S. Object detection based on template matching through use of best-so-far ABC. Computational intelligence and neuroscience. 2014 Jan 1;2014:7.

[39] Wu Z, Goshtasby A. Adaptive image registration via hierarchical voronoi subdivision. Image Processing, IEEE Transactions on. 2012 May;21(5):2464-73.

[40] Roy S, Rathod DP. REAL-TIME OBJECT TRACKING AND LEARNING USING TEMPLATE MATCHING.

[41] Chantara W, Mun JH, Shin DW, Ho YS. Object tracking using adaptive template matching. IEIE Trans. Smart Process. Comput. 2015 Feb;4(1):1-9.

[42] Sharmila R, Uma R. A new approach to image contrast enhancement using weighted threshold histogram equalization with improved switching median filter. International Journal Of Advanced Engineering Sciences and Technologies Vol. 2011(7):206-11.

[43] Otsu N. A threshold selection method from gray-level histograms. Automatica. 1975 Jun;11(285-296):23-7.

[44] Cheriet M, Said JN, Suen CY. A recursive thresholding technique for image segmentation. Image Processing, IEEE Transactions on. 1998 Jun;7(6):918-21.

[45] Yapa RD, Harada K. A connected component labelling algorithm for greyscale mammography image processing as a pre-processing tool. Machine Graphics & Vision International Journal. 2007 Jan 1;16(3):305-27.

[46] Walczyk R, Armitage A, Binnie D. Comparative study on connected component labeling algorithms for embedded video processing systems.(2010)

[47] Rudrapatna M, Sowmya A. Feature weighted minimum distance classifier with multi-class confidence estimation. InAI 2006: Advances in Artificial Intelligence 2006 Dec 4 (pp. 253-263). Springer Berlin Heidelberg.

[48] Booth DJ, Oldfield RB. A comparison of classification algorithms in terms of speed and accuracy after the application of a post-classification modal filter. Remote Sensing. 1989 Jul 1;10(7):1271-6.

[49] Gerstner W. Supervised learning for neural networks: A tutorial with Java Exercises. Recurso disponible on-line: http://diwww. epfl. ch/mantra/tutorial/english/supervised. pdf. 1998.

[50] Yu H, Wilamowski BM. Levenberg-marquardt training. Industrial electronics handbook. 2011;5(12):1-6.

[51] Neural Network Toolbox Documentation [Internet]. Mathworks.com. 2016 [cited 19 May 2016]. Available from: http://www.mathworks.com/help/nnet/index.html

[52] Fine S, Scheinberg K. Efficient SVM training using low-rank kernel representations. The Journal of Machine Learning Research. 2002 Mar 1;2:243-64.

[53] Kecman V. Learning and soft computing: support vector machines, neural networks, and fuzzy logic models. MIT press; 2001.

[54] [Internet]. 2016 [cited 19 May 2016]. Available from: 21. http://www.pharmtech.com/trends-and-best-practices-visual-inspection

[55] Langille SE. Particulate matter in injectable drug products. PDA Journal of Pharmaceutical Science and Technology. 2013 May 1;67(3):186-200.

[56] Wichtl M. Herbal drugs and phytopharmaceuticals: a handbook for practice on a scientific basis. CRC press; 2004.

[57] Chin RT, Harlow CA. Automated visual inspection: A survey. Pattern Analysis and Machine Intelligence, IEEE Transactions on. 1982 Nov(6):557-73.

[58] Singh S, Bharti M. Image processing based automatic visual inspection system for PCBs. ISOR J. Eng. 2012;2:1451-5.

[59] Gunatilake P, Siegel M, Jordan AG, Podnar GW. Image understanding algorithms for remote visual inspection of aircraft surfaces. InElectronic Imaging'97 1997 Apr 15 (pp. 2-13). International Society for Optics and Photonics.

[60] Histogram Equalization [Internet]. Fourier.eng.hmc.edu. 2016 [cited 19 May 2016]. Available from: http://fourier.eng.hmc.edu/e161/lectures/contrast_transform/node2.html

[61] Maini R, Aggarwal H. A comprehensive review of image enhancement techniques. arXiv preprint arXiv:1003.4053. 2010 Mar 22.

[62] Brinkmann R. The art and science of digital compositing: techniques for visual effects, animation and motion graphics. Morgan Kaufmann; 2008 May 24.

[63] Suzuki K, Horiba I, Sugie N. Linear-time connected-component labeling based on sequential local operations. Computer Vision and Image Understanding. 2003 Jan 31;89(1):1-23.

[64] Karasulu B, Korukoglu S. Moving Object Detection and Tracking in Videos. Springer New York; 2013.

[65] Matching F. Fast/Robust Template Matching - File Exchange - MATLAB Central [Internet]. Mathworks.com. 2016 [cited 19 May 2016]. Available from: http://www.mathworks.com/matlabcentral/fileexchange/24925-fast-robust-template-matching

[66] Introduction to SURF (Speeded-Up Robust Features) âĂŤ OpenCV 3.0.0-dev documentation [Internet]. Docs.opencv.org. 2016 [cited 29 June 2016]. Available from: http://docs.opencv.org/3.0-beta/doc/py_tutorials/py_feature2d/py_surf_intro/py_surf_intro.html

[67] Object Detection in a Cluttered Scene Using Point Feature Matching - MATLAB & Simulink Example [Internet]. Mathworks.com. 2016 [cited 19 May 2016]. Available from: http://www.mathworks.com/help/vision/examples/object-detection-in-a-cluttered-scene-using-point-feature-matching.html

[68] Zhang J, Yan Y, Lades M. Face recognition: eigenface, elastic matching, and neural nets. Proceedings of the IEEE. 1997 Sep;85(9):1423-35.

[69] Kriesel D. A brief Introduction on Neural Networks.

Appendix A

Source Code for MSS

The MSS is designed in Microsoft Visual Studio using C# language. Only the main program launcher is listed below, but the complete source and executable files for material selection using barcode reader can be found here:

https://drive.google.com/folderview?id=0B7M9qPY-omo8a2JwUVFvZGdUd28\&usp=sharing

A.1 Program Launcher

```
using System;
using System.Collections.Generic;
using System.ComponentModel;
using System.Data;
using System.Drawing;
using System.Linq;
using System.Text;
using System.Windows.Forms;
using Excel = Microsoft.Office.Interop.Excel;

namespace ApplicationV5262
```

```
{
    public partial class Form1 : Form
    {
        public Form1()
        {
            InitializeComponent();
        }
       private void loginTableBindingNavigatorSaveItem_Click(object
       sender, EventArgs e)
        {
            this.Validate();
            this.loginTableBindingSource.EndEdit();
            this.tableAdapterManager.UpdateAll(this.database1DataSet1);
        }
       private void Form1_Load(object sender, EventArgs e)
        {
            // TODO: This line of code loads data into the
            // 'database1DataSet1.LocalDataBase' table. You can move,
            // or remove it, as needed.
            this.localDataBaseTableAdapter.Fill
            (this.database1DataSet1.LocalDataBase);
            comboBox1.DataSource = database1DataSet1.Tables["LocalDataBase"];
            comboBox1.DisplayMember = "Category";
           // code to show only unique name on 1st list
            int count_len = comboBox1.Items.Count;
            comboBox2.Items.Clear();
            comboBox1.SelectedIndex = 1;
```

```
      comboBox2.Items.Add(comboBox1.Text);
      string prev_text = comboBox1.Text;
      for (int i = 2; i <= count_len; i++)
      {
        comboBox1.SelectedIndex = i;
        string  next_text = comboBox1.Text;
        if (prev_text != next_text)
        {
            comboBox2.Items.Add(next_text); prev_text = next_text;
        } }
    comboBox2.SelectedIndex = 1;
 }
private void button2_Click(object sender, EventArgs e)
 {
      DataBase database = new DataBase();
      this.Hide();
      database.Show();
 }
private void button3_Click(object sender, EventArgs e)
 {
      comboBox1.DataSource = database1DataSet1.Tables["LocalDataBase"];
      comboBox1.DisplayMember = "Name";
 }
private void button4_Click(object sender, EventArgs e)
 {
      Application.Exit();
 }
```

```
private void button1_Click(object sender, EventArgs e)
 {
     textBox1.Text = textBox1.Text + comboBox2.Text +
     comboBox3.Text + comboBox4.Text + "\r\n";
 }
private void button6_Click(object sender, EventArgs e)
 {
     DataTable table = database1DataSet1.Tables["LocalDataBase"];
     string[] tempstr = textBox1.Lines;
     for (int i = 0; i < tempstr.Length - 1; i++)
      {
       foreach (DataRow row in table.Rows)
        {
         int column = 5;  // Name Column
         if(String.Equals(row[column].ToString(),tempstr[i]))
          {
          textBox2.Text = textBox2.Text + row[0].ToString()
          +"\r\n";
      } } }
     button7.Enabled = true;
 }
private void button7_Click(object sender, EventArgs e)
 {
     SelectionWindow selwind = new SelectionWindow(textBox2);
     this.Hide();selwind.Show();
 }
private void button5_Click_1(object sender, EventArgs e)
```

```
  {
      this.loginTableBindingSource.AddNew();
  }
private void button8_Click(object sender, EventArgs e)
  {
      this.Validate();
      this.loginTableBindingSource.EndEdit();
      this.tableAdapterManager.UpdateAll(this.database1DataSet1);
  }
private void exitToolStripMenuItem_Click(object sender, EventArgs e)
  {
      Application.Exit();
  }
private void helpToolStripMenuItem_Click(object sender, EventArgs e)
  {
      string help_message = "Updated Later";
      MessageBox.Show(help_message);
  }
private void comboBox2_SelectedIndexChanged(object sender, EventArgs e)
  {
      comboBox3.Enabled = true;
      comboBox3.Items.Clear();
      DataTable table = database1DataSet1.Tables["LocalDataBase"];
      string filter_text = comboBox2.Text;
      DataRow[] foundrownew = table.Select("Category =" + "'" +
      filter_text + "'");
      string prev_text = foundrownew[0][2].ToString();
```

```
            comboBox3.Items.Add(prev_text);
            for (int i = 1; i < foundrownew.Length; i++)
            {
                if (prev_text != foundrownew[i][2].ToString())
                {
                    prev_text = foundrownew[i][2].ToString();
                    comboBox3.Items.Add(foundrownew[i][2].ToString());
                }
            }
            comboBox3.SelectedIndex = 0;
        }
    private void comboBox3_SelectedIndexChanged(object sender, EventArgs e)
       {
        comboBox4.Enabled = true;
        comboBox4.Items.Clear();
        DataTable table = database1DataSet1.Tables["LocalDataBase"];
        string filter_text1 = comboBox3.Text;
        DataRow[] foundrownew1 = table.Select("Name =" + "'" +
        filter_text1 + "'");
        string prev_text = foundrownew1[0][3].ToString();
        comboBox4.Items.Add(prev_text);
        for (int i = 0; i < foundrownew1.Length; i++)
          {
            if (prev_text != foundrownew1[i][3].ToString())
              {
                prev_text = foundrownew1[i][3].ToString();
                comboBox4.Items.Add(foundrownew1[i][3].ToString());
```

```
            } }
          comboBox4.SelectedIndex = 0;
      }
    private void goToDataBaseToolStripMenuItem_Click(object sender,
     EventArgs e)
        {
          DataBase database = new DataBase();
          this.Hide(); database.Show();
        }
    private void button2_Click_1(object sender, EventArgs e)
        {
            double dose_req = Convert.ToDouble(textBox4.Text);
            double concentration  = Convert.ToDouble(textBox3.Text);
            double volume_req = dose_req/concentration;
            textBox5.Text = volume_req.ToString();
        }  }
}
```

Appendix B

Source Code for VPS

This appendix consists the main program files for VPS that includes image acquisition, component detection, and procedure monitoring. The complete program files with sample recorded video of CSP can be found here:

https://drive.google.com/folderview?id=0B7M9qPY-omo8ZnM5VkJOT1RHV1k\
&usp=sharing

B.1 Program Launcher

```
% Master Program for all with connection to proper connection
clc; clear all; home;
 id = 0;
 disp('Waiting for Signal from Graphical User Interface!!!');
 while(id==0)
 fileid = fopen('C:\Users\Hem Regmi\Dropbox\Documentation
  Thesis\ApplicationV872015\ApplicationV5262\bin\
  Debug\test.txt','r');
 id = fscanf(fileid,'%d');
 fclose(fileid);
 %disp(string);
```

```
 end
if(id==1)
   % script for ampule
   Mainprogram_video_ampule();
elseif(id==2)
   % script for ampule
   Mainprogram_video_injection();
elseif(id==3)
   % script for ampule
   Mainprogram_video_powder();
end
ab = 0;
fileid = fopen('C:\Users\Hem Regmi\Dropbox\Documentation
 Thesis\ApplicationV872015\ApplicationV5262\bin\
 Debug\test.txt','w');
fprintf(fileid,'%d',ab);
fclose(fileid);
```

B.2 Detection of Component

```
% Surf detection script
clc; clear all; home;
hoodImage = imread('wholeimage.jpg');
figure(1),imshow(hoodImage);
hoodImage = uint8(rgb2gray(hoodImage));
title('Image of Hood with Items');
ivbagImage = imread('ivbag.jpg');
```

```
figure(2),imshow(ivbagImage);
ivbagImage = rgb2gray(ivbagImage);
title('Image of a IV bag');
hoodPoints = detectSURFFeatures(hoodImage);
ivbagPoints = detectSURFFeatures(ivbagImage);
[hoodFeatures, hoodPoints] = extractFeatures(hoodImage,
hoodPoints);
[ivbagFeatures, ivbagPoints] = extractFeatures(ivbagImage,
ivbagPoints);
hoodPairs = matchFeatures(hoodFeatures, ivbagFeatures);
matchedhoodPoints = hoodPoints(hoodPairs(:, 1), :);
matchedivbagPoints = ivbagPoints(hoodPairs(:, 2), :);
figure;
showMatchedFeatures(hoodImage,
ivbagImage, matchedhoodPoints,matchedivbagPoints,
 'montage');
title('Putatively Matched Points (Including Outliers)');
[tform, inlierhoodPoints, inlierivbagPoints] =
estimateGeometricTransform(matchedhoodPoints,
matchedivbagPoints, 'affine');
figure;
showMatchedFeatures(hoodImage, ivbagImage,
inlierhoodPoints, inlierivbagPoints,
'montage');
title('Matched Points (Inliers Only)');
hoodPolygon = [1, 1;...                           % top-left
        size(hoodImage, 2), 1;...                 % top-right
```

```
        size(hoodImage, 2), size(hoodImage, 1);... % bottom-right
        1, size(hoodImage, 1);...                  % bottom-left
        1, 1];
newhoodPolygon = transformPointsForward(tform, hoodPolygon);
figure;
imshow(hoodImage);
hold on;
line(newhoodPolygon(:, 1), newhoodPolygon(:, 2), 'Color', 'y');
title('Detected Box');
```

B.3 Region Extraction

```
function [sy_corr,ne_corr,vi_corr,ca_corr,sw_corr]
 = Get_Correlation_Manual_Injection
 (prev_picture,picture)
% Calculates the correlation between successive
 %frames supplied on input as
% a function
    sy_x = 946; sy_y = 545; sy_width = 103; sy_height = 202;
    vi_x = 1148; vi_y = 529; vi_width = 143; vi_height = 218;
    ca_x = 465;  ca_y = 556; ca_width = 134; ca_height = 188;
    sw_x = 104; sw_y = 610; sw_width = 124; sw_height = 89;
    ne_x = 703; ne_y = 550; ne_width = 126; ne_height = 195;
    % Extraction of previous template
sy_temp_prev = Get_Template_Manula(prev_picture,sy_x,sy_y,sy_width,sy_height);
vi_temp_prev = Get_Template_Manula(prev_picture,vi_x,vi_y,vi_width,vi_height);
ca_temp_prev = Get_Template_Manula(prev_picture,ca_x,ca_y,ca_width,ca_height);
```

```
ne_temp_prev = Get_Template_Manula(prev_picture,ne_x,ne_y,ne_width,ne_height);
sw_temp_prev = Get_Template_Manula(prev_picture,sw_x,sw_y,sw_width,sw_height);
    %extraction of current templates
    sy_temp = Get_Template_Manula(picture,sy_x,sy_y,sy_width,sy_height);
    vi_temp = Get_Template_Manula(picture,vi_x,vi_y,vi_width,vi_height);
    ne_temp = Get_Template_Manula(picture,ne_x,ne_y,ne_width,ne_height);
    ca_temp = Get_Template_Manula(picture,ca_x,ca_y,ca_width,ca_height);
    sw_temp = Get_Template_Manula(picture,sw_x,sw_y,sw_width,sw_height);
   % Correlation calculation
    sy_corr = corr2(sy_temp,sy_temp_prev);
     vi_corr = corr2(vi_temp,vi_temp_prev);
     ne_corr = corr2(ne_temp,ne_temp_prev);
     ca_corr = corr2(ca_temp,ca_temp_prev);
     sw_corr = corr2(sw_temp,sw_temp_prev);
end
```

B.4 VPS for Ampule Preparation

The source code below shows the video processing system for ampule preparation algorithm. The source code for injection vial and powdered reconstitution can be found in the link given at the beginning of the Appendix B.

```
clc; home; clear all;
% Setting Position, based on position of components in the lab
sy_x = 703; sy_y = 550; sy_width = 126; sy_height = 195;
iv_x = 1148; iv_y = 529; iv_width = 143; iv_height = 218;
```

```
ne_x = 465; ne_y = 556; ne_width = 134; ne_height = 188;
fn_x = 277; fn_y = 556; fn_width = 119; fn_height = 184;
sw_x = 104; sw_y = 610; sw_width = 124; sw_height = 89;
am_x = 946; am_y = 545; am_width = 103; am_height = 202;
% Position Setting ends
% Variable Declaration Section
 clean_detected_flag = 0; first_time_flag = 1;
 clean_counter = 0; syringe_clean_flag = 0;
 iv_clean_flag = 0; am_clean_flag = 0;
 needle_flag_stage2 = 0; syringe_flag_stage2 = 0;
 needle_change_flag = 0; prev_sw = 0;
 fn_flag_stage2 = 0;  sw = 0;
 prev_iv = 0; iv = 0;
 prev_k = 0; swab_use_counter = 0;
 ampule_break_flag = 0; Stage_index = 1;
 prev_logic_sw = 1; logic_sw = 1;
% Start Video Reading from webcam
 vid = videoinput('winvideo',1,'RGB24_1280x720');  % This image
 resolution is same as in video recorded
 preview(vid);
 while(1)
if(first_time_flag == 1)
 picture = uint8(getsnapshot(vid));
 picture = rgb2gray(picture); first_time_flag = 0;
 disp('Ampule Preparation Started');
 ne_temp_ref = Get_Template_Manula(picture,ne_x,ne_y,ne_width,ne_height);
 fn_temp_ref = Get_Template_Manula(picture,fn_x,fn_y,fn_width,fn_height);
```

```
am_temp_ref = Get_Template_Manula(picture,am_x,am_y,am_width,am_height);
else
prev_picture = picture;
picture = uint8(getsnapshot(vid));
picture = rgb2gray(picture);
[sy,iv,ne,fn,sw,am,status]=Get_Correlation_Manual(prev_picture,picture);
% Logic for Stage
    if(Stage_index == 1)
     if(sy < 0.5)
      syringe_clean_flag = 1;
     end
     prev_logic_sw = logic_sw;
     if(sw > 0.5)  % just to make work in my lab
     logic_sw = 1;
    else
           logic_sw = 0;
           end
           if(xor(prev_logic_sw,logic_sw))
               swab_use_counter = swab_use_counter + 1;
           else
               clean_counter = clean_counter + 1;
           end
           if(swab_use_counter >= 4)
               Stage_index = 2;
               disp('Cleaning Stage ended');
           end
           if(clean_counter > 30 && syringe_clean_flag == 1)
```

```
        disp('Cleaning Stage Missed'); break;
    end
end
 if(Stage_index == 2)
     if(sy < 0.5 && syringe_flag_stage2==0)
        syringe_flag_stage2 = 1;
        disp('Syringe use detected');
    end
    if(ne < 0.5 && needle_flag_stage2==0)
        needle_flag_stage2 = 1;
        disp('Needle use detected');
    end
    if(fn < 0.5 && fn_flag_stage2==0)
        fn_flag_stage2 = 1;
        disp('Regular Needle use detected');
     end
    if(syringe_flag_stage2 == 1 && needle_flag_stage2 == 1)
        disp('Opening of Syringe and Needle Stared');
    Stage_index = 3;
    elseif(syringe_flag_stage2 == 1 && fn_flag_stage2 == 1)
    disp('Filter Needle is not used');Stage_index = 3;
    end
 end
 % Logic for Stage 3
 if(Stage_index == 3)
    disp('Reached Stage 3');
    disp(am);
```

```
    if(am < 0.5 && ampule_break_flag==0)
        disp('Ampule Break Started');
        Stage_index = 4;
        ampule_break_flag = 1;
    end
end
% Logic for Stage 4
if(Stage_index == 4)
    if(iv < 0.5)
        Stage_index = 5;
    end
    if(fn < 0.5 && needle_change_flag == 0)
        disp('Changing of Needle reached');
        Stage_index = 5;
        needle_change_flag = 1;
    end
end
% Logic for Stage 5
if(Stage_index == 5)
    if(abs(iv < 0.5))
        disp('Injecting into IV Bag');
        ne_temp = Get_Template_Manula(picture,ne_x,ne_y,
        ne_width,ne_height);
        fn_temp = Get_Template_Manula(picture,fn_x,fn_y,
        fn_width,fn_height);
        am_temp = Get_Template_Manula(picture,am_x,am_y,
        am_width,am_height);
```

```
                corr_ne = corr2(ne_temp,ne_temp_ref);
                corr_fn = corr2(fn_temp,fn_temp_ref);
                corr_am = corr2(am_temp,am_temp_ref);
                if(corr_ne > 0.7)
                    disp('Filter Needle is not used..');
                end
                if(corr_fn > 0.7)
                    disp('Regular Needle is not used..');
                end
                if(corr_am > 0.7)
                    disp('Medicine is not Used');
                end
                Stage_index = 6; break;
            end
        end
          sy_temp = Get_Template_Manula(picture,sy_x,sy_y,sy_width,sy_height);
          iv_temp = Get_Template_Manula(picture,iv_x,iv_y,iv_width,iv_height);
          ne_temp = Get_Template_Manula(picture,ne_x,ne_y,ne_width,ne_height);
          fn_temp = Get_Template_Manula(picture,fn_x,fn_y,fn_width,fn_height);
          sw_temp = Get_Template_Manula(picture,sw_x,sw_y,sw_width,sw_height);
          am_temp = Get_Template_Manula(picture,am_x,am_y,am_width,am_height);
          subplot(321),imshow(sy_temp); subplot(322),
          imshow(iv_temp); subplot(323),imshow(ne_temp);
          subplot(324),imshow(fn_temp); subplot(325),
          imshow(sw_temp); subplot(326),imshow(am_temp);
          pause(0.5);
    end end
```

Appendix C

Source Code for SCVMS

This appendix includes the complete MATLAB program for the syringe classification and volume measurement system. The complete database of training data, trained model, and reference images can be found here:

https://drive.google.com/folderview?id=0B7M9qPY-omo8ek03SkVXN2swQk0\&usp=sharing

C.1 Program Launcher

```
% Complete program of classifying and volume measurement
% 3/4/2016
    clear all; home ; clc;%tic;
    %********Image Acquisition******
    vid = videoinput('winvideo',1,'RGB24_1920x1080');
    syringe_image = getsnapshot(vid);
    syringe_image = imrotate(syringe_image,90);
     %********Finding Syringe Cap centroid******%
     I = im2double(syringe_image);
     T=im2double(imread('syringe_cap_yellow.jpg'));
     [I_SSD,I_NCC]=template_matching(T,I);
```

```
    [x,y]=find(I_SSD==max(I_SSD(:)));
    if(x < 150 || x > 700)
    T=im2double(imread('syringe_cap_blue.jpg'));
    [I_SSD,I_NCC]=template_matching(T,I);
    [x,y]=find(I_SSD==max(I_SSD(:)));
    x = x + 14;
    end
    cap_x = y; cap_y = x;
%******Syringe Classification******%
    syringe_gray = rgb2gray(syringe_image);
    [w,h] = size(syringe_gray);
    syringe_binary = zeros(w,h);
        for i=1:w
           for j=1:h
               if(syringe_gray(i,j) < 100)
                   syringe_binary(i,j) = 1;
               end
           end
        end
      CC = bwconncomp(syringe_binary);
      numPixels = cellfun(@numel,CC.PixelIdxList);
      [biggest,idx] = max(numPixels);
      plunger_image = zeros(w,h);
      plunger_image(CC.PixelIdxList{idx}) = 1;
      S = regionprops(plunger_image, {'BoundingBox'});
      bbox = vertcat(S.BoundingBox);width = bbox(:,3);
     % Syringe Classification Testing
```

```
        Result = 'Default';
        if(x > 170 && x < 250)
            Result = 'Thirty';
        elseif(x > 250 && x < 370)
            Result = 'Twenty';
        elseif(x > 370 && x < 500)
            Result = 'Ten';
        elseif(x > 500 && x < 590)
            Result = 'One';
        elseif(x > 590 && x < 750)
            if(width < 125)
            Result = 'Three';
            else
                Result = 'Five';
            end
        end
    % To calculate Lowest points of Plunger Region
      lowest_x = 1;
        lowest_y = 1;
         for i=1:w
             for j=1:h
                 if(plunger_image(i,j)==1)
                     if(lowest_x < i)
                     lowest_x = i;lowest_y = j;
                     end
                 end
             end
```

```
 end
 % form rectangular window of size 40 by 80
 start_x = lowest_x;
 start_y = 10;window_w = 1000;window_h = 5;
 % extracting window image
 se = strel('disk',7);
 plunger_image = imerode(plunger_image,se);
 window_image = zeros(w,h);
 while(nnz(window_image)<200) % to make sure window image gets
 %lower few points of plunger
     for i=start_x:start_x + window_h
         for j=start_y:start_y + window_w
             window_image(i,j) = plunger_image(i,j);
         end
     end
     start_x = start_x - 1; window_h = window_h + 1;
end
 % calculate centroid of window image
 figure(3), imshow(plunger_image); hold on;
 rectangle('Position',[start_y,start_x,window_w,window_h],
 'Linewidth',2,'Linestyle','--','Edgecolor','r');
 stat1 = regionprops(window_image,'centroid');
 % calculating centroid of tip
 plunger_points = stat1(1).Centroid;
 plunger_x = plunger_points(1);  plunger_y = plunger_points(2);
 plot(plunger_x,plunger_y,'go','Linewidth',2); drawnow;
 plot(cap_x,plunger_y,'ro','Linewidth',4);drawnow;
```

```
        plot(cap_x,cap_y,'go','Linewidth',4); drawnow;
        drawLine([cap_x cap_y],[cap_x plunger_y]);  hold off
%******** Volume Measurent using image length ****%
        dist = abs(plunger_y - cap_y);
        volume = 0;
        if(strcmp(Result,'Thirty'))
            load Neuralnetwork_30ml
            volume = sim(net30,dist);
        elseif(strcmp(Result,'Twenty'))
            load Neuralnetwork_20ml
            volume = sim(net20,dist);
        elseif(strcmp(Result,'Ten'))
            load Neuralnetwork_10ml
            volume = sim(net10,dist);
        elseif(strcmp(Result,'Five'))
            load Neuralnetwork_5ml
            volume = sim(net5,dist);
        elseif(strcmp(Result,'Three'))
            load Neuralnetwork_3ml
            volume = sim(net3,dist);
        elseif(strcmp(Result,'One'))
            load Neuralnetwork_1ml
            volume = sim(net1,dist);
        end
 time_req = toc;
figure(1),imshow(syringe_image); hold on;
 plot(cap_x,plunger_y,'ro','Linewidth',4); drawnow;
```

```
plot(cap_x,cap_y,'go','Linewidth',4); drawnow;
figure(4), imshow(syringe_image); home;
output_string = strcat('Syringe Classified :',Result);
disp(output_string);
```

C.2 Neural Network Training

Source code for neural network training of 1 mL syringe is shown, and similar codes with different data were performed for other syringes. The complete source code could be found at the link provided at the beginning of Appendix C.

```
% Program for neural network training
filename = 'Data_1ml.xlsx';
[ndata, text, rawdata] = xlsread(filename);
rawdata = cell2mat(rawdata);
x = rawdata(:,1);x = transpose(x);t = rawdata(:,2);
t = transpose(t);figure(1),plot(x,t,'o');
xlabel('Length');ylabel('Volume');
title('Before Training');
net1 = feedforwardnet(10);net1 = configure(net1,x,t);
net1 = train(net1,x,t);y2 = net1(x);
figure(2),plot(x,t,'o',x,y2,'*');
xlabel('Length');ylabel('Volume');title('After Training');
save Neuralnetwork_1ml net1
```